ON THE NUMERICAL INTEGRATION OF SINGULARLY PERTURBED VOLTERRA INTEGRO-DIFFERENTIAL EQUATIONS

BAKULIKIRA IRAGI

A research project submitted in partial fulfilment of the requirements for the degree of Masters of Science in the Department of Mathematics and Applied Mathematics, University of the Western Cape.

Supervisor: Dr. Justin B. Munyakazi

September 2017

ON THE NUMERICAL INTEGRATION OF SINGULARLY PERTURBED VOLTERRA INTEGRO-DIFFERENTIAL EQUATIONS

BAKULIKIRA IRAGI

KEYWORDS

Singularly perturbed problems

Volterra integro-differential equations

Boundary layer

Maximum principle

Numerical integration

Fitted finite difference methods

Shishkin mesh

Stability analysis

Error bound

Uniform convergence.

Abstract

On the Numerical Integration of Singularly Perturbed Volterra Integro-differential Equations

Bakulikira Iragi

MSc Thesis, Department of Mathematics and Applied Mathematics, Faculty of Natural Sciences, University of the Western Cape.

Efficient numerical approaches for parameter dependent problems have been an interesting subject to numerical analysts and engineers over the past decades. This is due to the prominent role that these problems play in modeling many real life situations in applied sciences. Often, the choice and the efficiency of the approaches depend on the nature of the problem to solve. In this work, we consider the general linear first-order singularly perturbed Volterra integro-differential equations (SPVIDEs). These singularly perturbed problems (SPPs) are governed by integro-differential equations in which the derivative term is multiplied by a small parameter, known as "perturbation parameter". It is known that when this perturbation parameter approaches zero, the solution undergoes fast transitions across narrow regions of the domain (termed boundary or interior layer) thus affecting the convergence of the standard numerical methods. Therefore one often seeks for numerical approaches which preserve stability for all the values of the perturbation parameter, that is ε-numerical methods. This work seeks to investigate some ε-numerical methods that have been used to solve SPVIDEs. It also proposes alternative ones. The various numerical methods are composed of a fitted finite difference scheme used along with suitably chosen interpolating quadrature rules. For each method investigated or designed, we

analyse its stability and convergence. Finally, numerical computations are carried out on some test examples to confirm the robustness and competitiveness of the proposed methods.

September 2017.

Declaration

I declare that **On the numerical integration of singularly perturbed Volterra integro-differential equations** is my own work, that it has not been submitted before for any degree or examination in any other university, and that all the sources I have used or quoted have been indicated and acknowledged as complete references.

Bakulikira Iragi September 2017

Signed:.....

Acknowledgement

I wish to express my deep gratitude to my supervisor, Dr Justin B. Munyakazi for introducing me to the wide field of singularly perturbed problems. I am also thankful to him for his excellent advice, guidance, encouragement and constructive suggestions towards the completion of this thesis. My sincere gratitude goes also to the Department of Mathematics and Applied Mathematics for the academic, technical as well as financial support they gave me through a teaching assistant position. I also would like to convey my special thanks to my lovely mum, Mushiwalyahyage Zaluka , my brothers and sisters for being friendly and helpful during this work. Lastly and above all, I would like to thank the Almighty for his continuous blessings.

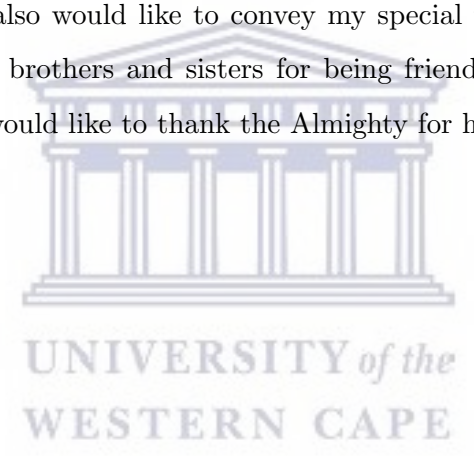

Dedication

To my lovely mum and my late father

Contents

List of Figures

List of Tables

Manuscripts submitted for publication

The following manuscripts which form part of this thesis have been submitted for publication and are under review:

1. Bakulikira C. Iragi and Justin B. Munyakazi, A uniformly convergent numerical method for a singularly perturbed Volterra integro-differential equation, submitted for publication.

2. Bakulikira C. Iragi and Justin B. Munyakazi, New parameter-uniform discretisations of singularly perturbed Volterra integro-differential equations, submitted for publication.

Chapter 1

General Introduction

1.1 Introduction

In his innovative work at the Third International Congress of Mathematicians in Heidelberg at the beginning of last century [49], Prandtl introduced, in the context of fluid dynamics, what is known now as "singular perturbation problems." Now-a-days, these problems turn out to be ubiquitous in various areas of applied mathematics and engineering. These include quantum mechanics, geophysical fluid dynamics, elasticity, chemical reactor theory, optimal control, oceanic and atmospheric circulation, fluid dynamics, fluid mechanics, diffraction theory, reaction-diffusion processes and meteorology.

In fluid dynamics, for example, the most striking example is Navier-Stokes equation in two dimensions [18]

$$\frac{\partial(u^2+p)}{\partial x}+\frac{\partial(uv)}{\partial y}=\frac{1}{Re}\left(\frac{\partial^2 u}{\partial x^2}+\frac{\partial^2 u}{\partial y^2}\right), \tag{1.1.1}$$

with appropriately chosen initial and boundary conditions. Here u and v are the velocity components in x and y directions and p is the pressure. The Reynolds number, Re, which is proportional to the length scale, velocity scale and inversely proportional to the kinematics viscosity of the fluid, gives rise to singularly perturbed nature of (1.1.1) for sufficiently large values (i.e. $Re \gg 1$).

In mathematical genetics, the time-independent Fokker-Planck equation for a one-dimensional dynamical system with state-independent random perturbation

$$\varepsilon^2\frac{d^2\Phi}{dt^2}+b(t)\frac{d\Phi}{dt}=0,\ \ 0<\varepsilon\ll 1,\ \ t\in(0,1),\ \ \Phi(0,\varepsilon)=\Phi_0,\ \ \Phi(1,\varepsilon)=\Phi_1; \tag{1.1.2}$$

is considered in [22]. Here $b(t)$ denotes a gradient field. Under the assumptions that the coeffi-

cient function $b'(t)$ is strictly negative throughout the interval $[0, 1]$ and that $b(t) = 0$ for some $0 < t < 1$, the above problem is aclearly a turning point problem. Φ_0 and Φ_1 are fixed constants.

Another significant model of singular perturbation problems is the free motion of the undamped linear spring mass system with a very resistant spring [65]. For more on singular perturbation models, interested readers are referred to [29, 44, 51].

In general, singular perturbation problems (SPPs) are differential equations (ordinary or partial) that depend on a small positive parameter ε, and whose solutions (their derivatives) approach a discontinuous limit as ε approaches zero [51]. The parameter ε is said to be the perturbation parameter. Technically, this definition simply means that the solution of the SPPs cannot be represented as asymptotic expansion in the powers of ε.

Notwithstanding the best effort of many researchers in finding solution to SPPs using analytical, semi-analytical or numerical techniques, the problem of inaccurate solution persists. The major difficulty that one faces when solving SPPs has always been associated with the small parameter multiplying the highest derivative terms. This parameter prevents one from getting satisfactory results. Several numerical methods have been adequately used to solve SPPs. However, most of them become unfit when the perturbation parameter takes small values. The solution of these problems varies abruptly across narrow regions of the domain (named layers) as the perturbation parameter becomes small. Depending on the location of these layers in the domain of the problem, they are called boundary or interior layers.

Before we proceed further, we give a clear overview of the layer behaviour of the solution of the SPPs. To this end, we discuss the following examples.

Example 1.1.1. [35] *Consider the following Volterra equation of the second kind*

$$\varepsilon u(t) = \sin(t) - \int_0^t u(s)ds. \tag{1.1.3}$$

For $\varepsilon > 0$ the exact solution is given by

$$u(t) = \frac{1}{1+\varepsilon^2}(\cos(t) + \varepsilon \sin(t)) - \frac{1}{1+\varepsilon^2} \exp\left(\frac{-t}{\varepsilon}\right), \text{ and satisfies } \quad u(0) = 0. \tag{1.1.4}$$

Putting $\varepsilon = 0$, in (1.1.3) we obtain the reduced equation which we denote by

$$0 = \sin(t) - \int_0^t u_0(s)ds, \tag{1.1.5}$$

and its solution is given

$$u_0(t) = \cos(t), \text{ and one has } \quad u_0(0) = 1. \tag{1.1.6}$$

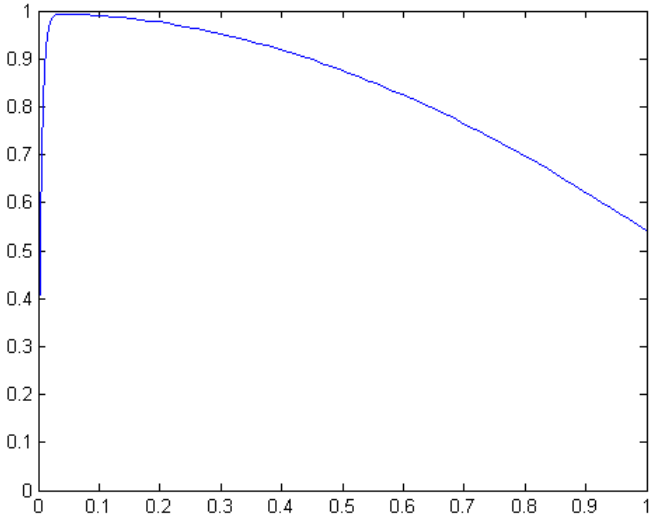

Figure 1.1: Exact solution of Example 1.1.1 for ε =0.005

Clearly $u(0) \neq u_0(0)$. The solution u_0 of the reduced problem is not a uniformly valid approximation of u near $t = 0$ and therefore one observes the presence of a boundary layer term containing $\exp(-t/\varepsilon)$. This boundary layer is responsible for the quick changes of the solution u from $u(0) = 0$ to $u_0(t) = \cos(t)$ near $t = 0$.

Example 1.1.2. [44] *On the interval* Ω =$(0, 1)$*, consider the initial value problem*

$$\varepsilon u'(t) + u(t) = 0, \;\; u(0) = u_0, \tag{1.1.7}$$

where $u_0 \in \mathbb{R}$ *is an arbitrary constant and* $\varepsilon \in (0, 1]$.

The exact solution of equation (1.1.7) when $\varepsilon > 0$ is given by

$$u_\varepsilon(t) = u_0 \exp\left(\frac{-t}{\varepsilon}\right), \text{ for every } t \in \Omega. \tag{1.1.8}$$

Setting $\varepsilon = 0$, equation (1.1.7) is reduced to a trivial equation $v_0(t) = 0$ for every $t \in (0, 1]$. It can be easily seen that no initial condition can be imposed at $t = 0$, as a result of $v_0(t) \equiv 0$ being completely solved. The solution of the differential equation and that of the reduced equation diverge except when $u_0 = 0$. Therefore, there exists one boundary layer in the neighbourhood of $t = 0$.

Example 1.1.3. [44] *Consider the two-point boundary value problem*

$$-\varepsilon u''(t) + u(t) = 0, \quad u(0) = u_0, \; u(1) = u_1, \tag{1.1.9}$$

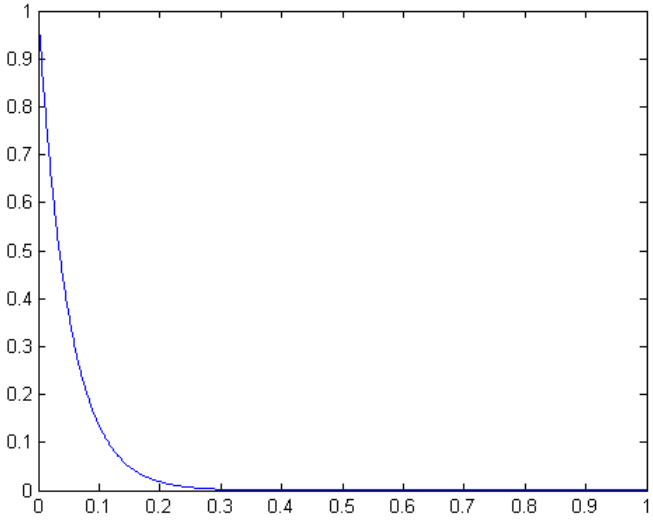

Figure 1.2: Exact solution of Example 1.1.2 for ε =0.005

where $u_0, u_1 \in \mathbb{R}$ *are arbitrary constants and* $\varepsilon \in (0, 1]$.

The exact solution $u_\varepsilon(t)$ is given by

$$u_\varepsilon(t) = \exp\left(\frac{-t}{\sqrt{\varepsilon}}\right) + \exp\left(\frac{-(1-t)}{\sqrt{\varepsilon}}\right). \tag{1.1.10}$$

Putting $\varepsilon = 0$ in (1.1.9), we obtain the reduced equation which is of order zero. Since the boundary conditions should be prescribed depending on the order of the derivative involved in differential equation, it is easy to observe that no boundary condition can be imposed to exact solution of the reduced equation, $v_0 = 0$. It therefore follows that the solution will display a boundary layer at $t = 0$ unless $u_0 = 0$ and similarly at $t = 1$ unless $u_1 = 0$.

1.2 Some basic notions on Volterra integral equations

To avoid a lengthy section, we only include some basic but important information on Volterra integral equations. A Volterra integral equation is a functional equation in which the unknown function (to be determined) appears under the integral sign and the upper limit of the integral is a variable [66]. As far as Volterra integral equations are concerned, one distinguishes between the first and the second kind. Indeed, for a closed and bounded interval $I := [0, T], \{(t, s)\ 0 \leq s \leq t \leq T\}$, the Volterra integral equations of the first and the second kinds in the unknown

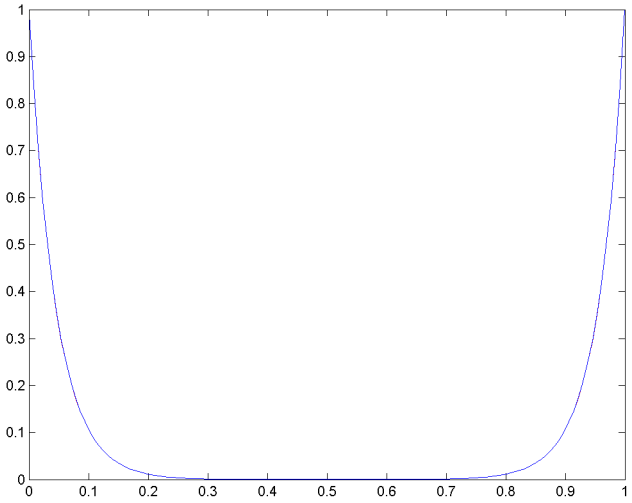

Figure 1.3: Exact solution of Example 1.1.3 for ε =0.005

function $u(t)$ are respectively

$$\int_{t_0}^{t} K(t,s,u(s))ds = f(t) \tag{1.2.1}$$

and

$$u(t) = f(t) + \int_{t_0}^{t} K(t,s,u(s))ds, \tag{1.2.2}$$

where the function $f(.)$ and the kernel $K(.,.,.)$ are known, t_0 is a constant and $u(.)$ is the unknown function to be determined. Note that, if the two limits of integration are constants, equations (1.2.1) and (1.2.2) are called first and second kind Fredholm integral equations respectively. The distinction between Fredholm and Volterra equations is similar to the one between boundary and initial value problems in ODEs [45]. Volterra integral equations are extensively applied in demography, viscosity, biology, chemistry, insurance mathematics [58]. In 1900, while working on population growth, Volterra came up with a special type of equation in which both the differential and integral operators of the unknown function appeared [66]. This new equation was named Volterra integro-differential equation. It's general form is

$$u^{(n)}(t) = f(t) + \int_{t_0}^{t} K(t,s,u(s))ds; \quad t \in [t_0, T] \text{ where } u^{(n)}(t) = \frac{d^n u(t)}{dt^n}, \tag{1.2.3}$$

with the initial conditions $u(t_0), u'(t_0), u''(t_0), ..., u^{(n-1)}(t_0)$ to be defined. In the same manner as (1.2.1) and (1.2.2), the corresponding Fredholm integro-differential equation can be obtained

by letting the two limits to be constants. As shown in [12], the interval $[t_0, T]$ may be interpreted as $[t_0, \infty]$ if T is unbounded. For our purposes and without lost of generality, we will assume that T is finite. The functions $f(.) \in C[t_0, T]$ and the kernel $K(t, s, v)$ are continuous for $t_0 \leq s \leq t \leq T$. In addition, the function $K(t, s, v)$ satisfies a uniform Lipschitz condition in v for $t_0 \leq s \leq t \leq T$. These conditions are sufficient to guarantee that (1.2.1)-(1.2.3) have a unique continuous solution [66]. In some cases, alternative equation to (1.2.3) is

$$u^{(n)}(t) = F\left(t, u(t), \int_{t_0}^{t} K(t, s, u(s))ds\right), \quad t \in [t_0, T] \quad \text{with} \tag{1.2.4}$$

the initial conditions $u(t_0), u'(t_0), u''(t_0), ..., u^{(n-1)}(t_0)$, where as before, $F(.,.,)$, and $K(.,.,.)$ are given functions and $u(.)$ is the unknown function to be found. Moreover, the function $F(.,.,)$ satisfies appropriate Lipschitz conditions.

1. If $K(t, s, v)$=$K(t, s)v$, equations (1.2.1)-(1.2.3) are linear.

2. If at least one of the limits of integration is infinite or the kernel $K(t, s, v)$ becomes unbounded at some point inside the interval $[t_0, T]$, then equations (1.2.1)-(1.2.3) are said to be singular equations, not to be confused with singularly perturbed equations.

In [12], it is said that there could be a link between the solution $u_\varepsilon(.)$ of the singularly perturbed Volterra equation

$$\varepsilon u'(t) = \int_{t_0}^{t} K(t, s, u_\varepsilon(s))ds - f(t), \tag{1.2.5}$$

of the second kind and the solution $u_0(.)$ of the corresponding reduced Volterra integro-differential equation (1.2.1), (see discusions in example (1.1.3)). However, such link can only be established under special conditions. This said, one can develop special discretization techniques that are candidates to solve equation a (1.2.1) by modifying them for the singularly perturbed equation (1.2.5). This dissertation falls under the design of these techniques.

1.3 The model problem

There exists several types of SPPs. In this work, we consider the general linear first order singularly perturbed Volterra integro-differential equation (SPVIDE)

$$Lu := \varepsilon u'(t) + a(t)u(t) + \int_0^t K(t, s)u(s)ds = f(t), \quad t \in I := [0, 1], \tag{1.3.1}$$

along with the initial condition

$$u(0) = u_0, \tag{1.3.2}$$

where a prime indicates the first derivative of u with respect to t, $0 < \alpha \leq a(t)$ and $a(t), f(t)$, $K(t,s)$ $((t,s) \in I \times I)$ are sufficiently smooth functions. The perturbation parameter ε is assumed to take arbitrary small positive values in the semi-open interval $(0, 1]$ and u_0 is a given fixed constant.

Under these conditions, the solution $u(t)$ of the problem (1.3.1)-(1.3.2) displays one boundary layer near $t = 0$ [4]. Setting $\varepsilon = 0$ in equation (1.3.1), we obtain the reduced equation

$$a(t)u_0(t) + \int_0^t K(t,s)u_0(s)ds = f(t) \tag{1.3.3}$$

which is a Volterra integral equation of the second kind. The singularly perturbed nature of (1.3.1) arises when the properties of the solution with $\varepsilon > 0$ are incompatible with those when $\varepsilon = 0$ [4]. Problems which do imply such an incompatibility in the behaviour of u near $t = 0$ form the subject matter of this dissertation.

1.4 Fitted finite difference methods to solve singularly perturbed problems

Problems with a small parameter multiplying the derivative have been solved successfully using various computational methods such as Finite Element Method (FEM), Finite Volume Method (FVM) and Finite Difference Method (FDM). These methods are generally referred to as standard or classical numerical methods. However, it is known that if any discretization technique is applied to a parameter-dependent problem, then the behaviour of the discretization depends on the parameter. With this in mind, unless extremely large number of mesh points is provided, standard numerical methods fail to provide fairly accurate approximate solution of the exact solution for all the values of the perturbation parameter. The truncation error becomes unbounded on one hand, on the other hand, when $\varepsilon = 0$, the order of the differential equation drop by one as a result, the number of initial or boundary condition to be imposed is lowered [44].

To resolve this issue, ε-uniformly convergent methods are desirable. These are numerical methods whose accuracy does not depend on the value of the perturbation parameter and for

which the size of the error depends only on the number of mesh points [24]. Throughout this work, we focus on ε-uniform numerical methods to derive approximate solutions.

In order to achieve ε-uniform convergent behavior, two approaches are often used in the context of finite difference methods. The first one involves designing a method which reflects the nature of the solution in the layer regions using uniform meshes with reasonable number of mesh points. This approach forms the class of Fitted Operator Finite Difference Methods (FOFDMs). The second approach is to use meshes adapted to the layers [31]. This technique falls under the class of Fitted Mesh Finite Difference Methods (FMFDMs). We give a brief description of both techniques in this section.

1.4.1 Fitted Operator Finite Difference Methods (FOFDMs)

This first approach which reduces to a discrete operator involving either a fitting factor (of exponential type for example) or a denominator function, consists in replacing the standard finite difference operator suitably by a finite difference operator which reflects the singularly perturbed nature of the differential operator [44, 51]. In other words, modifying the difference scheme coefficients in such a way that the scheme becomes more stable and achieves that the truncation error becomes uniformly bounded with respect to the perturbation parameter.

The concept denominator function is recent and developed on the basis of some rules first introduced by Mickens [43]. The advent of this book seem to have been the principal motivation for introducing the concept of denominator function in the wide area of numerical analysis. The fundamental idea behind the construction of this FOFDMs is to substitute the denominator functions of the classical derivatives with a positive functions derived in such a way that they capture significant properties of the governing differential equation and provide trustworthy numerical results [10]. Numerous scientific works have been dedicated to construction of FOFDMs for singularly perturbed differential equations (see e.g.; [40, 46, 47, 48]) and in a number of other works as well.

In the case of linear equations, the FOFDMs are developed by choosing their coefficients so that some or all the exponential functions in the null space of the differential operator, or part of it, are also in the null space of the finite difference operator [18]. Here, the FOFDM is termed Exponentially Fitted Operator Finite Difference Method and generally require the introduction of artificial viscosity.

Introduced by Allen and Southwell [1], FOFDMs of exponential type have been used by

many authors [3, 4, 32] to solve several different type of SPPs.

Note that in either case, the FOFDMs consist in a special discretization of the continuous problem on a uniform mesh and are known to be more accurate than FMFDMs. An other attractive advantage is that FOFDMs are easy to implement and generally do not require a priori knowledge of the location and the breadth of the layer [47] . However, they are difficult to extend to nonlinear and higher order dimensional problems.

1.4.2 Fitted Mesh Finite Difference Method (FMFDM)

The FMFDM consists of a simple discretization with fittingly chosen non-uniform grid. It involves transforming the continuous problem into a discrete problem on a non-uniform partition and uses a mesh which is adapted to the singularly perturbed nature of the problem [44, 51].

Towards the design of FMFDMs, numerous works have been done (see for instance [16, 29, 41, 46, 51]).

The idea of layer adapted meshes was addressed for the first time by Bakhvalov about six decades ago [11] in the framework of a reaction-diffusion problem. For singularly perturbed boundary value problems whose solution contains an exponential term of the form $y = \exp(-\beta x/\varepsilon)$, where β is a fixed constant, the exponential layer appears near $x = 0$ [39]. In fact, Bakhvalov's idea is to use an equidistant y-grid near $y = 1$ (which corresponds to $x = 1$), then to map this grid back to the x-axis by means of a logarithmic function.

A mesh generating function of this type for a problem whose solution exhibits two layers is as follows [60]: for an even positive integer N, we consider the following partition $I_h := 0 = x_0 < x_1 < ... < x_{N-1} < x_N = 1,\ \ x_i = \Psi(i/N),\ h = 1/N,\ i = 0(1)N$. Note that the mesh generating function Ψ consists of three parts: Ψ_1, Ψ_2 and Ψ_3. The functions Ψ_1 and Ψ_3 generate points in the boundary layers near $x = 0$ and $x = 1$ respectively, while the function Ψ_2 generates mesh points outside the boundary layers and is tangent to both Ψ_1 and Ψ_3 and satisfies $\Psi_2(1/2) = 1/2$. Hence, Bakhvalov's mesh generating function in the three subintervals is given by

$$\Psi(t) = \begin{cases} \Phi(t) = -a\sqrt{\varepsilon}\ln(\frac{q}{q-t}), & t \in [0, \eta], \\ \Phi(\eta) + \Phi'(\eta)(t-\eta), & t \in [\eta, 1/2], \\ 1 - \Psi(1-t), & t \in [1/2, 1], \end{cases} \tag{1.4.1}$$

where a, q are constants independent of ε and satisfy $q \in (0, 1/2), \quad a \in (0, q/\sqrt{\varepsilon})$, η is the abscissa of the contact point of the tangent line from the point $(1/2, 1/2)$ to $\Phi(x)$.

The graded grids of Bakhvalov are equally spaced outside the layer and characterized by a gradual transition from the coarse in a very fine mesh at the layer. This mesh has been investigated and improved by many authors, like Gartland in [21] and Vulanović [64].

Soon after, the Russian mathematician Grigorii Ivanovich Shishkin [59] introduced a simple layer adapted mesh which consists in a blend of finite number of uniform meshes with different transition points. Unlike Bakhvalov meshes, Shishkin meshes are piecewise uniform meshes. That is, they divide the domain into subdomains on which an equidistant mesh is developed.

For illustration purposes, we present piecewise-uniform meshes [44]. Consider the following piecewise-uniform mesh Ω_δ^N which we generate as follows: choose a point δ such that $0 < \delta \leq 1/2$ and assume that N is an even positive number. We divide the interval $[0, 1]$ into two subintervals $[0, \delta]$ and $[\delta, 1]$. Then the mesh size in each of the two subintervals is given by

$$x_j - x_{j-1} = \begin{cases} h_1 = 2\delta/N, & j = 0, 1, ..., N/2, \\ h_2 = 2(1-\delta)/N, & j = N/2+1, ..., N. \end{cases} \tag{1.4.2}$$

The transition parameter, δ which separates the inner and outer regions is located and defined according to the nature of the problem to be solved. In other words, δ is chosen in accordance with the position of the layer. An example of a Shishkin mesh with $N = 8$ is given in Figure 1.4, where the transitions parameter is

$$\delta = \min\{1/2, \varepsilon \ln N\}. \tag{1.4.3}$$

Note that for the above case, the boundary layer is located at $x = 0$. On the other hand, if

Figure 1.4: Shishkin mesh Ω_δ^8 where the boundary layer is located at $x = 0$

the layer occurs near $x = 1$, then the mesh is as the in Figure 1.5 where δ is still defined as in (1.4.3) and mesh size in the two subdomains then becomes

$$x_j - x_{j-1} = \begin{cases} h_1 = 2(1-\delta)/N, & j = N/2+1, ..., N, \\ h_2 = 2\delta/N, & j = 0, 1, 2, ..., N/2. \end{cases} \tag{1.4.4}$$

In the above two cases, we dealt with problems whose solutions exhibit one boundary layer. Next, we look at example (1.1.3) whose solution displays two boundary layers, one near $x = 0$ and

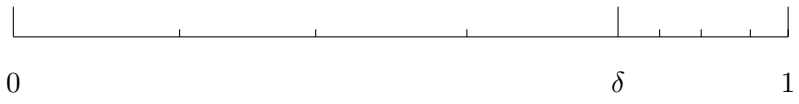

Figure 1.5: Shishkin mesh Ω_δ^8 where the boundary layer is located at $x = 1$

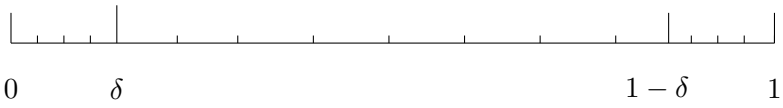

Figure 1.6: Shishkin mesh Ω_δ^{16} where the boundary layers occur at $x = 0$ and $x = 1$

another one at $x = 1$. Because of these two boundary layers, the mesh should be condensing near each of these points. Therefore, the interval $\Omega = (0, 1)$ is then divided into three subintervals, $(0, \delta)$, $(1 - \delta, 1)$ and $1 - \delta$. As before, δ is still ranging in the semi-open interval $(0, 1/2]$ but in this case there are two transition points. One located at $x = \delta$ and other one at $x = 1 - \delta$. Each of the intervals $(0, \delta)$ and $(1 - \delta, 1)$ is divided uniformly into $N/4$ subintervals whilst the interval $(\delta, 1 - \delta)$ is devided into $N/2$ subintervals. In this case, we define δ as

$$\delta = \min\{1/4, \sqrt{\varepsilon} \ln N\}. \tag{1.4.5}$$

The mesh size in each of the three subintervals is given by

$$x_j - x_{j-1} = \begin{cases} h_1 = 4\delta/N, & j = 0, 1, 2, ..., N/4 + 1, \\ h_2 = 2(1 - 2\delta)/N, & j = N/4 + 1, ..., 3N/4, \\ h_3 = 4\delta/N, & j = 3N/4 + 1, ..., N. \end{cases} \tag{1.4.6}$$

A model presentation of the mesh of this kind is shown in Figure 1.6. Note that the choice of $\delta = 1/4$ results in a uniform mesh. For all other permissible values of δ, $0 < \delta \leq 1/2$, each of the subintervals $(0, \delta)$ and $(1 - \delta, 1)$ is small than the subinterval $(\delta, 1 - \delta)$. In this case the mesh becomes piecewise-uniform rather than uniform. The same idea holds true for $\delta = 1/2$ in each of the first two cases.

As reported by Kadalbajoo et al. [29], though Shishkin meshes are simpler than Bakhvalov meshes, the latter produces much better numerical results. The chief reason is that Bakhvalov meshes are better adapted to the layer structure. However, since higher order schemes are much easier developed on an equidistant grid than on an entirely nonequidistant one, the piecewise uniform Shihskin mesh presents more advantage than Bakhvalov ones. Another advantage of

Shishkin meshes over Bakhvalov's is observed in their simplicity which allows application to different type of problem, more precisely flexibility and smoothness to tackle complicated and higher order dimensional problems [31, 48].

The above approaches have been used extensively to solve singularly perturbed differential equations. However, very little effort in their use is observed for singularly perturbed integro-differential equations.

1.5 Literature review on Volterra equations

In this section, we present some of the works recorded in the literature on numerical treatment of Volterra integral equations over the past half century. These classes of equations play a primordial role in modelling numerous problems in engineering and applied sciences, and therefore have attracted the attention of many researchers in developing a wide theory and numerical analysis.

A number of recent papers have been devoted to the investigation of various approximation techniques including quadrature rules, finite difference method, finite element methods, variational iteration method, homotopy perturbation methods and spline collocation methods for Volterra, Fredholm, Fredholm-Volterra and Volterra-Abel integral and integro-differential equations [7, 14, 19, 50, 52, 55, 56, 62].

If we restrict the above mentioned classes of problems to the corresponding classes in which the terms with the highest derivatives are multiplied by a small parameter, then they are said to be singularly perturbed Volterra, Fredholm, Fredholm-Volterra and Volterra-Abel integral and integro-differential equations respectively. The solution of these problems undergoes fast variations in the boundary or interior layers thus rendering the classical numerical approaches impractical. This fact motivates the design of special techniques which preserve stability for all the values of the perturbation parameter. In this regard, tremendous works have been done for singularly perturbed Volterra integro-differential equations.

Kauthen [35] surveyed the existing literature on singularly perturbed Volterra integral and integro-differential equations. He also analyzed an implicit Runge-Kutta method for singularly perturbed Volterra integro-differential equation [33]. In [34] the same author studied the convergence of the extended implicit Pouzet-Volterra-Runge-Kutta methods applied to singularly perturbed systems of Volterra integro-differential equations.

An exponentially fitted scheme for a fixed perturbation parameter ε is derived and stability analysis of the scheme is discussed in [53]. Some discretizations of singularly perturbed Volterra integro-differential equation and Volterra integral equations by tension spline collocation methods in tension spline spaces can be found in [25].

In 1978, Lodge et al. [42] established many qualitative properties of the solution of a nonlinear singularly perturbed Volterra integro-differential equation. They also proved existence and uniqueness of the solution. Jordan [28, 26] extended the results of [42] to the general nonconvolution problem.

Angell and Olmstead developed [9] a formal methodology for obtaining asymptotic expansion of the solution to a singularly perturbed Volterra equation which they appplied to several examples. In [8], they used a formal asymptotic scheme and determined the leading order behaviour of a certain singularly perturbed integro-differential equation which models the process of stretching a polymer filament. Bijura [15] demonstrated in 2006 the existence of the initial layers whose thickness is not of order of magnitude $O(\varepsilon), \varepsilon \longmapsto 0$, and constructed approximate solutions using the initial layer theory.

In [61], Zhao et al. investigate the delay-dependent stability of the symmetric boundary value methods (BVMs). Four families of symetric boundary value methods, namely the Extended Trapezoidal Rules of first (ETR_1) and second (ETR_2) kinds, the Top Order Methods (TOMs) and the B-spline linear multistep methods (BS methods) were considered. The authors analyzed the delay-dependent stability region of symmetric BVM using the boundary locus technique and proved that under suitably chosen hypothesis the symmetric schemes preserve the delay-dependent stability of the test equation. A convergent collocation method based on the use of the Taylor polynomials to approximate the solution of the delay integro-differential equation in spline space $S^0_{m-1}(\Pi_N)$ is presented by Bellour and Bousselsar [13]. In [23], He and Xa discussed the exponential stability of impulsive singularly perturbed Volterra delay integro-differential equation.

Koto [37] studied stability of a Runge-Kutta method for Volterra delay integro-differential equation with a constant delay. For singularly perturbed problem, the issues associated with their numerical treatments and several approaches to sort out these difficulties we used [20, 44, 51]. The authors in [67] examined a singularly perturbed Volterra integro-differential equation with a delay. Using a linear multistep method, they investigated error behaviour and derived global error estimates $A(\alpha)$-stable linear multistep method with convergent quadrature rule.

None of the works above mentioned on singularly perturbed Volterra integro-differential equations (SPVIDE) have used fitted finite difference methods for their solution.

Using a method of integral identities with weights and remainder terms in the integral form, Amiraliyev and Yilmaz [2] developed a fitted difference method of exponential type to solve a delayed singularly perturbed Volterra integro-differential equation. The scheme was fully analyzed for convergence and stability and proved to have a first order parameter-uniform convergence. In [54], Şevgin derived a uniformly convergence ε-numerical method on a graded mesh for the numerical solution of a nonlinear SPVIDE and was proved to be of first order accurate in the maximum norm.

Using the midpoint difference operator with trapezoidal integration, Zhongdi and Lifeng [63] studied the convergence properties of a finite difference scheme on Shishkin mesh for problem (1.3.1)-(1.3.2), they derived a priori error estimate that is ε-uniform and proved that the finite difference scheme is almost second order accurate. On the other hand, Amiraliyev and Şevgin [4] presented an exponentially fitted finite difference method to solve the same problem. The fitting factor was introduced via the method of integral identities with the use of exponential basis functions and interpolating quadrature rules with weight and remainder terms in integral form. Their method was first order uniformly convergent, in the maximum norm, with respect to ε.

Recently Kudu et al. [38] designed an implicit finite difference scheme on a piecewise-uniform mesh of Shishkin-type for solving a singularly perturbed delay integro-differential equation. The scheme was constructed utilising the procedure in [4]. It was proved that under some appropriate conditions, the scheme is stable with respect to ε and is convergent with oder $0(N^{-1}\ln N)$.

To our knowledge, fitted finite difference methods are not fully explored to solve singularly perturbed Volterra integro-differential equations. In this work, we solve first order linear singularly Perturbed Volterra Integro-differential Equation (SPVIDE). Our aim is to investigate some existing fitted finite difference methods. Then design and analyse new discretizations in the framework of fitted finite difference methods for these problems. In this regard, we have reached some successes. Apart from the technique used in chapter 2, the approach to construct discrete problems and to perform convergence analysis of approximate solution is analogous to the ones from [4, 54, 38] and based upon some quadratures rule introduced by Amiraliyev [5]. An extension and summary of these rules are given in Amiraliyev and Mamedou [6].

1.6 Outline of the thesis

In this work, we investigate, construct and analyse FMFDMs and exponentially FOFDMs to solve singularly perturbed Volterra integro-differential equations (SPVIDEs). Apart from this introductory chapter, this dissertation consists of five chapters and a conclusion. In each chapter, we investigate/design a numerical method and provide a complete theoretical analysis of its convergence. Computational results are presented in tabular form to support the theoretical results.

The problem under consideration in this work is composed of a differential and integral operators. Therefore, to construct the numerical methods, we use the upwinding finite difference discretization for the differential part and several different suitably chosen interpolating quadrature rules to discretize the intergral part.

The exponentially fitted operator finite difference scheme of [4] is considered in Chapter 2. The chapter commences with an important qualitative result which gives a better understanding of the behaviour of the solution of the problem under study and its derivatives. Then we present the difference scheme. The method is based on the use of exponential basis functions and some interpolating quadrature rules with weights and remainder terms in integral form. The method is analyzed for stability and convergence and proved to be first order accurate in the maximum norm.

In Chapter 3, we investigate the fitted mesh finite difference method of [63]. The method consists of the midpoint finite difference operator along with the trapezoidal integration. The method is applied on an appropriate piecewise uniform mesh of Shishkin type. We show that the method is parameter uniformly convergent of almost second order.

As outlined earlier in the chapter, fitted mesh and fitted operator finite difference methods are not fully exploited for singularly perturbed Volterra integro-differential equations. In the next 3 Chapters we suggest more discretizations for (1.3.1)-(1.3.2). In Chapter 4, we design and analyze an implicit finite difference scheme on a piecewise-uniform mesh. The scheme is developed using right and composite left side rectangle rules with the weights and remainder terms in integral form. We prove that the method is first order accurate in the maximum norm. A similar method has been suggested by Kudu et al. [38] to solve singularly perturbed integro-differential equations with delay. In Chapter 5, we wish to improve the results obtained with the method in Chapter 4. To this end, we combine the obtained result with Simpson and trapezoidal quadrature rules. We remark that the two quadrature rules have greatly contributed

to the accrued accuracy of the schemes, however, the rates of convergence remain the same.

In Chapter 6, we introduce a new discretization on a uniform mesh. Unlike the method in Chapter 2, this new FOFDMs is based on the right side rectangle rule and use of exponential basis functions to compute a fitting factor which is employed for the discretization of the derivative part. Then the trapezoidal integration with weight and remainder terms in the integral form is used to deal with the integral part. This method is shown to be stable, of first order convergence and more accurate than the one in Chapter 2. The performance of our method is illustrated through numerical computations.

Lastly some concluding remarks and directions for further research are given in Chapter 7.

Chapter 2

An Exponentially Fitted Operator Finite Difference Method for SPVIDEs

In the previous chapter, we discussed singularly perturbed problems as well as the issues associated with their numerical treatment. We have noticed that the major difficulty with SPPs lies in resolving the layer. The solution to these problems vary abruptly within some thin regions of the domain (boundary layer) thus making numerical methods unsatisfactory. To overcome this difficulty, two approaches are often used in the framework of finite difference methods namely fitted operator finite difference methods and fitted mesh finite difference methods.

This chapter presents a fitted operator finite difference method of exponential type to solve (1.3.1)-(1.3.2). The proposed numerical method is constructed via the integral identities approach along with the exponential basis function to compute a fitting factor. This approach is used to discretize the differential part. Then, a blend of some suitable interpolating quadrature rules with weights and remainder terms in the integral form are used for the integral part. We show that this method is first order convergent in the maximum norm. We carry out some computations on two test examples to support the theoretical results.

2.1 Introduction

Over the past half century, numerical solution of singularly perturbed Volterra integro-differential equations have attracted the attention of researchers in applied sciences and engineering. Numer-

ous analytical, semi-analytical and numerical approaches have been developed to approximate the solution of these equations (see [33, 34, 25] and the references therein). However, when the perturbation parameter approaches zero, the solution of the these problems is known to have a steep gradient within the boundary layer which affects the convergence of the solution obtained utilizing classical numerical techniques.

To get the best of this difficulty, two ways have been followed in the context of finite defference methods. Those are FMFDMs and FOFDMs.

Except the works in [4, 54, 63], not much work have been done so far towards the design of fitted finite difference methods for solving singularly perturbed Volterra integro-differential equations (SPVIDEs). In this chapter, we aim to explore a class of fitted operator finite difference methods. More specifically the Exponentially Fitted Operator Finite Difference Method (EFOFDM) constructed by Amiraliyev and Şevgin [4].

The rest of the chapter is organized as follows. Bounds on the solution and its derivatives are provided in the next Section. In Section 2.3, we present the numerical method. Stability and convergence analysis of the numerical method are carried out in Section 2.4. Two test examples to confirm our theoretical results are given in Section 2.5 and lastly, a short conclusion is provided in Section 2.6.

Throughtout the dissertation, C, sometimes subscripted, denotes a generic positive constant which is independent of ε and the mesh parameter. The set $C^n(I \times I)$ denotes a space of real-valued functions which are n-times continuously differentiable on $I \times I$. The set $C_m^n(I \times I)$ denotes the space of two real-valued functions which are n-times continuously differentiable with respect to the first argument and m-times continuously differentiable with respect to the second argument on $I \times I$. Moreover, the constant $\bar{K}$ denotes the maximum of the function $K(t,s)$ i.e., $\bar{K} = \max_{I \times I} |K(t,s)|$.

2.2 Bounds on the solution and its derivatives

In this section, we study the qualitative behaviour of the solution of (1.3.1)-(1.3.2) and its derivatives which are required in the convergence analyis of the numerical methods.

Lemma 2.2.1. *Let $a, f \in C^3(I)$ and $K \in C^3(I \times I)$. Then the solution $u(t)$ of the problem*

(1.3.1)-(1.3.2) satisfies the following inequalities.

$$||u||_{\infty,I} \leq C, \tag{2.2.1}$$

$$|u^k(t)| \leq C\left(1 + \frac{1}{\varepsilon^k}\exp\left(\frac{-\alpha t}{\varepsilon}\right)\right), \quad t \in I, \quad k = 1, 2, 3. \tag{2.2.2}$$

Proof. We first show that (2.2.1) holds true. To do that, we rewrite (1.3.1) in the form

$$u'(t) + \frac{1}{\varepsilon}a(t)u(t) = Q(t) \quad t \in I, \quad u(0) = A, \tag{2.2.3}$$

where

$$Q(t) = \frac{1}{\varepsilon}f(t) - \frac{1}{\varepsilon}\int_0^t K(t,s)u(s)ds.$$

It is clear that (2.2.3) is a first order linear differential equation. From here, using the theory of integrating factor for linear differential equation, we obtain

$$\begin{aligned} u(t) =& u(0)\exp\left(-\frac{1}{\varepsilon}\int_0^t a(\eta)d\eta\right) + \int_0^t Q(\xi)\exp\left(-\frac{1}{\varepsilon}\int_\xi^t a(\eta)d\eta\right)d\xi \\ =& u(0)\exp\left(-\frac{1}{\varepsilon}\int_0^t a(\eta)d\eta\right) + \frac{1}{\varepsilon}\int_0^t f(\xi)\exp\left(-\frac{1}{\varepsilon}\int_\xi^t a(\eta)d\eta\right)d\xi \\ & -\frac{1}{\varepsilon}\int_0^t\left[\int_0^\xi K(\xi,s)u(s)ds\right]\exp\left(-\frac{1}{\varepsilon}\int_\xi^t a(\eta)d\eta\right)d\xi. \end{aligned}$$

From this expression we can write

$$\begin{aligned} |u(t)| \leq& |u(0)|\exp\left(-\frac{1}{\varepsilon}\int_0^t a(\eta)d\eta\right) + \frac{1}{\varepsilon}\int_0^t |f(\xi)|\exp\left(-\frac{1}{\varepsilon}\int_\xi^t p(\eta)d\eta\right)d\xi + \\ & \frac{1}{\varepsilon}\int_0^t\left[\int_0^\xi |K(\xi,s)||u(s)|ds\right]\exp\left(-\frac{1}{\varepsilon}\int_\xi^t p(\eta)d\eta\right)d\xi. \end{aligned}$$

If $\bar{K} = \max_{I\times I}|K(t,s)|$ and since $a(t) \geq \alpha$, it follows that

$$\begin{aligned} |u(t)| \leq& |A|\exp\left(\frac{-\alpha t}{\varepsilon}\right) + \frac{1}{\alpha}||f||_\infty\left(1 - \exp\left(\frac{-\alpha t}{\varepsilon}\right)\right) + \\ & \frac{1}{\varepsilon}\bar{K}\int_0^t\left[\int_0^\xi |u(s)|ds\right]\exp\left(-\frac{\alpha(t-\xi)}{\varepsilon}\right)d\xi \\ \leq& |A|\exp\left(\frac{-\alpha t}{\varepsilon}\right) + \frac{1}{\alpha}||f||_\infty\left(1 - \exp\left(\frac{-\alpha t}{\varepsilon}\right)\right) + \\ & \frac{1}{\alpha}\bar{K}\left(1 - \exp\left(\frac{-\alpha t}{\varepsilon}\right)\right)\int_0^t |u(s)|ds \\ \leq& |A| + \frac{1}{\alpha}||f||_\infty + \frac{1}{\alpha}\bar{K}\int_0^t |u(s)|ds. \end{aligned}$$

Then, applying the Gronwall's inequality to this last estimate, we obtain

$$|u(t)| \leq \left(|A| + \frac{1}{\alpha}||f||_\infty\right) \exp\left(\frac{1}{\alpha}\bar{K}t\right),$$

which proves (2.2.1).

Next, to show (2.2.2) for $k = 1$, we differentiate equation (1.3.1) to obtain

$$v'(t) + a(t)v(t) = F(t), \tag{2.2.4}$$

where

$$\begin{aligned} &u'(t) = v(t), \quad u'(0) = v(0), \quad \text{and} \\ &F(t) = f'(t) - a'(t)u(t) - K(t,t)u(t) - \int_0^t \frac{\partial}{\partial t}K(t,s)u(s)ds. \end{aligned} \tag{2.2.5}$$

Futhermore, from (1.3.1) and taking into account (1.3.2) we obtain

$$|u'(0)| \leq \frac{|f(0) - a(0)u(0)|}{\varepsilon} = \frac{|f(0) - a(0)A|}{\varepsilon} \leq \frac{C}{\varepsilon}. \tag{2.2.6}$$

It follows from (2.2.4) that

$$v(t) = v(0)\exp\left(-\frac{1}{\varepsilon}\int_0^t a(\eta)d\eta\right) + \frac{1}{\varepsilon}\int_0^t F(\xi)\exp\left(-\frac{1}{\varepsilon}\int_\xi^t a(\eta)d\eta\right)d\xi,$$

which means in view of (2.2.5) that

$$u'(t) \quad = \quad u'(0)\exp\left(-\frac{1}{\varepsilon}\int_0^t a(\eta)d\eta\right) + \frac{1}{\varepsilon}\int_0^t F(\xi)\exp\left(-\frac{1}{\varepsilon}\int_\xi^t a(\eta)d\eta\right)d\xi.$$

Next, using (2.2.6) we get

$$|u'(t)| \leq \frac{C}{\varepsilon}\exp\left(-\frac{1}{\varepsilon}\int_0^t a(\eta)d\eta\right) + \frac{1}{\varepsilon}\int_0^t |F(\xi)|\exp\left(-\frac{1}{\varepsilon}\int_\xi^t a(\eta)d\eta\right)d\xi. \tag{2.2.7}$$

Evidently, if $a, f \in C^1(I)$ and $K \in C^1(I \times I)$, then

$$\frac{1}{\varepsilon}\left|\int_0^t F(\xi)\exp\left(-\frac{1}{\varepsilon}\int_\xi^t a(\eta)d\eta\right)d\xi\right| \leq C.$$

And hence, (2.2.7) becomes

$$|u'(t)| \leq \frac{C}{\varepsilon}\exp\left(\frac{-\alpha t}{\varepsilon}\right) + C. \tag{2.2.8}$$

Thus, this completes the proof for $k = 1$.

To prove (2.2.2) for $k = 2$, we differentiate (2.2.4) to obtain

$$v''(t) + a(t)v'(t) = G(t) \tag{2.2.9}$$

where

$$u''(t) = v'(t), \quad u''(0) = v'(0), \quad \text{and}$$
$$G(t) = F'(t) - a'(t)v(t).$$

From (2.2.4) and taking into consideration (2.2.6) we obtain

$$|u''(0)| \leq \frac{|F(0) - a(0)u'(0)|}{\varepsilon} \leq \frac{C}{\varepsilon^2}. \tag{2.2.10}$$

It follows from (2.2.9) that

$$v'(t) = v'(0)\exp\left(-\frac{1}{\varepsilon}\int_0^t a(\eta)d\eta\right) + \frac{1}{\varepsilon}\int_0^t G(\xi)\exp\left(-\frac{1}{\varepsilon}\int_\xi^t a(\eta)d\eta\right)d\xi.$$

Consequently,

$$u''(t) = u''(0)\exp\left(-\frac{1}{\varepsilon}\int_0^t a(\eta)d\eta\right) + \frac{1}{\varepsilon}\int_0^t G(\xi)\exp\left(-\frac{1}{\varepsilon}\int_\xi^t a(\eta)d\eta\right)d\xi,$$

so that from (2.2.10) we have

$$|u''(t)| \leq \frac{C}{\varepsilon^2}\exp\left(-\frac{1}{\varepsilon}\int_0^t a(\eta)d\eta\right) + \frac{1}{\varepsilon}\int_0^t |G(\xi)|\exp\left(-\frac{1}{\varepsilon}\int_\xi^t a(\eta)d\eta\right)d\xi. \tag{2.2.11}$$

Obviously, if $a, f \in C^2(I)$ and $K \in C^2(I \times I)$, then

$$\frac{1}{\varepsilon}\left|\int_0^t G(\xi)\exp\left(-\frac{1}{\varepsilon}\int_\xi^t a(\eta)d\eta\right)d\xi\right| \leq C,$$

And from (2.2.11), we obtain

$$|u''(t)| \leq \frac{C}{\varepsilon^2}\exp\left(\frac{-\alpha t}{\varepsilon}\right) + C. \tag{2.2.12}$$

Thus, this completes the proof for $k = 2$. Following a similar procedure, we obtain (2.2.2) for $k = 3$. □

2.3 The numerical method

Now, we shall provide a few notations and define some finite difference operators which will be employed to discretize the continuous problem in this section and the subsequent sections. Let N be an even and positive integer. Consider the following uniform partition of the unit interval $[0,1]$: $t_0 = 0, t_i = t_0 + ih,\ h = 1/N,\ i = 1(1)N, t_N = 1$. We denote the above mesh by ω_h, with $\overline{\omega}_h = \omega_h \cup \{t = 0\}$. Notice that the above uniform partition breaks up the interval $[0,1]$ into N subintervals of equal length.

To simplify the notations, we set $g_i = g(t_i)$ for any function g while y_i denotes an approximation of u at the point t_i. Throughout the work, we use $g_{\widetilde{t},i} = (g_i - g_{i-1})/h$ and $g_{i-1/2} = g(t_i - h/2)$ for any mesh function g_i defined on $\overline{\omega}_h$.

In our estimates, we use the maximum norm defined by $||g||_\infty = \max_{[0,1]}|g(t)|$ and for any discrete function $g_{\widetilde{t},i}$, we also define the corresponding discrete norm $||g||_{\infty,\omega_h} \equiv ||g|| = \max_{1\le i\le N}|g_i|$.

2.3.1 Fitting factor and difference scheme

This section deals with the discretization of the continuous problem on the uniform mesh ω_h. To this end, a fitting factor [4] is constructed and then blended with some quadrature rules to contruct the fully fledged numerical method.

Using the exponential basis function and interpolating quadrature rules with weights and remainder terms in the integral form, Amiraliyev and Şevgin [4] designed an exponential fitted operator finite difference method to solve (1.3.1)-(1.3.2) as follows. They considered the identity

$$\chi_i^{-1}h^{-1}\int_{t_{i-1}}^{t_i} Lu\varphi_i(t)dt = \chi_i^{-1}h^{-1}\int_{t_{i-1}}^{t_i} f(t)\varphi_i(t)dt, \;\; 1 \le i \le N, \tag{2.3.1}$$

where the exponential basis function $\varphi_i(t)$ is given by

$$\varphi_i(t) = \exp\left(\frac{a_{i-\frac{1}{2}}}{\varepsilon}(t - t_i)\right), \tag{2.3.2}$$

and the coefficient function χ_i in (2.3.1) can be explicitly expressed by evaluating the exponential function $\varphi_i(t)$ over the interval $[t_i, t_{i-1}]$, that is

$$\begin{aligned}
\chi_i = h^{-1}\int_{t_{i-1}}^{t_i}\varphi_i(t) &= h^{-1}\int_{t_{i-1}}^{t_i}\exp\left(\frac{a_{i-\frac{1}{2}}}{\varepsilon}(t-t_i)\right)dt \\
&= \frac{h^{-1}\varepsilon}{a_{i-\frac{1}{2}}}\exp\left(-\frac{a_{i-\frac{1}{2}}}{\varepsilon}t_i\right)\left[\exp\left(\frac{a_{i-\frac{1}{2}}}{\varepsilon}t\right)\right]_{t_{i-1}}^{t_i} \\
&= \frac{h^{-1}\varepsilon}{a_{i-\frac{1}{2}}}\exp\left(\frac{a_{i-\frac{1}{2}}}{\varepsilon}(-t_i)\right)\left[\exp\left(\frac{a_{i-\frac{1}{2}}}{\varepsilon}t_i\right) - \exp\left(\frac{a_{i-\frac{1}{2}}}{\varepsilon}t_{i-1}\right)\right] \\
&= \frac{\varepsilon}{ha_{i-\frac{1}{2}}}\left(1 - \exp\left(\frac{a_{i-\frac{1}{2}}}{\varepsilon}(-(t_i - t_{i-1}))\right)\right) \\
&= \frac{\varepsilon}{ha_{i-\frac{1}{2}}}\left(1 - \exp\left(a_{i-\frac{1}{2}}\left(-\frac{h}{\varepsilon}\right)\right)\right).
\end{aligned}$$

It then follows that

$$h^{-1}\int_{t_{i-1}}^{t_i}\varphi_i(t)dt = \frac{1}{\rho a_{i-\frac{1}{2}}}\left(1 - \exp(-\rho a_{i-\frac{1}{2}})\right), \tag{2.3.3}$$

where $\rho = \frac{h}{\varepsilon}$. Note that the function $\varphi_i(t)$ satisfies

$$-\varepsilon\varphi_i'(t) + a_{i-\frac{1}{2}}\varphi_i(t) = 0, \;\; \varphi(t_i) = 1, \tag{2.3.4}$$

and that

$$\chi_i^{-1}h^{-1}\int_{t_{i-1}}^{t_i}\varphi_i(t)dt = 1. \tag{2.3.5}$$

Rearranging (2.3.1) leads to

$$\begin{aligned}\chi_i^{-1}h^{-1}\varepsilon\int_{t_{i-1}}^{t_i}u'(t)\varphi_i(t)dt + \chi_i^{-1}h^{-1}a_{i-\frac{1}{2}}\int_{t_{i-1}}^{t_i}u(t)\varphi_i(t)dt \\ +\chi_i^{-1}h^{-1}\int_{t_{i-1}}^{t_i}\varphi_i(t)\left(\int_0^t K(t,s)u(s)ds\right)dt = f_{i-\frac{1}{2}} - R_i^{(1)}.\end{aligned} \tag{2.3.6}$$

where

$$R_i^{(1)} = \chi_i^{-1}h^{-1}\int_{t_{i-1}}^{t_i}[a(t) - a(t_{i-\frac{1}{2}})]u(t)\varphi_i(t)dt + \chi_i^{-1}h^{-1}\int_{t_{i-1}}^{t_i}[f(t_{i-\frac{1}{2}}) - f(t)]\varphi_i(t)dt.$$

To reduce the integrals in (2.3.6), the following quadrature rules will be used [6]:

- $$\begin{aligned}\int_a^b p(t)f(t)dt =& \left[\int_a^b p(t)dt\right]\{\sigma f(b) + (1-\sigma)f(a)\} \\ &+ f(a;b)\int_a^b (t - t^{(\sigma)})p(t)dt + R(f).\end{aligned} \tag{2.3.7}$$
- $$\int_a^b p(t)f'(t)dt = f(a;b)\int_a^b p(t)dt + \widetilde{R}(f). \tag{2.3.8}$$

The truncation errors $R(f)$ and $\widetilde{R}(f)$ are given by

$$R(f) = \int_a^b dtp(t)\int_a^b f^{(n)}(\xi)K_{n-1}(t,\xi)d\xi, \; n = 1 \text{ or } 2, \tag{2.3.9}$$

and

$$\widetilde{R}(f) = -\int_a^b dtp'(t)\int_a^b f^{(n)}(\xi)K_{n-1}(t,\xi)d\xi, \; n = 1 \text{ or } 2, \tag{2.3.10}$$

with

$$\begin{aligned}t^{(\sigma)} =& \sigma b + (1-\sigma)a, \;\; f(a;b) = \frac{[f(b) - f(a)]}{b-a}, \\ T_s(\lambda) =& \frac{\lambda^s}{s!} \text{ if } \lambda > 0; \;\; T_s(\lambda) = 0, \text{ if } \lambda < 0, \\ K_s(t,\xi) =& T_s(t-\xi) - (b-a)^{-1}(t-a)(b-\xi)^s, \; s = 0 \text{ or } 1,\end{aligned}$$

and σ a real parameter. In some cases, very often the case when approximating by time, the second term in (2.3.7) is included in the remainder. Thus, employing (2.3.7) and (2.3.8) on the

interval $[t_{i-1}, t_i]$ and taking into consideration the fact that $\varphi_i(t)$ satisfies (2.3.4) we have

$$\begin{aligned}
&\chi_i^{-1}h^{-1}\varepsilon\int_{t_{i-1}}^{t_i} u'(t)\varphi_i(t)dt + \chi_i^{-1}h^{-1}a_{i-\frac{1}{2}}\int_{t_{i-1}}^{t_i} u(t)\varphi_i(t)dt \\
&+ \chi_i^{-1}h^{-1}\int_{t_{i-1}}^{t_i}\varphi_i(t)\left(\int_0^t K(t,s)u(s)ds\right)dt \\
&= \varepsilon u_{\widetilde{t},i}\chi_i^{-1}h^{-1}\int_{t_{i-1}}^{t_i}\varphi_i(t)dt + a_{i-\frac{1}{2}}\chi_i^{-1}h^{-1}\int_{t_{i-1}}^{t_i}\varphi_i(t)dt \\
&[\sigma u_i + (1-\sigma)u_{i-1}] + u_{\widetilde{t},i}\chi_i^{-1}h^{-1}a_{i-\frac{1}{2}} \times \int_{t_{i-1}}^{ti}(t-t_i^{\sigma})\varphi_i(t)dt \\
&+ \chi_i^{-1}h^{-1}\int_{t_{i-1}}^{t_i}\varphi_i(t)dt\left[\sigma\int_0^{t_i}K(t_i,s)u(s)ds + (1-\sigma)\int_0^{t_{i-1}}K(t_{i-1},s)u(s)ds\right] \\
&+ \chi_i^{-1}h^{-1}\int_{t_{i-1}}^{t_i}\varphi_i(t)dt \times \int_{t_{i-1}}^{t_i}\frac{d}{d\xi}\left[\int_0^{\xi}K(\xi,s)u(s)ds\right][H(T-\xi)-\sigma]d\xi.
\end{aligned}$$

We can write the above expression in the form.

$$\begin{aligned}
&\varepsilon u_{\widetilde{t},i}\left[\chi_i^{-1}h^{-1}\int_{t_{i-1}}^{t_i}\varphi_i(t)dt + a_{i-\frac{1}{2}}\int_{t_{i-1}}^{ti}(t-t_i^{\sigma})\varphi_i(t)dt\right] \\
&+ a_{i-\frac{1}{2}}\chi_i^{-1}h^{-1}\int_{t_{i-1}}^{t_i}\varphi_i(t)dt\,[\sigma u_i + (1-\sigma)u_{i-1}] \\
&+ \chi_i^{-1}h^{-1}\int_{t_{i-1}}^{t_i}\varphi_i(t)dt\left[\sigma\int_0^{t_i}K(t_i,s)u(s)ds + (1-\sigma)\int_0^{t_{i-1}}K(t_{i-1},s)u(s)ds\right] \\
&+ \chi_i^{-1}h^{-1}\int_{t_{i-1}}^{t_i}\varphi_i(t)dt \times \int_{t_{i-1}}^{t_i}\frac{d}{d\xi}\left[\int_0^{\xi}K(\xi,s)u(s)ds\right][H(T-\xi)-\sigma]d\xi. \\
&= \varepsilon\theta_i u_{\widetilde{t},i} + a_{i-\frac{1}{2}}u_i^{\sigma} + \left[\sigma\int_0^{t_i}K(t_i,s)u(s)ds + (1-\sigma)\int_0^{t_{i-1}}K(t_{i-1},s)u(s)ds\right] \\
&+ \int_{t_{i-1}}^{t_i}\frac{d}{d\xi}\left[\int_0^{\xi}K(\xi,s)u(s)ds\right][H(T-\xi)-\sigma]d\xi, \qquad (2.3.11)
\end{aligned}$$

where we have used (2.3.5),

$$\theta_i = 1 + \chi_i^{-1}h^{-1}a_{i-\frac{1}{2}}\varepsilon^{-1}\int_{t_{i-1}}^{t_i}(t-t_i^{\sigma})\varphi_i(t)dt, \qquad (2.3.12)$$

and

$$u_i^{\sigma} = \sigma u_i + (1-\sigma)u_{i-1}.$$

The function $H(T-\xi)$ is a Heaviside function.

Furthermore, applying also (2.3.7) for $\sigma = \frac{1}{2}$ to the following two integrals in the right hand side of the relation (2.3.11) :

$$\int_0^{t_i}K(t_i,s)u(s)ds \qquad \int_0^{t_{i-1}}K(t_{i-1},s)u(s)ds$$

we obtain

$$\int_0^{t_i} K(t_i,s)u(s)ds = \sum_{j=1}^{i} \frac{h_i}{2}\left[K(t_i,t_j)u_j + K(t_i,t_{j-1})u_{j-1}\right] + R_i^{(3)} \tag{2.3.13}$$

$$\int_0^{t_{i-1}} K(t_{i-1},s)u(s)ds = \sum_{j=1}^{i-1} \frac{h_i}{2}\left[K(t_{i-1},t_j)u_j + K(t_{i-1},t_{j-1})u_{j-1}\right] + R_i^{(4)} \tag{2.3.14}$$

$$R_i^{(3)} = \sum_{j=1}^{i} \int_{t_{j-1}}^{t_j} (t_{j-\frac{1}{2}} - \xi)\frac{d}{d\xi}[K(t_i,\xi)u(\xi)]d\xi$$

$$R_i^{(4)} = \sum_{j=1}^{i-1} \int_{t_{j-1}}^{t_j} (t_{j-\frac{1}{2}} - \xi)\frac{d}{d\xi}[K(t_{i-1},\xi)u(\xi)]d\xi$$

As a result, from (2.3.6) and (2.3.11) we obtain the expression

$$\varepsilon\theta_i u_{\widetilde{t},i} + a_{i-\frac{1}{2}}u_i^{\sigma} + \sigma\frac{h}{2}\sum_{j=1}^{i}[K(t_i,t_j)u_j + K(t_i,t_{j-1})u_{j-1}] +$$

$$(1-\sigma)\frac{h}{2}\widetilde{K}(t_0,...,t_{i-1};u_0,...,u_{i-1}) = f_{i-\frac{1}{2}} - R_i, \tag{2.3.15}$$

where

$$\widetilde{K}(t_0,...,t_{i-1};u_0,...,u_{i-1}) = \begin{cases} 0 & \text{for } i=1, \\ \sum_{j=1}^{i-1}[K^{\sigma}(t_i,t_j)u_j + K^{\sigma}(t_i,t_{j-1})u_{j-1}] & \text{for } i>2. \end{cases}$$

The remainder term is

$$R_i = \chi_i^{-1}h^{-1}\int_{t_{i-1}}^{t_i}[a(t) - a(t_{i-\frac{1}{2}})]u(t)\varphi_i(t)dt + \chi_i^{-1}h^{-1}\int_{t_{i-1}}^{t_i}[f(t_{i-\frac{1}{2}}) - f(t)]\varphi_i(t)dt$$
$$+ \int_{t_{i-1}}^{t_i}\frac{d}{d\xi}\left[\int_0^{\xi}K(\xi,s)u(s)ds\right][H(T-\xi)-\sigma]d\xi$$
$$+ \sum_{j=1}^{i}\int_{t_{j-1}}^{t_j}(t_{j-\frac{1}{2}} - \xi)\frac{d}{d\xi}[K(t_i,\xi)u(\xi)]d\xi + \widetilde{w_i}, \tag{2.3.16}$$

where

$$\widetilde{w_i} = \begin{cases} 0 & \text{for } i=1, \\ \sum_{j=1}^{i-1}\int_{t_{j-1}}^{t_j}(t_{j-\frac{1}{2}} - \xi)\frac{d}{d\xi}[K(t_{i-1},\xi)u(\xi)]d\xi & \text{for } i>2, \end{cases}$$

and

$$K^{\sigma}(t_i,.) = \sigma K(t_i,.) + (1-\sigma)K(t_{i-1},.). \tag{2.3.17}$$

Simplifying (2.3.12) yields

$$\theta_i = \frac{\rho a_{i-\frac{1}{2}}[(1-\sigma) + \sigma\exp(-\rho a_{i-\frac{1}{2}})]}{1-\exp(-\rho a_{i-\frac{1}{2}})},$$

which we refer to as the fitting factor. Neglecting the remainder term R_i in (2.3.15) we obtain the following scheme to approximate the solution of the problem (1.3.1)-(1.3.2):

$$L^h y_i \equiv \varepsilon\theta_i y_{\widetilde{t},i} + a_{i-\frac{1}{2}} y_i^{\sigma} + \frac{\sigma h}{2}\left[K(t_i,t_i)y_i + K(t_i,t_{i-1})y_{i-1}\right] + \frac{h}{2}\widetilde{K}(t_0,...,t_{i-1};y_0,...,y_{i-1}),$$
$$= f_{i-\frac{1}{2}}, \quad i = 1(1)N, \tag{2.3.18}$$
$$y(0) = y_0, \tag{2.3.19}$$

where

$$\widetilde{K}(t_0,...,t_{i-1};y_0,...,y_{i-1}) = \begin{cases} 0 & \text{for } i = 1, \\ \sum_{j=1}^{i-1}[K^{\sigma}(t_i,t_j)y_j + K^{\sigma}(t_i,t_{j-1})y_{j-1}] & \text{for } i > 2. \end{cases}$$

In matrix notation, the scheme in (2.3.18) is a lower triangular linear system

$$W\widetilde{Y} = \widetilde{F},$$

where W is the matrix of the system and F the unknown column vector. The different entries of the matrix W and components of the column vector $\widetilde{F}$ are given by

$$W_{11} = \tfrac{\varepsilon\theta_1}{h} + \tfrac{\sigma}{2}(a_0 + a_1) + \tfrac{h\sigma}{2}K_{11}, \quad i = 1,$$
$$W_{ii} = r_i^c, \quad i = 2(1)N,$$
$$W_{i,i-1} = r_{1i,i-1}^-, \quad i = 2(1)N,$$
$$W_{i,j} = r_{2i,i-1}^-, \quad i = 3(1)N; j = 1(1)i-2,$$
$$F_1 = \tfrac{1}{2}(f_0 + f_1) - (\tfrac{-\varepsilon\theta_1}{h} + \tfrac{1}{2}(1-\sigma)(aa_1 + a_1) + \tfrac{h\sigma}{2}K_{11})U_0, \quad i = 1,$$
$$F_i = \tfrac{1}{2}(f_{i-1} + f_i) - (\tfrac{h}{2}(\sigma K_{i,0} + (1-\sigma)K_{i-1,0}))U_0, \quad i = 2(1)N.$$

where

$$r_i^c = \tfrac{\varepsilon\theta_i}{h} + \tfrac{\sigma}{2}(a_i + a_{i-1}) + \tfrac{h\sigma}{2}K_{ii},$$
$$r_{i,i-1}^- = \tfrac{-\varepsilon\theta_i}{h} + \tfrac{(1-\sigma)}{2}(a_i + a_{i-1}) + \tfrac{h\sigma}{2}K_{i,i-1} + \tfrac{1}{2}h(\sigma K_{i,i-1} +$$
$$\tfrac{h}{2}(\sigma K_{i,i-1} + (1-\sigma)K_{i-1,i-1}),$$
$$r_{i,i-1}^- = h(\sigma K_{i,j} + (1-\sigma)K_{i-1,j}).$$

2.3.2 Some useful features of the scheme

In this section, we provide statements and proofs of lemmas which are required in the analysis of the numerical method presented above.

Lemma 2.3.1. *Consider the following difference operator*

$$ly_i \equiv A_i y_i - B_i y_{i-1}, \quad 1 \le i \le N, \tag{2.3.20}$$

where

$$A_i = \frac{\varepsilon\theta_i}{h} + a_{i-\frac{1}{2}}\sigma + \frac{\sigma h K(t_i, t_i)}{2}, \quad B_i = \frac{\varepsilon\theta_i}{h} - a_{i-\frac{1}{2}}(1-\sigma). \tag{2.3.21}$$

(I) The difference operator (2.3.20) satisfies the discrete maximum principle: If the operator $ly_i \geq 0, \quad i \geq 1$, *and* $y_0 \geq 0$, *then* $y_i \geq 0$, $i \geq 0$.

(II) The solution of the difference initial value problem

$$ly_i = F_i, \quad i \geq 1,$$
$$y_0 = \mu$$

satisfies the inequality

$$||y_i||_\infty \leq |\mu| + \alpha^{-1} \max_{0\leq i\leq N} |F_i|. \tag{2.3.22}$$

(III) If $F_i \geq 0$ *is nondecreasing and* $A_i - B_i \geq \alpha > 0$, *then*

$$|y_i| \leq |\mu| + \alpha^{-1} F_i, \quad i \geq 1. \tag{2.3.23}$$

Proof.

(I) Let j be such that $\Psi_j = \min_{0\leq i\leq N} \Psi_i$ and assume that $\Psi_j < 0$. Then it is clear that $\Psi_j \leq \Psi_{j-1}$. It follows that

$$\begin{aligned} l\Psi_j &= A_j\Psi_j - B_j\Psi_{j-1} \\ &= A_j\Psi_j - B_j\Psi_j + B_j\Psi_j - B_j\Psi_{j-1} \\ &= (A_j - B_j)\Psi_j + B_j(\Psi_j - \Psi_{j-1}) < 0. \end{aligned}$$

Which contradicts our assumptions. Therefore $\Psi_j \geq 0$. Thus $\Psi_i \geq 0$, $i = 0(1)N$.

(II) Consider two mesh functions which we define by

$$\Psi_i = |\mu| + \frac{1}{\alpha} \max_{0\leq i\leq N} |F_i| \pm y_i. \tag{2.3.24}$$

It is clear that for $i = 0$

$$\begin{aligned} \Psi_0 &= |\mu| + \frac{1}{\alpha} \max_{0\leq i\leq N} |F_0| \pm y_0 \\ &\geq 0, \end{aligned}$$

and that for $i \geq 1$

$$\begin{aligned}
l\Psi_i &= A_i\Big[|\mu| + \frac{1}{\alpha}\max_{0\leq i\leq N}|F_i| \pm y_i\Big] - B_i\Big[|\mu| + \frac{1}{\alpha}\max_{0\leq i\leq N}|F_{i-1}| \pm y_{i-1}\Big] \\
&= (A_i - B_i)|\mu| + \frac{1}{\alpha}\Big[A_i \max_{1\leq i\leq N}|F_i| - B_i \max_{1\leq i\leq N}|F_{i-1}|\Big] + A_i(\pm y_i) - B_i(\pm y_{i-1}) \\
&= (A_i - B_i)|\mu| + \frac{1}{\alpha}\Big[A_i \max_{1\leq i\leq N}|F_i| - B_i \max_{1\leq i\leq N}|F_{i-1}|\Big] \pm (A_i y_i) - B_i y_{i-1}) \\
&= (A_i - B_i)|\mu| + \frac{1}{\alpha}\Big[A_i \max_{1\leq i\leq N}|F_i| - B_i \max_{1\leq i\leq N}|F_{i-1}|\Big] \pm l y_i \\
&= (A_i - B_i)|\mu| + \frac{1}{\alpha}\Big[A_i \max_{1\leq i\leq N}|F_i| - B_i \max_{1\leq i\leq N}|F_{i-1}|\Big] \pm F_i \\
&\geq (A_i - B_i)|\mu| + \frac{1}{\alpha}\Big[A_i \max_{1\leq i\leq N}|F_i| - B_i \max_{1\leq i\leq N}|F_i|\Big] \pm F_i \\
&\geq (A_i - B_i)|\mu| + \frac{A_i - B_i}{\alpha}\max_{1\leq i\leq N}|F_i| \pm F_i.
\end{aligned}$$

Since $(A_i - B_i)/\alpha \geq 1$, we have.

$$l\Psi_i \geq 0.$$

Employing the discrete maximum principle (part I) of this Lemma yields $\Psi_i \geq 0$ and so

$$||y_i||_\infty \leq |\mu| + \frac{1}{\alpha}\max_{0\leq i\leq N}|F_i|, \tag{2.3.25}$$

as required.

(III) Likewise, consider the two mesh functions,

$$\Psi_i = |\mu| + \frac{1}{\alpha}F_i \pm y_i.$$

It can be easily seen that for $i = 0$, $\Psi_0 \geq 0$ and that for $i \geq 1$ we have

$$\begin{aligned}
l\Psi_i &= A_i\big[|\mu| + \frac{1}{\alpha}|F_i| \pm y_i\big] - B_i[|\mu| + \frac{1}{\alpha}|F_{i-1}| \pm y_{i-1}|] \\
&= (A_i - B_i)|\mu| + \frac{1}{\alpha}[A_i|F_i| - B_i|F_{i-1}|] + A_i(\pm y_i) - B_i(\pm y_{i-1}) \\
&= (A_i - B_i)|\mu| + \frac{1}{\alpha}[A_i|F_i| - B_i|F_{i-1}|] \pm (A_i y_i - B_i y_{i-1}) \\
&= (A_i - B_i)|\mu| + \frac{1}{\alpha}[A_i|F_i| - B_i|F_{i-1}|] \pm l y_i \\
&= (A_i - B_i)|\mu| + \frac{1}{\alpha}[A_i|F_i| - B_i|F_{i-1}|] \pm F_i,
\end{aligned}$$

Since F_i is nondecreasing, we have

$$\begin{aligned}
l\Psi_i &\geq (A_i - B_i)|\mu| + \frac{1}{\alpha}[A_i|F_i| - B_i|F_i|] \pm F_i \\
&\geq (A_i - B_i)|\mu| + \frac{A_i - B_i}{\alpha}|F_i| \pm F_i. \\
&\geq 0.
\end{aligned}$$

In virtue of the discrete maximum principle (part I) of this Lemma, we conclude that $\Psi_i \geq 0$, thus

$$|y_i| \leq |\mu| + \frac{1}{\alpha} F_i.$$

□

The uniqueness of the solution is guaranteed by the discrete maximum principle. The existence follows easily since, for linear problems, the existence of the solution is implied by its uniqueness.

Lemma 2.3.2. *Under the condition*

$$\alpha + \frac{\sigma k h}{2} \geq \alpha_* > 0 \tag{2.3.26}$$

for the difference operator

$$l^h v_i := \varepsilon \theta_i v_{\overline{t},i} + a_{i-\frac{1}{2}} v_i^{\sigma} + \frac{\sigma h}{2} K_{ii} v_i \tag{2.3.27}$$

we have

$$||v||_{\infty} \leq |v_0| + \frac{1}{\alpha_*} \max_{1 \leq i \leq N} |l v_i|, \tag{2.3.28}$$

where

$$k = \begin{cases} K_*, \sigma > 0 \\ K_*, \sigma < 0, \ K_* \leq K_{ii} \leq K^* \text{and } K_{ii} = K(t_i, t_i). \end{cases}$$

Proof. The difference expression (2.3.27) can be rewritten as

$$l y_i \equiv A_i y_i - B_i y_{i-1},$$

where A and B are given by (2.3.21). From here, it is clear that

$$A_i > a_{i-\frac{1}{2}} + \frac{\sigma h K(t_i, t_i)}{2} > 0 \ \text{ and } \quad B_i = \frac{a_{i-\frac{1}{2}} \exp(-\rho a_{i-\frac{1}{2}})}{1 - \exp(-\rho a_{i-\frac{1}{2}})} > 0,$$

since from (2.3.26),

$$A_i - B_i \ = a_{i-\frac{1}{2}} + \tfrac{\sigma h K(t_i, t_i)}{2} > 0. \tag{2.3.29}$$

Therefore, (2.3.28) is direct consequence of (2.3.22). □

The next lemma shows the stability of the discrete problem (2.3.18)-(2.3.19).

Lemma 2.3.3. *Let the difference operator $l^h y_i$ be defined by (2.3.27). Then for discrete problem (2.3.18)-(2.3.19), we have*

$$|l^h y_i| \le Ch \sum_{j=1}^{i} |y_{j-1}| + ||f||_\infty, \quad 1 \le i \le N. \tag{2.3.30}$$

Proof. Using (2.3.17), we rewrite (2.3.18) as

$$\begin{aligned}
|l^h y_i| &\le \left|f_{i-\frac{1}{2}}\right| + \left|\frac{\sigma h}{2}\sum_{j=1}^{i-1} K(t_i,t_j)y_j\right| + \left|\frac{h\sigma}{2}K(t_i,t_{i-1})y_{i-1}\right| + \left|\frac{h\sigma}{2}\sum_{j=1}^{i-1} K(t_i,t_{j-1})y_{j-1}\right| \\
&\quad + \left|\frac{h(1-\sigma)}{2}\sum_{j=1}^{i-1}[K(t_{i-1},t_j)y_j + K(t_{i-1},t_{j-1})y_{j-1}]\right| \\
&\le \left|f_{i-\frac{1}{2}}\right| + \left|\frac{\sigma h}{2}\sum_{j=1}^{i-1} K(t_i,t_j)y_j\right| + \left|\frac{h\sigma}{2}\sum_{j=1}^{i} K(t_i,t_{j-1})y_{j-1}\right| \\
&\quad + \left|\frac{h(1-\sigma)}{2}\sum_{j=1}^{i-1}[K(t_{i-1},t_j)y_j + K(t_{i-1},t_{j-1})y_{j-1}]\right|
\end{aligned}$$

From here, taking into account the fact that the kernel is bounded, we obtain

$$\begin{aligned}
l^h y_i \le& ||f|| + Ch\sum_{j=1}^{i}|y_{j-1}| + Ch\sum_{j=1}^{i-1}|y_j| + Ch\sum_{j=1}^{i-1}|y_{j-1}| \\
\le& Ch\sum_{j=1}^{i}|y_{j-1}| + |f|_\infty.
\end{aligned}$$

This ends the proof. □

Lemma 2.3.4. *Under the condition (2.3.26) for the solution of the difference scheme (2.3.18)-(2.3.19) we have*

$$|y_i| \le (\alpha_*^{-1}||f||_\infty + |A|)\exp(\alpha_*^{-1}Ct_i), \quad 1 \le i \le N. \tag{2.3.31}$$

Proof. Let

$$v_i = \begin{cases} h\sum_{j=1}^{i}|y_{j-1}|, & i > 0, \\ 0, & i = 0, \end{cases}$$

where

$$v_{\widetilde{t},i} = |y_{i-1}|.$$

It follows from inequality (2.3.30) that

$$l^h y_i \leq Cv_i + ||f||_\infty,$$
$$y_0 = A.$$

By the discrete maximum principle we have

$$|y_i| \leq w_i,$$

where w_i is the solution of the problem

$$l^h w_i \leq Cv_i + ||f||_\infty,$$
$$w_0 = |A|.$$

From here, in view of (2.3.22) we have

$$|y_i| \leq w_i \leq \alpha_*^{-1}(Cv_i + ||f||_\infty) + |A| \tag{2.3.32}$$

as a result

$$v_{\widetilde{t},i} = |y_{i-1}| \leq \alpha_*^{-1}(Cv_{i-1} + ||f||_\infty) + |A|.$$

Then applying the difference analogue of the differential inequality gives

$$w_i \leq \alpha_*^{-1}(||f||_\infty + |A|)\alpha_* C^{-1}(\exp(\alpha_*^{-1} Ct_i - 1)),$$

which together with (2.3.32) proves (2.3.31). □

2.4 Uniform error estimate

In this section, we carry out the convergence analysis of the method presented in section (2.3). To this end, we use the following error function $z_i = y_i - u_i$, where y_i is the solution of the difference problem (2.3.18)-(2.3.19) and u_i the solution of the continuous problem (1.3.1)-(1.3.2) at the mesh point t_i. Note that the error function z_i, $i = 0(1)N$, satisfies the discrete problem

$$\begin{aligned} l^h z_i \equiv & \varepsilon\theta_i z_{\widetilde{t},i} + [a_{i-\frac{1}{2}} y_i^\sigma - a_{i-\frac{1}{2}} u_i^\sigma] + \frac{\sigma h}{2}[K(t_i,t_i)y_i - K(t_i,t_i)u_i] + \\ & \frac{\sigma h}{2}[K(t_i,t_{i-1})y_{i-1} - K(t_i,t_{i-1})u_{i-1}] + \widetilde{K} = R_i, \quad i = 1(1)N \end{aligned} \tag{2.4.1}$$

$$z_0 = 0, \tag{2.4.2}$$

where R_i is given by (2.3.16) and

$$\widetilde{K} = \begin{cases} 0 & i = 1, \\ \frac{h}{2}\sum_{j=1}^{i-1}\{[K^\sigma(t_i,t_j)y_j - K^\sigma(t_i,t_j)u_j] + [K^\sigma(t_i,t_{j-1})y_{j-1} - K^\sigma(t_i,t_{j-1})u_{j-1}]\} & i > 2. \end{cases}$$

The next Lemma gives the main estimates of the truncation error for the method (2.3.18)-(2.3.19).

Lemma 2.4.1. *Let $a, f \in C^1(I)$, $K \in C_1^1(I\times I)$. Then for the remainder term R_i of the scheme (2.3.18)-(2.3.19), we have*

$$||R_i||_{\infty,\omega_h} \leq Ch. \tag{2.4.3}$$

Proof. The remainder term (2.3.16) of the scheme (2.3.18) can be rewritten as

$$R_i = R_i^{(1)} + R_i^{(2)} + R_i^{(3)} + R_i^{(4)},$$

where

$$R_i^{(1)} = \chi_i^{-1}h^{-1}\int_{t_{i-1}}^{t_i}[a(t) - a(t_{i-\frac{1}{2}})]u(t)\varphi_i(t)dt + \chi_i^{-1}h^{-1}\int_{t_{i-1}}^{t_i}[f(t_{i-\frac{1}{2}}) - f(t)]\varphi_i(t)dt, \tag{2.4.4}$$

$$R_i^{(2)} = \int_{t_{i-1}}^{t_i}\left[\frac{d}{d\xi}\int_0^\xi K(\xi,s)u(s)ds\right][H(t-\xi)-\sigma]d\xi, \tag{2.4.5}$$

$$R_i^{(3)} = \sum_{j=1}^{i}\int_{t_{j-1}}^{t_j}(t_{j-\frac{1}{2}} - \xi)\frac{d}{d\xi}\left[K(t_i,\xi)u(\xi)\right]d\xi, \tag{2.4.6}$$

$$R_i^{(4)} = \begin{cases} 0 & \text{for } i = 1, \\ \sum_{j=1}^{i-1}\int_{t_{j-1}}^{t_j}(t_{j-\frac{1}{2}} - \xi)\frac{d}{d\xi}[K(t_{i-1},\xi)u(\xi)]d\xi & \text{for } i > 1. \end{cases} \tag{2.4.7}$$

We first prove that for (2.4.4) the estimate

$$|R_i^{(1)}| \leq Ch, \quad 1 \leq i \leq N, \tag{2.4.8}$$

holds true. We rewrite (2.4.4) as

$$\begin{aligned} |R_i^{(1)}| &= \left|\chi_i^{-1}h^{-1}\int_{t_{i-1}}^{t_i}\Big[a(t) - a(t_{i-\frac{1}{2}})\Big]u(t)\varphi_i(t)dt + \chi_i^{-1}h^{-1}\int_{t_{i-1}}^{t_i}\Big[f(t_{i-\frac{1}{2}}) - f(t)\Big]\varphi_i(t)dt\right| \\ &\leq \chi_i^{-1}h^{-1}\int_{t_{i-1}}^{t_i}\left|\Big[a(t) - a(t_{i-\frac{1}{2}})\Big]u(t)\varphi_i(t)\right|dt + \chi_i^{-1}h^{-1}\int_{t_{i-1}}^{t_i}\left|\Big[f(t_{i-\frac{1}{2}}) - f(t)\Big]\varphi_i(t)\right|dt. \end{aligned}$$

Using the intermediate value theorem we obtain

$$\begin{aligned} |a(t) - a(t_{i-1/2})| &= |a'(\vartheta_i)||t - t_{i-\frac{1}{2}}| \leq C_1h, \quad \vartheta_i \in (t_{i-\frac{1}{2}}, t), \\ |f(t_{i-1/2}) - f(t)| &= |f'(\upsilon_i)||t_{i-\frac{1}{2}} - t| \leq C_2h, \quad \upsilon_i \in (t, t_{i-\frac{1}{2}}). \end{aligned}$$

Thus, it is clear that (2.4.8) is true.

For $R_i^{(2)}$ we have,

$$|R^{(2)}| \leq \int_{t_{i-1}}^{t_i} \Big| \Big[\frac{d}{d\xi}\int_0^{\xi} K(\xi,s)u(s)ds\Big][H(t-\xi)-\sigma]\Big| d\xi,$$

and after applying Leibnitz rule we get

$$\begin{aligned}|R^{(2)}| \leq & \max(|\sigma|,|1-\sigma)|)\Big\{\int_{t_{i-1}}^{t_i}|K(\xi,\xi)|\,|u(\xi)|\,d\xi + \int_{t_{i-1}}^{t_i}\Big|\int_0^{\xi}\frac{\partial}{\partial_\xi}K(\xi,s)u(s)ds\Big|\,d\xi\Big\}\\ \leq & \max(|\sigma|,|1-\sigma)|)\left\{\int_{t_{i-1}}^{t_i}\bar{K}|u(\xi)|d\xi + \int_{t_{i-1}}^{t_i}\Big|\int_0^{\xi}\bar{K}u(s)ds\Big|\,d\xi\right\}.\end{aligned}$$

Hence, using (2.2.1) we get

$$|R_i^{(2)}| \leq \quad Ch. \tag{2.4.9}$$

Next, for $R_i^{(3)}$ we have

$$\begin{aligned}|R_i^{(3)}| &= \left|\sum_{j=1}^{i}\int_{t_{j-1}}^{t_j}(t_{j-\frac{1}{2}}-\xi)\frac{\partial}{\partial_\xi}K(t_i,\xi)u(\xi)d\xi + \sum_{j=1}^{i}\int_{t_{j-1}}^{t_j}(t_{j-\frac{1}{2}}-\xi)K(t_i,\xi)u'(\xi)d\xi\right|\\ &\leq \left|\sum_{j=1}^{i}\int_{t_{j-1}}^{t_j}(t_{j-\frac{1}{2}}-\xi)\frac{\partial}{\partial_\xi}K(t_i,\xi)u(\xi)d\xi\right| + \left|\sum_{j=1}^{i}\int_{t_{j-1}}^{t_j}(t_{j-\frac{1}{2}}-\xi)K(t_i,\xi)u'(\xi)d\xi\right|\\ &\leq \left|\sum_{j=1}^{i}\int_{t_{j-1}}^{t_j}(t_{j-\frac{1}{2}}-\xi)\bar{K}u(\xi)d\xi\right| + \left|\sum_{j=1}^{i}\int_{t_{j-1}}^{t_j}(t_{j-\frac{1}{2}}-\xi)\bar{K}u'(\xi)d\xi\right|\\ &\leq Ch\left(\int_0^{t_i}|u(\xi)|dt + \int_0^{t_i}|u'(\xi)|dt\right)\end{aligned} \tag{2.4.10}$$

Since, by (2.2.2) for $k=1$,

$$\int_0^{t_i}|u'(t)|dt \leq C,$$

It follows from (2.4.10) that

$$|R_i^{(3)}| \leq Ch. \tag{2.4.11}$$

Analogous to the proof for $R_i^{(3)}$, we have for (2.4.7),

$$|R_i^{(4)}| \quad \leq \quad Ch. \tag{2.4.12}$$

Finally, the inequalities (2.4.8),(2.4.9),(2.4.11) and (2.4.12) imply the assertion of the lemma. □

Lemma 2.4.2. *Under condition of (2.3.26), the solution z_i of problem (2.4.1)-(2.4.2) satisfies*

$$||z||_{\infty,\omega_h} \leq \max_{1\leq i\leq N}|R_i| \tag{2.4.13}$$

Proof. The proof follows directly from (2.3.31) by setting $f = R$ and $A = 0$. □

Combining the estimates in the two previous lemmas leads to the following theorem

Theorem 2.4.1. *Suppose that the conditions of Lemma 2.4.1 are satisfied. Then the difference scheme (2.3.18)-(2.3.19) applied to the continuous problem (1.3.1)-(1.3.2) on uniform mesh is first order ε-uniformly convergent in the discrete maximum norm, i.e.,*

$$||y - u||_{\infty,\omega_h} \leq Ch.$$

2.5 Numerical results

To illustrate the numerical method described in this chapter, we solve two Volterra integro-differential equations. The numerical results are presented in tabular form. In each table, we present the maximum pointwise errors for various values of ε and N along with the corresponding computational rates of convergence.

Example 2.5.1. [63] *Consider Problem (1.3.1)-(1.3.2) where the coefficient functions are given by*

$$\begin{aligned} &a(t) = t + 1, \quad K(t,s) = t + s, \\ &f(t) = \varepsilon \cos t + t \sin t + 2 \sin t + (t - 2t\varepsilon + \varepsilon^2) \exp(-t/\varepsilon) + t - 2t \cos t + \varepsilon t - \varepsilon^2, \\ &u(0) = 1. \end{aligned}$$

The exact solution to this problem is given by

$$u(t) = \sin t + \exp(-t/\varepsilon).$$

Example 2.5.2. [4] *Consider Problem (1.3.1)-(1.3.2) where the coefficient functions are given by*

$$\begin{aligned} &a(t) = 1, \quad K(t,s) = s, \\ &f(t) = (2 + 9\varepsilon + \varepsilon t + 11t + t^2) \exp(-t) - 10(\varepsilon t + \varepsilon^2) \exp(-t/\varepsilon) + 5t^2 + 10\varepsilon^2 - 2, \\ &u(0) = 10. \end{aligned}$$

The exact solution to this problem is given by

$$u(t) = 10 - (10 + t) \exp(-t) + 10 \exp(-t/\varepsilon).$$

Since the exact solutions are available for the two test examples, the maximum errors at all the mesh points are computed using the formula

$$e_{\varepsilon,N} := \max_{[0\leq j\leq 1]} |u_j - y_j| \tag{2.5.1}$$

for all the values of N. The numerical rates of convergence are calculated using the formula

$$r_{\varepsilon,k} := \log 2 \left(\frac{e_{N_{k,\varepsilon}}}{e_{2N_{k,\varepsilon}}} \right), k = 1, 2, 3, ... \tag{2.5.2}$$

To evaluate the uniform maximum errors we use the formula

$$E_N := \max_{0<\varepsilon\leq 1} |e_{\varepsilon,k}| \tag{2.5.3}$$

with the corresponding ε-uniform rates of convergence obtained using

$$r_N := \log 2 \left(\frac{E_{N_{k,\varepsilon}}}{E_{2N_{k,\varepsilon}}} \right), k = 1, 2, 3, ... \tag{2.5.4}$$

Table 2.1: Results for Example 2.5.1: Maximum errors and maximum rates of convergence obtained via EFOFDM (2.3.18)-(2.3.19) for $\sigma = 0.5$

ε	n=40	n=80	n=160	n=320	n=640	n=1280	n=2560
10^{-2}	2.52E-02	1.22E-02	5.64E-03	2.36E-03	8.21E-04	2.81E-04	7.02E-05
	1.26	1.52	1.55	2.00	1.97	1.85	
10^{-3}	2.61E-02	1.30E-02	6.49E-03	3.20E-03	1.55E-03	7.30E-04	3.18E-04
	1.02	1.04	1.09	1.20	1.44	1.52	
10^{-4}	2.61E-02	1.31E-02	6.58E-03	3.29E-03	1.64E-03	8.15E-04	4.03E-04
	1.00	1.00	1.00	1.00	1.00	1.00	
10^{-5}	2.62E-02	1.31E-02	6.58E-03	3.30E-03	1.65E-03	8.24E-04	4.12E-04
	1.00	1.00	1.00	1.00	1.00	1.00	
10^{-6}	2.62E-02	1.31E-02	6.59E-03	3.30E-03	1.65E-03	8.25E-04	4.12E-04
	1.00	1.00	1.00	1.00	1.00	1.00	
⋮	⋮	⋮	⋮	⋮	⋮	⋮	⋮
E_N	2.62E-02	1.31E-02	6.59E-03	3.30E-03	1.65E-03	8.25E-04	4.12E-04
r_N	1.00	1.00	1.00	1.00	1.00	1.00	

Table 2.2: Results for Example 2.5.1: Maximum errors and maximum rates of convergence obtained via EFOFDM (2.3.18)-(2.3.19) for $\sigma = 1$

ε	$N = 40$	$N = 80$	$N = 160$	$N = 320$	$N = 640$	$N = 1280$	$N = 2560$
10^{-2}	2.75E-02	1.24E-02	5.64E-03	2.64E-03	1.28E-03	6.64-04	3.33E-04
	1.26	1.52	1.55	2.00	1.97	1.85	
10^{-3}	3.21E-02	1.58-02	7.64E-03	3.57-03	1.61E-03	7.23E-04	3.34E-04
	1.02	1.04	1.09	1.20	1.44	1.52	
10^{-4}	3.26E-02	1.63E-02	8.16E-03	4.05E-03	2.00E-03	9.70E-04	4.95E-04
	1.00	1.00	1.00	1.00	1.00	1.00	
10^{-5}	3.27E-02	1.64E-02	8.21E-03	4.11E-03	2.05E-03	1.02E-03	5.09E-04
	1.00	1.00	1.00	1.00	1.00	1.00	
10^{-6}	3.27E-02	1.64E-03	8.21E-03	4.11E-03	2.06E-03	1.03E-03	5.57E-04
	1.00	1.00	1.00	1.00	1.00	1.00	
$\vdots$	$\vdots$	$\vdots$	$\vdots$	$\vdots$	$\vdots$	$\vdots$	$\vdots$
E_N	3.27E-02	1.64E-03	8.21E-03	4.11E-03	2.06E-03	1.03E-03	5.57E-04
r_N	1.00	1.00	1.00	1.00	1.00	1.00	

The maximum errors E_N and the corresponding rates of convergence r_N computed for the numerical solution y are given in tables (2.1)-(2.4) for Examples (2.5.1) and (2.5.2). A careful look at these tables show that the rates of convergence are monotonically growing towards one which simply means that the method is convergent of order one and that the numerical results are in good agreement with theoretical results as summarized in theorem 2.4.1.

2.6 Conclusion

We have investigated a numerical method for solving singularly perturbed Volterra integro-differential equations whose solution displays one boundary layer. To construct the difference scheme, a fitting factor was developed via the method of integral identities and exponential basis function along with some interpolating quadrature rules with weights and remainder terms in the integral form. We analyzed the method for stability and convergence and found it to be convergent of order one in the maximum norm. Robustness behaviour have been displayed both theoretical and numerical. The computations carried out on two test examples for $\sigma = 1$ and

Table 2.3: Results for Example 2.5.2: Maximum errors and maximum rates of convergence obtained via EFOFDM (2.3.18)-(2.3.19) for $\sigma = 0.5$

ε	$N = 40$	$N = 80$	$N = 160$	$N = 320$	$N = 640$	$N = 1280$	$N = 2560$
10^{-2}	1.02E-01	4.71E-02	2.47E-02	1.30E-02	6.81E-03	3.49E-03	1.77E-03
	0.93	0.92	0.94	0.96	0.98	0.99	
10^{-3}	1.10E-01	5.50E-02	2.71E-02	1.31E-02	6.13E-03	3.07E-03	1.61E-03
	1.02	1.05	1.10	1.00	0.93	0.93	
10^{-4}	1.11E-01	5.59E-02	2.80E-02	1.40E-02	6.94E-03	3.42E-03	1.67E-03
	1.00	1.00	1.01	1.02	1.04	1.08	
10^{-5}	1.11E-01	5.59E-02	2.80E-02	1.40E-02	7.03E-03	3.51E-03	1.76E-03
	1.00	1.00	1.00	1.00	1.00	1.00	
10^{-6}	1.11E-01	5.59E-02	2.80E-02	1.40E-02	7.03E-03	3.51E03	1.76E-03
	1.00	1.00	1.00	1.00	1.00	1.00	
$\vdots$	$\vdots$	$\vdots$	$\vdots$	$\vdots$	$\vdots$	$\vdots$	$\vdots$
E_N	1.11E-01	5.59E-02	2.80E-02	1.40E-02	7.03E-03	3.51E-03	1.76E-03
r_N	1.00	1.00	1.00	1.00	1.00	1.00	

$\sigma = 0.5$ confirm the analytically findings given in Theorem 2.4.1.

In the next chapter, we discretize (1.3.1)-(1.3.2) on a piecewise-uniform mesh using the midpoint difference operator along with the trapezoidal integration.

Table 2.4: Results for Example 2.5.2: Maximum errors and maximum rates of convergence obtained via EFOFDM (2.3.18)-(2.3.19) for $\sigma = 1$

ε	$N = 40$	$N = 80$	$N = 160$	$N = 320$	$N = 640$	$N = 1280$	$N = 2560$
10^{-2}	1.02E-01	4.74E-02	2.48E-02	1.31E-02	6.82E-03	3.49E-03	1.77E-03
	0.94	0.92	0.94	0.96	0.98	0.99	
10^{-3}	1.10E-01	5.50E-02	2.71E-02	1.31E-02	6.13E-03	3.08E-03	1.61E-03
	1.02	1.05	1.10	0.99	0.93	0.93	
10^{-4}	1.11E-01	5.58E-02	2.80E-02	1.40E-02	6.94E-03	3.42E-03	1.67E-03
	1.00	1.00	1.01	1.02	1.04	1.08	
10^{-5}	1.11E-01	5.59E-02	2.80E-02	1.40E-02	7.02E-03	3.51E-03	1.75E-03
	1.00	1.00	1.00	1.00	1.00	1.00	
10^{-6}	1.11E-01	5.59E-02	2.80E-02	1.40E-02	7.03E-03	3.51E-03	1.76E-03
	1.00	1.00	1.00	1.00	1.00	1.00	
$\vdots$	$\vdots$	$\vdots$	$\vdots$	$\vdots$	$\vdots$	$\vdots$	$\vdots$
E_N	1.11E-01	5.59E-02	2.80E-02	1.40E-02	7.03E-03	3.51E-03	1.76E-03
r_N	1.00	1.00	1.00	1.00	1.00	1.00	

Chapter 3

A Fitted Mesh Finite Difference Method for SPVIDEs based on Midpoint and Trapezoidal rules

In chapter 1, we discussed Fitted Mesh Finite Difference Methods (FMFDMs). We also surveyed works showing how FMFDMs have been widely employed to various classes of singularly perturbed differential equations. We noticed that only few researchers have engaged with this approach for the case of singularly perturbed Volterra integro-differential equations. In this chapter, we follow Zhongdi and Lifeng [63] to show how this approach can be used efficiently to approximate the solution of problem (1.3.1)-(1.3.2).

We start by presenting the FMFDM followed by its convergence analysis. We then present some computational results to attest the robustness of the scheme.

3.1 Difference scheme and mesh

In this section, we introduce a FMFDM for our model problem. Note that the piecewise-uniform mesh constructed here is based on the bounds of the exact solution and its derivatives. Thus, let N be a positive even integer and $\lambda \in (0,1)$. We divide the unit interval $[0,1]$ into subintervals $[0,\lambda]$ and $[\lambda,1]$. Each of these two subintervals is divided into a uniform mesh of $N/2$ mesh elements. Clearly, the mesh is uniform with N mesh subintervals if $\lambda = 1/2$. The value of λ is

$$\lambda = \min\left\{\frac{1}{2}, 2\varepsilon\alpha^{-1}\ln N\right\}. \tag{3.1.1}$$

Therefore, the mesh is given by

$$t_i = \begin{cases} 2i\lambda/N & i = 0(1)N/2, \\ 1 - 2(1-\lambda)(N-i)/N & i = N/2+1(1)N. \end{cases} \tag{3.1.2}$$

Further, we denote the mesh size in the subinterval $[0, \lambda]$ by $h_i = h$, with

$$h = 4\varepsilon\alpha^{-1}N^{-1}\ln N, \text{ for } i = 0(1)N/2, \tag{3.1.3}$$

and in $[\lambda, 1]$ by $h_i = H$ with

$$H = 2(1-\lambda)N^{-1}, \text{ for } i = N/2+1(1)N. \tag{3.1.4}$$

In the next section, to analyse the convergence of the method which we introduce below, we shall only consider the case where $\lambda = 2\varepsilon\alpha^{-1}\ln N$,

and assume that $\varepsilon \leq CN^{-1}$ which is generally reasonable in practice.

On the above piecewise-uniform mesh, we denote $g_i := g(t_i)$ for all the mesh points $(t_i)_{i=0}^N$ in $[0, 1]$. In order to solve (1.3.1)-(1.3.2) numerically, [63] proposed the following finite difference scheme.

$$\begin{aligned} Lu_i^N \equiv & \varepsilon\frac{u_i^N - u_{i-1}^N}{h_i} + a_{i-\frac{1}{2}}(u_i^N + u_{i-1}^N)/2 + \frac{h_i}{4}\left[\frac{3}{2}K(t_{i-\frac{1}{2}}, t_{i-1})u_{i-1}^N + \frac{1}{2}K(t_{i-\frac{1}{2}}, t_i)u_i^N\right] + \\ & \widetilde{K}(t_0, ..., t_{i-1}; u_0^N, ..., u_{i-1}^N) = f_{i-\frac{1}{2}}, \quad i = 1(1)N, \end{aligned} \tag{3.1.5}$$

$$u_0^N = \gamma_0, \tag{3.1.6}$$

where

$$\widetilde{K}(t_0, ..., t_{i-1}; u_0^N, ..., u_{i-1}^N) = \begin{cases} 0, & \text{for } i = 1, \\ \sum_{j=1}^{i-1}\frac{h_j}{2}[K(t_{i-\frac{1}{2}}, t_j)u_j^N + K(t_{i-\frac{1}{2}}, t_{j-1})u_{j-1}^N] & \text{for } i > 1, \end{cases} \tag{3.1.7}$$

and $a_{i-\frac{1}{2}} = a(\frac{t_{i-1}+t_i}{2})$, similarly for $f_{i-\frac{1}{2}}$ and $K(t_{i-\frac{1}{2}}, t_j)$. In matrix form, the scheme (3.1.5) is given by a lower triangular linear system

$$Av = G,$$

where A is the matrix of the system and G the unknown vector. The entries of the matrix A

and components of the vector G are given by

$$
\begin{aligned}
&A_{11} = \tfrac{\varepsilon}{h_1} + \tfrac{\sigma}{4}(a_0 + a_1) + \tfrac{h_1}{16}(K_{i,0} + K_{11}) \quad i = 1;\\
&A_{ii} = r_i^c, \quad i = 2(1)N;\\
&A_{i,i-1} = r_{i,i-1}^- \quad i = 2(1)N;\\
&A_{i,j} = r_{i,i-1}^- \quad i = 3(1)N; j = 1(1)i-2;\\
&G_1 = \tfrac{1}{2}(f_0 + f_1) - (\tfrac{-\varepsilon}{h_1} + \tfrac{1}{4}(a_0 + a_1) + \tfrac{3h_1}{16}(K_{11} + K_{1,0})y_0 \quad i = 1;\\
&G_i = \tfrac{1}{2}(f_{i-1} + f_i) - (\tfrac{h}{4}(KK_i + KK_{i-1}))y_0, \quad i = 2(1)N;
\end{aligned}
$$

with

$$
\begin{aligned}
&r_i^c = \tfrac{\varepsilon}{h_i} + \tfrac{1}{4}(a_i + a_{i-1}) + \tfrac{h_i}{16}(K_{i-1,i} + K_{ii});\\
&r_{i,i-1}^- = \tfrac{-\varepsilon}{h_i} + \tfrac{1}{4}(a_i + a_{i-1}) + \tfrac{3h_i}{16}(K_{i-1,i-1} + K_{i,i-1}) + \tfrac{1}{4}h_{i-1}(K_{i-1,i-1} + K_{i,i-1});\\
&r_{i,i-1}^- = \tfrac{1}{4}(h_j + h_{j+1})(K_{i-1,j} + K_{i,j}).
\end{aligned}
$$

3.2 Error analyis of the scheme

Following ideas of [63] we present the convergence analysis of the method developed in previous section. Note that the analysis of the difference scheme is based on the discrete comparison principle and barrier function technique introduced respectively by Styness and Kellogg [36, 57]. We now introduce a number of results in forms of Lemmas on which the analyis will be based.

Lemma 3.2.1. *Assume that*

$$a(t) + \frac{H}{4}K(t,t) \geq 2\alpha^* > 0. \tag{3.2.1}$$

Then the operator l^N defined by

$$l^N u_i^N \equiv \varepsilon \frac{u_i^N + u_{i-1}^N}{h_i} + \left[\frac{1}{2}a_{i-\frac{1}{2}} + \frac{h_i}{8}K(t_{i-\frac{1}{2}}, t_i)\right] u_i^N, \quad 1 \leq i \leq N \tag{3.2.2}$$

satisfies a discrete comparison principle, i.e., if $\{v_i\}$ and $\{w_i\}$ are mesh functions that satisfy $v_0 \leq w_0$ and $l^N v_i \leq l^N w_i$, for $i = 1(1)N$, then $v_i \leq w_i$ for all i.

Proof. The operator l^N can be considered as a system of N linear equations in the unknowns u_i^N. It is easy to verify that the coefficient matrix associated with the operator l^N is diagonally dominant and that all off diagonal entries are positives. Therefore, the matrix is an irreducible M-matrix and has a positive inverse. Thus, if there exists two solutions v_i and w_i for $1 \leq i \leq N$, such that $v_0 \leq w_0$ and $l^N v_i \leq l^N w_i$, for $i = 1(1)N$, then $v_i \leq w_i$, $1 \leq i \leq N$. □

This discrete comparison principle is then used to prove the following stability lemma

Lemma 3.2.2. *Under the condition (3.2.1), the solution of the difference initial value problem*

$$l^N u_i^N = F_i, \;\; i = 1(1)N, \quad u_0^N = \beta \tag{3.2.3}$$

satisfies the estimate.

$$|u_i^N| \leq |\beta| + \alpha_*^{-1}|F_i|, \quad i = 1(1)N, \tag{3.2.4}$$

where $F_i \geq 0$ is nondecreasing.

Proof. Consider the barrier function given by

$$W_i = |\beta| + \alpha_*^{-1}|F_i| \pm u_i^N,$$

Then

$$\begin{aligned}
l^N W_i =& \varepsilon \frac{|\beta| + \alpha_*^{-1}|F_i| \pm u_i^N - (|B| + \alpha_*^{-1}|F_{i-1}| \pm u_{i-1}^N)}{h_i} + \\
& \left[\frac{1}{2}a_{i-\frac{1}{2}} + \frac{h_i}{8}K(t_{i-\frac{1}{2}}, t_i)\right](|B| + \alpha_*^{-1}|F_i| \pm u_i^N) \\
=& \frac{\varepsilon}{h_i}\left[\frac{|F_i| - |F_{i-1}|}{\alpha_*} + (\pm u_i^N - (\pm u_{i-1}^N))\right] + \left[\frac{1}{2}a_{i-\frac{1}{2}} + \frac{h_i}{8}K(t_{i-\frac{1}{2}}, t_i)\right](|B| + \alpha_*^{-1}|F_i| \pm u_i^N) \\
=& \frac{\varepsilon}{h_i}\left[\frac{|F_i| - |F_{i-1}|}{\alpha_*}\right] + \left[\frac{1}{2}a_{i-\frac{1}{2}} + \frac{h_i}{8}K(t_{i-\frac{1}{2}}, t_i)\right](|B| + \alpha_*^{-1}|F_i|) + \\
& \frac{\varepsilon}{h_i}(\pm u_i^N - (\pm u_{i-1}^N)) + \left[\frac{1}{2}a_{i-\frac{1}{2}} + \frac{h_i}{8}K(t_{i-\frac{1}{2}}, t_i)\right](\pm u_i^N) \\
=& \frac{\varepsilon}{h_i \alpha_*}[|F_i| - |F_{i-1}|] + \left[\frac{1}{2}a_{i-\frac{1}{2}} + \frac{h_i}{8}K(t_{i-\frac{1}{2}}, t_i)\right](|B| + \alpha_*^{-1}|F_i|) \pm l^N u_i^N \\
=& \frac{\varepsilon}{h_i}\left[\frac{|l^N u_i^N| - |l^N u_{i-1}^N|}{\alpha_*}\right] + \left[\frac{1}{2}a_{i-\frac{1}{2}} + \frac{h_i}{8}K(t_{i-\frac{1}{2}}, t_i)\right](|B| + \alpha_*^{-1}|F_i|) \pm l^N u_i^N \geq 0 \\
\geq& 0.
\end{aligned}$$

It then follows from the discrete comparison principle (Lemma 3.2.1) that

$$W_i \geq 0, \;\; \forall_i.$$

Thus

$$|\beta| + \alpha_*^{-1}|F_i| \pm u_i^N > 0,$$

which implies that

$$|u_i^N| \leq |\beta| \pm \alpha_*|F_i| \tag{3.2.5}$$

as required. □

Lemma 3.2.3. *There exists a constant C such that*

$$\int_{t_{j-1}}^{t_j}(1+\varepsilon^{-1}\exp(-\alpha t/2\varepsilon))dt \leq CN^{-1}\ln N, \quad \text{for } j=1(1)N.$$

Proof. For $j = N/2+1(1)N$, we write

$$\begin{aligned}
\int_{t_{j-1}}^{t_j}(1+\varepsilon^{-1}\exp(-\alpha t/(2\varepsilon)))dt &= \left[t+2\varepsilon\alpha^{-1}(\varepsilon^{-1}\exp(-\alpha t/(2\varepsilon)))\right]_{t_{j-1}}^{t_j} \\
&= \left[t+2\alpha^{-1}\exp(-\alpha t/(2\varepsilon))\right]_{t_{j-1}}^{t_j} \\
&= h_j - 2\alpha^{-1}[\exp(-\alpha t_j/(2\varepsilon)) - \exp(-\alpha t_{j-1}/2\varepsilon)] \\
&= CN^{-1} - 2\alpha^{-1}\left[\exp\left(-\alpha t_j/(2\varepsilon)\right) - \exp(-\alpha t_{j-1}/(2\varepsilon))\right] \\
&\leq CN^{-1} - 2\alpha^{-1}\exp(-\alpha t_{N/2}/(2\varepsilon)) \\
&\quad \{t_{N/2} = 2\varepsilon\alpha^{-1}\ln N \ at\ N/2 = j-1\} \\
&\leq CN^{-1} - 2\alpha^{-1}N^{-1} \\
&\leq CN^{-1}. \qquad (3.2.6)
\end{aligned}$$

For $j = 1(1)N/2$

$$\begin{aligned}
\int_{t_{j-1}}^{t_j}(1+\varepsilon^{-1}\exp(-\alpha t/2(\varepsilon))dt &= \left[t+2\varepsilon\alpha^{-1}(\varepsilon^{-1}\exp(-\alpha t/(2\varepsilon)))\right]_{t_{j-1}}^{t_j} \\
&= h_j - 2\alpha^{-1}\left[\exp(-\alpha t_j/(2\varepsilon)) - \exp(-\alpha t_{j-1}/(2\varepsilon))\right] \\
&\leq CN^{-1} - 2\alpha^{-1}(\exp(-\alpha t_j/2\varepsilon) - \exp(-\alpha t_j/(2\varepsilon)) \times \\
&\quad \exp(\alpha t_j/(2\varepsilon)) \times \exp(\alpha t_{j-1}/(2\varepsilon))) \\
&\leq CN^{-1} - 2\alpha^{-1}\exp(-\alpha t_j/2\varepsilon)(1-\exp(\alpha h_j/(2\varepsilon)) \\
&\leq CN^{-1} + C\varepsilon^{-1}h_j\exp(\alpha t_j/(2\varepsilon)) \\
&\leq CN^{-1}\ln N. \ \text{Since } h_j = 4\varepsilon\alpha^{-1}N^{-1}\ln N \qquad (3.2.7)
\end{aligned}$$

Combining (3.2.6) and (3.2.7) completes the proof. □

The next lemma deals with the analyis of the truncation error of the trapezoidal integration in approximating the Volterra integral.

Lemma 3.2.4. *For $1 \leq i \leq N$, there exists a constant C such that*

$$\tau_i = \Big|\frac{h_i}{4}\left[\frac{3}{2}K(t_{i-\frac{1}{2}},t_{i-1})u_{i-1} + \frac{1}{2}K(t_{i-\frac{1}{2}},t_i)u_i\right] + \widetilde{K}(t_0,...,t_{i-1};u_0,...,u_{i-1}) - \int_0^{t_{i-\frac{1}{2}}} K(t_{i-\frac{1}{2}},s)u(s)ds\Big| \leq CN^{-2}\ln^2 N,$$

where $\widetilde{K}(t_0, ..., t_{i-1}; u_0, ..., u_{i-1})$ is given by (3.1.7).

Proof. The truncation error of the trapezoidal integration in the approximation of the Volterra integral satisfies the following inequality

$$\begin{aligned}\tau_i \quad \leq \quad & \left| \frac{h_i}{4} \left[\frac{3}{2} K(t_{i-\frac{1}{2}}, t_{i-1}) u_{i-1} + \frac{1}{2} K(t_{i-\frac{1}{2}}, t_i) u_i \right] - \int_{t_{i-1}}^{t_{i-\frac{1}{2}}} K(t_{i-\frac{1}{2}}, s) u(s) ds \right| + \\ & \left| \widetilde{K}(t_0, ..., t_{i-1}; u_0, ..., u_{i-1}) - \int_0^{t_{i-1}} K(t_{i-\frac{1}{2}}, s) u(s) ds \right|.\end{aligned}$$

Since the kernel $K(s,t)$ is bounded by $\bar{K} = \max_{I \times I} |K(t,s)|$, we have

$$\tau_i \leq \left| Ch_i[u_{i-1} + u_i] - C \int_{t_{i-1}}^{t_{i-\frac{1}{2}}} u(s) ds \right| + \left| C \sum_{j=1}^{i-1} h_j [u_j^N + u_{j-1}^N] - C \int_0^{t_{i-1}} u(s) ds \right|.$$

From here, taking Taylor series expansion with integral form of the remainder for u, u_{i-1} and u_{j-1} around the points t_i and t_j respectively leads to

$$\tau_i \leq Ch_i \int_{t_{i-1}}^{t_{i-\frac{1}{2}}} |u''(t)|(t - t_{i-1}) dt + C \sum_{j=1}^{i-1} h_j \int_{t_{j-1}}^{t_j} |u''(t)|(t - t_{j-1}) dt.$$

Thereafter employing Lemma 2.2.1 for $k = 2$, we obtain

$$\begin{aligned}\tau_i \leq & Ch_i \int_{t_{i-1}}^{t_{i-\frac{1}{2}}} (1 + \varepsilon^{-2} \exp(-\alpha t/\varepsilon))(t - t_{i-1}) dt + C \sum_{j=1}^{i-1} h_j \int_{t_{j-1}}^{t_j} (1 + \varepsilon^{-2} \exp(-\alpha t/\varepsilon))(t - t_{j-1}) dt \\ \leq \quad & C \max_{1 \leq j \leq i} \int_{t_{j-1}}^{t_j} (1 + \varepsilon^{-2} \exp(-\alpha t/\varepsilon))(t - t_{j-1}) dt. \qquad (3.2.8)\end{aligned}$$

Now, we shall utilize the following inequality [17]: For any positive monotonically decreasing function g defined on $[a, b]$ and arbitrary $k \in N$, we have

$$\int_a^b g(x)(x - a)^{k-1} \leq \frac{1}{k} \left[\int_a^b g(x)^{1/k} dx \right]^k \qquad (3.2.9)$$

Hence, the above inequality for $k = 2$ implies that

$$\tau_i \leq \int_{t_{j-1}}^{t_j} (1 + \varepsilon^{-2} \exp(-\alpha t/\varepsilon))(t - t_{j-1}) dt \leq \frac{1}{2} \left\{ \int_{t_{j-1}}^{t_j} (1 + \varepsilon^{-2} \exp(-\alpha t/\varepsilon)) dt \right\}^2.$$

The proposition of the Lemma follows from this inequality and the result of Lemma 3.2.3. □

Combining the results in Lemma 2.2.1, 3.2.3 and 3.2.4, we obtain the following theorem [63] which shows that in practice the method (3.1.5)-(3.1.6) developed on the piecewise-uniform mesh is uniformly convergent of almost second kind.

Theorem 3.2.1. *Let u be the exact solution of (1.3.1)-(1.3.2) and u^N the solution of the discrete problem (3.1.5)-(3.1.6). Then under the condition (3.2.1), for the difference problem (3.1.5)-(3.1.6) we have*

$$|u_i - u_i^N| \leq CN^{-2}\ln^2 N, \quad 0 \leq i \leq N. \tag{3.2.10}$$

Proof. For $0 \leq i \leq N$, in view of (3.1.5) and (3.2.2) we have

$$\begin{aligned}
&\left|l^N(u_i - u_i^N)\right| = \\
&|l^N u_i - \{f_{i-\frac{1}{2}} + \frac{1}{2}a_{i-\frac{1}{2}}u_{i-1}^N - \frac{3h_i}{8}K(t_{i-\frac{1}{2}}, t_{i-1})u_{i-1}^N\} - \widetilde{K}(t_0, ..., t_{i-1}; u_0^N, ..., u_{i-1}^N)| \\
&\leq \left|\varepsilon\left(\frac{u_i - u_{i-1}}{h_i} - u'_{i-\frac{1}{2}}\right)\right| + \left|\frac{h_i}{8}K(t_{i-\frac{1}{2}}, t_i)u_i - \int_0^{t_{i-\frac{1}{2}}} K(t_{i-\frac{1}{2}}, s)u(s)ds + \frac{1}{2}a_{i-\frac{1}{2}}u_i - \right. \\
&\left. a_{i-\frac{1}{2}}u_{i-\frac{1}{2}} + \frac{1}{2}a_{i-\frac{1}{2}}u_{i-1}^N + \frac{3h_i}{8}K(t_{i-\frac{1}{2}}, t_{i-1})u_{i-1}^N - \widetilde{K}(t_0, ..., t_{i-1}; u_0^N, ..., u_{i-1}^N)\right| \\
&\leq \left|\varepsilon\left(\frac{u_i - u_{i-1}}{h_i} - u'_{i-\frac{1}{2}}\right)\right| + \left|\frac{1}{2}a_{i-\frac{1}{2}}u_i - a_{i-\frac{1}{2}}u_{i-\frac{1}{2}} + \frac{1}{2}a_{i-\frac{1}{2}}u_{i-1}\right| + \left|\frac{1}{2}a_{i-\frac{1}{2}}(u_{i-1} - u_{i-1}^N)\right| + \\
&\left|\frac{h_i}{4}\left[\frac{3}{2}K(t_{i-\frac{1}{2}}, t_{i-1})u_{i-1} + \frac{1}{2}K(t_{i-\frac{1}{2}}, t_i)u_i\right] + \widetilde{K}(t_0, ..., t_{i-1}; u_0, ..., u_{i-1}) - \int_0^{t_{i-\frac{1}{2}}} K(t_{i-\frac{1}{2}}, s)u(s)ds\right| + \\
&\left|\frac{3h_i}{8}K(t_{i-\frac{1}{2}}, t_i)(u_{i-1} - u_{i-1}^N)\right| + \left|\widetilde{K}(t_0, ..., t_{i-1}; u_0 - u_0^N, ..., u_{i-1} - u_{i-1}^N)\right|.
\end{aligned}$$

Using the assumption that the kernel and all its derivatives are bounded, we get

$$\begin{aligned}
&\leq \left|\varepsilon\left(\frac{u_i - u_{i-1}}{h_i} - u'_{i-\frac{1}{2}}\right)\right| + \left|\frac{1}{2}a_{i-\frac{1}{2}}u_i - a_{i-\frac{1}{2}}u_{i-\frac{1}{2}} + \frac{1}{2}a_{i-\frac{1}{2}}u_{i-1}\right| + \left|\frac{1}{2}a_{i-\frac{1}{2}}(u_{i-1} - u_{i-1}^N)\right| + \\
&\quad C\left|h_i\left[u_{i-1} + u_i\right] + C\sum_{j=1}^{i-1} h_j[u_j + u_{j-1}] - C\int_0^{t_{i-\frac{1}{2}}} u(s)ds\right| + C\left|(u_{i-1} - u_{i-1}^N)\right| + \\
&\quad C\left|\sum_{j=1}^{i-1} h_j[u_j - u_j^N + u_{j-1} - u_{j-1}^N]\right|.
\end{aligned}$$

Again, using Taylor series expansion with integral form of the remainder for $u'_{i-\frac{1}{2}}$, $u_{i-\frac{1}{2}}$, u_{i-1}, u_{j-1}, u_{j-1}^N respectively about the points t_i and t_j together with the result of Lemma 3.2.4 we have

$$\begin{aligned}
\left|l^N(u_i - u_i^N)\right| \leq & C\varepsilon\int_{t_{i-1}}^{t_i} |u'''(t)|(t - t_{i-1})dt + C\int_{t_{i-1}}^{t_i} |u''(t)|(t - t_{i-1})dt + \\
& CN^{-2}\ln^2 N + C\sum_{j=1}^{i-1} h_j|u_j - u_j^N|.
\end{aligned}$$

Further, using Lemma 2.2.1 for $k = 2$, leads to the inequality

$$\left|l^N(u_i - u_i^N)\right| \leq C\int_{t_{i-1}}^{t_i} (1 + \varepsilon^{-2}\exp(\alpha t/\varepsilon))(t - t_{i-1})dt + CN^{-2}\ln^2 N + C\sum_{j=1}^{i-1} h_j|u_j - u_j^N|.$$

Furthermore, to bound the integral in this last expression we utilize again the inequality (3.2.9) for $k = 2$:

$$\left|l^N(u_i - u_i^N)\right| \leq C\left\{\int_{t_{i-1}}^{t_i}(1+\varepsilon^{-1}\exp(\alpha t/(2\varepsilon)))dt\right\}^2 + CN^{-2}\ln^2 N + C\sum_{j=1}^{i-1}h_j|u_j - u_j^N|,$$

which in view of Lemma 3.2.3 we write

$$\left|l^N(u_i - u_i^N)\right| \leq CN^{-2}\ln^2 N + C\sum_{j=1}^{i-1}h_j|u_j - u_j^N|.$$

Applying the discrete comparison principle (Lemma 3.2.1) we obtain

$$|u_i - u_i^N| \leq w_i, \quad 0 \leq i \leq N,$$

where w_i satisfies the problem

$$l^N w_i = \begin{cases} CN^{-2}\ln^2 N, \ \ i = 1, \\ CN^{-2}\ln^2 N + C\sum_{j=1}^{i-1}h_j|u_j - u_j^N|, \ \ 1 \leq i \leq N, \end{cases}$$

$$w_0 = 0.$$

From here, it is clear from the stability result (Lemma 3.2.2) that

$$|u_i - u_i^N| \leq |w_i| \leq CN^{-2}\ln^2 N + C\sum_{j=1}^{i-1}h_j|u_j - u_j^N|$$

and consequently

$$|u_{i-1} - u_{i-1}^N| \leq CN^{-2}\ln^2 N + C\sum_{j=1}^{i-2}h_j|u_j - u_j^N|.$$

Finaly, application of the recurrence inequality gives

$$|u_i - u_i^N| \leq CN^{-2}\ln^2 N, \ \ \text{for} \ \ i = 0(1)N.$$

□

3.3 Numerical results

To illustrate the performance of the proposed numerical method, we give some numerical results for three test examples. The maximum error of solution and the rates of convergence are evaluated using fomulae (2.5.1)-(2.5.4).

Example 3.3.1. [63] *Consider problem (1.3.1)-(1.3.2) with*

$$a(t) = t + 1, K(t, s) = t + s,$$
$$f(t) = \varepsilon \cos t + t \sin t + 2 \sin t + (t - 2t\varepsilon + \varepsilon^2) \exp\left(\frac{-t}{\varepsilon}\right) + t - 2t \cos t + \varepsilon t - \varepsilon^2,$$
$$u(0) = 1.$$

The exact solution to this problem is

$$u(t) = \sin t + \exp\left(\frac{-t}{\varepsilon}\right).$$

Example 3.3.2. [63] *Consider problem (1.3.1)-(1.3.2) with*

$$a(t) = 2, K(t, s) = s,$$
$$f(t) = \varepsilon - \exp\left(\frac{-t}{\varepsilon}\right) + 2t + 2\exp\left(\frac{-t}{\varepsilon}\right) + \frac{1}{3t^3} - t\varepsilon \exp\left(\frac{-t}{\varepsilon}\right) - \varepsilon^2 \exp\left(\frac{-\varepsilon}{t}\right) + \varepsilon^2,$$
$$u(0) = 1.$$

The exact solution to this problem is given by

$$u(t) = t + \exp\left(\frac{-t}{\varepsilon}\right).$$

Example 3.3.3. [4] *Consider problem (1.3.1)-(1.3.2) with*

$$a(t) = 1, K(t, s) = s,$$
$$f(t) = (2 + 9\varepsilon + \varepsilon t + 11t + t^2)\exp(-t) - 10(\varepsilon t + \varepsilon^2)\exp\left(\frac{-t}{\varepsilon}\right) + 5t^2 + 10\varepsilon^2 - 2,$$
$$u(0) = 10.$$

The exact solution to this problem is given by

$$u(t) = 10 - (10 + t)\exp(-t) + 10\exp\left(\frac{-t}{\varepsilon}\right).$$

Table 3.1 and 3.3 provide the maximum ε-uniform errors and the corresponding rates of convergence. From these two tables, one can observe that the rate of convergence are increasing towards 2 which indicates that the numerical results are essentially in agreement with our theoretical outcomes outlined in Theorem 3.2.1.

Table 3.1: Results for Example 3.3.1: Maximum errors and maximum rates of convergence obtained via FMFDM (3.1.5)-(3.1.6)

ε	n=40	n=80	n=160	n=320	n=640	n=1280	n=2560
10^{-2}	2.92E-03	9.91E-04	3.15E-04	8.84E-05	4.72E-05	4.73E-05	4.73E-05
	1.55	1.65	1.83	0.90	-0.00	-0.00	
10^{-3}	2.94E-03	1.01E-03	3.36E-04	1.08E-04	3.38E-05	1.02E-05	2.93E-06
	1.53	1.59	1.63	1.67	1.72	1.80	
10^{-4}	2.94E-03	1.01E-03	3.36E-04	1.08E-04	3.40E-05	1.04E-05	3.13E-06
	1.53	1.59	1.63	1.67	1.70	1.73	
10^{-5}	2.94E-03	1.01E-03	3.36E-04	1.08E-04	3.40E-05	1.04E-05	3.13E-06
	1.53	1.59	1.63	1.67	1.70	1.73	
⋮	⋮	⋮	⋮	⋮	⋮	⋮	⋮
E_N	2.94E-03	1.01E-03	3.36E-04	1.08E-04	3.40E-05	1.04E-05	3.13E-06
r_N	1.53	1.59	1.63	1.67	1.70	1.73	

Table 3.2: Results for Example 3.3.2: Maximum errors and maximum rates of convergence obtained via FMFDM (3.1.5)-(3.1.6)

ε	n=40	n=80	n=160	n=320	n=640	n=1280	n=2560
10^{-2}	4.38E-03	1.57E-03	5.65E-04	2.38E-04	1.89E-04	1.87E-04	1.87E-04
	1.47	1.24	0.33	0.01	0.00	0.00	
10^{-3}	4.22E-03	1.48E-03	4.96E-04	1.60E-04	5.07E-05	1.59E-05	5.21E-06
	1.57	1.62	1.66	1.67	1.60	1.24	
10^{-4}	4.21E-03	1.47E-03	4.94E-04	1.60E-04	5.00E-05	1.53E-05	4.62E-06
	1.57	1.63	1.67	1.70	1.73	1.75	
10^{-5}	4.21E-03	1.47E-03	4.94E-04	1.59E-04	5.00E-05	1.53E-05	4.61E-06
	1.57	1.63	1.67	1.70	1.73	1.75	
⋮	⋮	⋮	⋮	⋮	⋮	⋮	⋮
E_N	4.21E-03	1.47E-03	4.94E-04	1.59E-04	5.00E-05	1.53E-05	4.61E-06
r_N	1.57	1.63	1.67	1.70	1.73	1.75	

Table 3.3: Results for Example 3.3.3: Maximum errors and maximum rates of convergence obtained via FMFDM (3.1.5)-(3.1.6)

ε	n=40	n=80	n=160	n=320	n=640	n=1280	n=2560
10^{-2}	1.89E-02	4.69E-03	1.17E-03	2.93E-04	7.32E-05	1.83E-05	4.57E-06
	2.00	2.00	2.00	2.00	2.00	2.00	
10^{-3}	4.21E-02	1.47E-02	4.94E-03	1.59E-03	5.00E-04	1.53E-04	4.61E-05
	1.57	1.63	1.67	1.70	1.73	1.75	
10^{-4}	4.21E-02	1.47E-02	4.94E-03	1.59E-03	5.00E-04	1.53E-04	4.61E-05
	1.57	1.63	1.67	1.70	1.73	1.75	
10^{-5}	4.21E-02	1.47E-02	4.94E-03	1.59E-03	5.00E-04	1.53E-04	4.61E-05
	1.57	1.63	1.67	1.70	1.73	1.75	
⋮	⋮	⋮	⋮	⋮	⋮	⋮	
E_N	4.21E-02	1.47E-02	4.94E-03	1.59E-03	5.00E-04	1.53E-04	4.61E-05
r_N	1.57	1.63	1.67	1.70	1.73	1.75	

3.4 Conclusion

In this chapter, we have investigated a class of FMFDMs to solve (1.3.1)-(1.3.2). The problem was discretized using the standard backward difference operator along with the midpoint difference operator and trapezoidal integration on a piecewise-uniform mesh of Shishkin type. The method was analysed for convergence and stability and shown to be convergent of almost second order. The numerical results displayed in table 3.1 and 3.3 are in agreement with the theoretical results summarized in the Theorem 3.2.1.

Chapter 4

A Fitted Mesh Finite Difference Method for SPVIDEs based on Right and Left Side Rectangle Rules

This chapter presents another FMFDM to solve (1.3.1)-(1.3.2). The method is composed of an implicit finite difference scheme on a piecewise-uniform mesh of Shiskin type. The right and composite left side rectangle rules with the weights and remainder terms in intergral form have been used to discretize the integral part of the problem. This method was applied by Kudu et al. [38] to solve a linear singularly perturbed Volterra delayed integro-differential equation. In the next Section, we construct the scheme. The analysis of the fitted mesh finite difference method proposed is given in Section 4.3. Section 4.4 deals with numerical verifications. Section 4.5 is devoted to conclusion of the chapter.

4.1 Mesh and scheme

We derive the fitted finite difference scheme on the following piecewise-uniform division: $\psi_N = \{0 = t_0 < t_1 < t_2 < ... < t_{N-1} < t_N = 1\}$, where the mesh widths will be defined as $h_i = t_i - t_{i-1}$. The notations and assumptions used in chapter 2 are again considered here. It is known that the class of problems given by (1.3.1)-(1.3.2) exhibits one boundary layer, hence we define the piecewise-uniform mesh as follows. Let N be a positive even integer. We consider a slight variant

of the transition parameter given by Şevgin in [54]

$$\delta = \min\{1/2, \alpha^{-1}\varepsilon|\ln\varepsilon|\} \tag{4.1.1}$$

and partition evenly each of the subintervals $[0,\delta]$ and $[\delta,1]$ into $N/2$ subintervals. The mesh is uniform if $\delta = 1/2$ and piecewise uniform if $\delta = \alpha^{-1}\varepsilon|\ln\varepsilon|$. Then the corresponding mesh points are

$$t_i = \begin{cases} -\alpha^{-1}\varepsilon \ln\left[1-(1-\varepsilon)\frac{2i}{N}\right], & i = 0(1)N/2, \\ \delta + \frac{2(1-\delta)}{N}(i-\frac{N}{2}), & i = N/2+1(1)N. \end{cases} \tag{4.1.2}$$

Assumption: we shall assume that $\delta = \alpha^{-1}\varepsilon|\ln\varepsilon|$, so that the mesh is fine on $[0,\delta]$ and coarse in $[\delta,1]$. To construct the numerical method, we integrate (1.3.1) over the interval $[t_{i-1}, t_i]$:

$$\varepsilon h_i^{-1}\int_{t_{i-1}}^{t_i} u'(t)dt + h_i^{-1}\int_{t_{i-1}}^{t_i} a(t)u(t)dt + h_i^{-1}\int_{t_{i-1}}^{t_i}\left\{\int_0^t K(t,s)u(s)ds\right\}dt = h_i^{-1}\int_{t_{i-1}}^{t_i} f(t)dt.$$

Applying right side rectangle rule we obtain the relation

$$\varepsilon u_{\tilde{t},i} + a_i u_i + h_i^{-1}\int_{t_i-1}^{t_i}\left\{\int_0^t K(t,s)u(s)ds\right\}dt + R_i^{(1)} \tag{4.1.3}$$

where the error $R_i^{(1)}$ term is calculated using the formula (2.3.10):

$$R_i^{(1)} = -h_i^{-1}\int_{t_{i-1}}^{t_i}(t-t_{i-1})\frac{d}{dt}\left[a(t)u(t)-f(t)\right]dt. \tag{4.1.4}$$

Next, repeating this process for the integral part in (4.1.3), we get

$$h_i^{-1}\int_{t_{i-1}}^{t_i}\left\{\int_0^t K(t,s)u(s)ds\right\}dt = h_i^{-1}(t_i-t_{i-1})\int_0^{t_i} K(t_i,s)u(s)ds + R_i^{(2)}, \tag{4.1.5}$$

where the discretization error $R_i^{(2)}$ is evaluated using (2.3.9):

$$R_i^{(2)} = -h_i^{-1}\int_{t_{i-1}}^{t_i}(t-t_{i-1})\frac{d}{dt}\Big[\int_0^t K(t,s)u(s)ds\Big]dt. \tag{4.1.6}$$

Moreover, applying the composite left side rectangle rule to the integral term in (4.1.5), we obtain

$$\int_0^{t_i} K(t_i,s)u(s)ds = \sum_{j=0}^{i-1} h_{j+1}K(t_i,t_j)u_j + R_i^{(3)}$$

where utilizing the formula (2.3.9), we obtain

$$R_i^{(3)} = \sum_{j=1}^{i}\int_{t_{j-1}}^{t_j}(t_j-s)\frac{d}{ds}[K(t_i,s)u(s)]ds. \tag{4.1.7}$$

As a result, we obtain the following equation

$$\varepsilon u_{\tilde{t},i} + a_i u_i + \sum_{j=0}^{i-1} h_{j+1} K(t_i, t_j) u_j + R_i = f_i \;\; i = 1(1)N, \tag{4.1.8}$$

where R_i is given by the linear combination

$$R_i = R_i^{(1)} + R_i^{(2)} + R_i^{(3)}. \tag{4.1.9}$$

Neglecting R_i in (4.1.8), we obtain the finite difference scheme

$$L^N y_i = \varepsilon y_{\tilde{t},i} + a_i y_i + \sum_{j=0}^{i-1} h_{j+1} K(t_i, t_j) y_j = f_i \quad i = 1(1)N, \tag{4.1.10}$$

$$y(0) = B. \tag{4.1.11}$$

In matrix notation, the scheme (4.1.10)-(4.1.11) is given by lower triangular system $Ay = F$, where A is the matrix of the system and F is the unknown vector. The entries of the matrix A and the vector F are given by

$$\begin{aligned}
&A_{ii} = r_i^c, \quad i = 1(1)N;\\
&A_{i,i-1} = r_{1i,i-1}^- \quad i = 2(1)N;\\
&A_{i,j} = r_{2i,i-1}^- \quad i = 3(1)N; j = 1(1)i-2;\\
&F_1 = f_1 - (\tfrac{\varepsilon}{h_1} - h_1 K_{10}) y_0 \quad i = 1;\\
&F_i = f_i - h_1 K_{10}, \quad i = 2(1)N;
\end{aligned}$$

with

$$\begin{aligned}
&r_i^c = \tfrac{\varepsilon}{h_i} + a_i;\\
&r_{1i,i-1}^- = \tfrac{-\varepsilon}{h_i} + h_i K_{i,i-1};\\
&r_{2i,i-1}^- = h_{j+1} K_{i,j}.
\end{aligned}$$

4.2 Stability and convergence analysis of scheme

This section presents the stability results and the error analysis for the numerical method proposed in Section 4.1. The main ε-uniform convergence result in this chapter is also given at the end of the section.

The error function, which we define by $\tau_i = y_i - u_i,\ i = 0(1)N$, is the solution of the discrete problem

$$l^N \tau_i = R_i \;\; i = 0(1)N \tag{4.2.1}$$

$$\tau = 0 \tag{4.2.2}$$

where R_i is given by (4.1.9). The next two Lemmas are devoted to the stability bound of the scheme.

Lemma 4.2.1. [38] *Consider the following difference problem*

$$l^N v_i := \varepsilon v_{\widetilde{t},i} + a_i v_i = F_i \;\; i = 0(1)N, \tag{4.2.3}$$

$$v_0 = B. \tag{4.2.4}$$

Let $|F_i| \leq \mathcal{F}_i$ and $\mathcal{F}_i$ a nondecreasing function. Then the solution of (4.2.3)-(4.2.4) satisfies

$$|v_i| \leq |B| + \alpha^{-1}\mathcal{F}_i, \quad i = 0(1)N. \tag{4.2.5}$$

Proof. Consider the barrier function

$$\Phi_i^{\pm} = \pm v_i + |B| + \alpha^{-1}\mathcal{F}_i. \tag{4.2.6}$$

For i=0, we have

$$\begin{aligned}\Phi_0^{\pm} &= \pm v_0 + |B| + \alpha^{-1}\mathcal{F}_0 \\ &= \pm B + |B| + \alpha^{-1}\mathcal{F}_0 \\ &\geq 0,\end{aligned}$$

and for $i \geq 1$,

$$\begin{aligned}l^N\Phi_i^{\pm} &:= \varepsilon\Phi_{\widetilde{t},i}^{\pm} + a_i\Phi_i^{\pm} \\ &:= \varepsilon(\pm v_{\widetilde{t},i} + |B| + \alpha^{-1}\mathcal{F}_{\widetilde{t},i}) + a_i(\pm v_i + |B| \pm \alpha^{-1}\mathcal{F}_i) \\ &:= [\varepsilon(\pm v_{\widetilde{t},i}) + a_i(\pm v_i)] + (\varepsilon + a_i)|B| \pm \varepsilon\alpha^{-1}\mathcal{F}_{\widetilde{t},i} + a_i\alpha^{-1}\mathcal{F}_i \\ &:= \pm F_i + a_i\alpha^{-1}\mathcal{F}_i + (\varepsilon + a_i)|B| + \varepsilon\alpha^{-1}\mathcal{F}_{\widetilde{t},i},\end{aligned}$$

we have

$$\begin{aligned}l^N\Phi_i^{\pm} &\geq \pm F_i + a_i\alpha^{-1}\mathcal{F}_{\widetilde{t},i}. \;\; (\text{ Since as } \mathcal{F} \text{ is nondecreasing}, \mathcal{F}_{\widetilde{t},i} = (\mathcal{F}_i - \mathcal{F}_{i-1})/h \geq 0) \\ &\geq F_i + \mathcal{F}_i \\ &\geq 0.\end{aligned}$$

Applying the maximum principal, yields

$$\Phi_i^{\pm} \geq 0,$$

which means that

$$|v_i| \leq |B| + \alpha^{-1}\mathcal{F}_i, \quad i = 0(1)N, \tag{4.2.7}$$

as required. □

Lemma 4.2.2. *Let y_i be the solution of (4.1.10)-(4.1.11). Then result*

$$||y||_{\infty,\psi_N} \leq (B + \alpha^{-1}||f_i||_{\infty}, \psi_N) \exp(\alpha^{-1}\bar{K}). \tag{4.2.8}$$

Proof. The difference equation (4.1.10) can be rewritten in the form

$$\varepsilon y_{\tilde{t},i} + a_i y_i = F_i, \tag{4.2.9}$$

where

$$F_i = f_i - \sum_{j=0}^{i-1} h_{j+1} K(t_i, t_j) y_j.$$

Thus, we have

$$|F_i| \leq |f_i| + \sum_{j=0}^{i-1} h_{j+1}\bar{K}|y_j|) \leq ||f||_{\infty,\psi_N} + \sum_{j=0}^{i-1} h_{j+1}\bar{K}|y_j|.$$

Furthermore applying Lemma 4.2.1, we have

$$\begin{aligned} |y_i| &\leq |B| + \alpha^{-1}||f||_{\infty,\psi_N} + \alpha^{-1}\sum_{j=0}^{i-1} h_{j+1}\bar{K}|y_j|, \\ &\leq |B| + \alpha^{-1}||f||_{\infty,\psi_N} + \alpha^{-1}\sum_{j=1}^{i} h_j\bar{K}|y_{j-1}|, \end{aligned}$$

so that according to Grownall's inequality we obtain

$$|y_i| \leq (|B| + \alpha^{-1}||f||_{\infty,\psi_N}) \exp(\alpha^{-1}\bar{K}t_j) \leq (|B| + \alpha^{-1}||f||_{\infty,\psi_N}) \exp(\alpha^{-1}\bar{K}).$$

□

We now carry out the error analysis of the method.

Lemma 4.2.3. *Let the assumptions of Lemma 2.2.1 be satisfied. Then for the truncation error R_i, we have*

$$||R||_1, \psi_N \leq CN^{-1}. \tag{4.2.10}$$

Proof. To prove (4.2.10), it suffices to establish that the functions $||R_i^d||_1$, $(d = 1, 2, 3)$ involved in the expression for R_i admit the estimate

$$||R_i^k||_1 \leq CN^{-1}, \quad k = 1, 2, 3. \tag{4.2.11}$$

Using the hypothesis of Lemma 2.2.1 on an arbitrary mesh we obtain

$$R_i^{(1)} \leq C\{h_i + \int_{t_{i-1}}^{t_i} |u'(t)|dt\}, \quad i = 1(1)N, \tag{4.2.12}$$

which in view of (2.2.2), for $k = 1$, yields

$$R_i^{(1)} \leq C\{h_i + \frac{1}{\varepsilon}\int_{t_{i-1}}^{t_i} \exp(-\alpha t/\varepsilon)dt\}, \quad i = 1(1)N. \tag{4.2.13}$$

For (4.1.6) we have,

$$|R_i^{(2)}| = h_i^{-1}\int_{t_{i-1}}^{t_i}(t - t_{i-1})\Big|\frac{d}{dt}\Big[\int_0^t K(t, s)u(s)ds\Big]\Big|dt$$

Upon applying Leibniz rule, we obtain

$$\begin{aligned}|R_i^{(2)}| &\leq \int_{t_{i-1}}^{t_i} |K(t, t)||u(t)|dt + \int_{t_{i-1}}^{t_i}\Big|\int_0^t \frac{\partial}{\partial t}K(t, s)u(s)ds\Big|dt \\ &\leq \int_{t_{i-1}}^{t_i} \bar{K}|u(t)|dt + \int_{t_{i-1}}^{t_i}\Big|\int_0^t \bar{K}u(s)ds\Big|dt.\end{aligned}$$

In virtue of Lemma 2.2.1, we obtain

$$|R_i^{(2)}| \leq Ch_i, \quad i = 1(1)N. \tag{4.2.14}$$

Further,

$$\begin{aligned}|R_i^{(3)}| &= \Big|\sum_{j=1}^{i}\int_{t_{j-1}}^{t_j}(t_j - s)\frac{d}{dt}\Big[K(t_i, s)u(s)\Big]ds\Big| \\ &\leq \sum_{j=1}^{i}\int_{t_{j-1}}^{t_j}(t_j - s)\Big|\frac{\partial}{\partial t}K(t_i, s)u(s)\Big|ds + \Big|\sum_{j=1}^{i}\int_{t_{j-1}}^{t_j}(t_j - s)K(t_i, s)u'(s)\Big|ds \\ &\leq \sum_{j=1}^{i}\int_{t_{j-1}}^{t_j}(t_j - s)\Big|\bar{K}u(s)\Big|ds + \Big|\sum_{j=1}^{i}\int_{t_{j-1}}^{t_j}(t_j - s)\bar{K}u'(s)\Big|ds \\ &\leq Ch_i\Big\{\int_0^{t_i}|u(s)|ds + \int_0^{t_i}|u'(s)|ds\Big\}.\end{aligned} \tag{4.2.15}$$

Now, applying (2.2.1) and (2.2.2) for $k = 1$ we get

$$|R_i^{(3)}| \leq Ch_i, \quad i = 1(1)N, \tag{4.2.16}$$

where

$$h_i = \begin{cases} -\alpha^{-1}\varepsilon \ln\left[1-(1-\varepsilon)\frac{2i}{N}\right] + \alpha^{-1}\varepsilon \ln\left[1-(1-\varepsilon)\frac{2(i-1)}{N}\right], & i = 0(1)N/2, \\ \frac{2(1-\delta)}{N}, & i = N/2+1(1)N. \end{cases} \tag{4.2.17}$$

As indicated earlier, we only consider the case where $\delta < 1/2$ i.e., $\delta = \alpha^{-1}\varepsilon|\ln\varepsilon|$ and analyse the truncation error R_i on the inner region, $[0,\delta]$ and the outer region, $[\delta,1]$ separately. In the layer region $[0,\delta]$, by (2.2.2) for $k=1$, the inequality (4.2.12) becomes

$$|R_i^{(1)}| \le C\left[h_i + \alpha^{-1}\left(\exp\left(-\frac{\alpha t_{i-1}}{\varepsilon}\right) + \exp\left(-\frac{\alpha t_i}{\varepsilon}\right)\right)\right], \quad i = 1(1)N/2, \tag{4.2.18}$$

and, since [54]

$$\begin{aligned} h_i = t_i - t_{i-1} &= -\alpha^{-1}\varepsilon \ln\left[1-(1-\varepsilon)\frac{2i}{N}\right] + \alpha^{-1}\varepsilon \ln\left[1-(1-\varepsilon)\frac{(2(i-1))}{N}\right] \\ &\le 2\alpha^{-1}(\varepsilon-1)N^{-1} \end{aligned} \tag{4.2.19}$$

and

$$\exp(-\alpha t_{i-1}/\varepsilon) + \exp(-\alpha t_i/\varepsilon) = 2(1-\varepsilon)N^{-1}. \tag{4.2.20}$$

It then follows from (4.2.18) that

$$|R_i^{(1)}| \le C\{2\alpha^{-1}(1-\varepsilon)N^{-1} + 2(1-\varepsilon)\alpha^{-1}N^{-1}\} = 4\alpha^{-1}CN^{-1}, \;\; i = 0(1)N/2. \tag{4.2.21}$$

Analogously for the estimate (4.2.14) and (4.2.16) we have

$$|R_i^{(2)}| \le 2\alpha^{-1}\varepsilon CN^{-1}, \;\; i = 0(1)N/2, \tag{4.2.22}$$

and

$$|R_i^{(3)}| \le 2\alpha^{-1}\varepsilon CN^{-1}, \;\; i = 0(1)N/2. \tag{4.2.23}$$

Combining (4.2.21), (4.2.22) and (4.2.23) for the inner region $[0,\delta]$, we get

$$|R_i| \le CN^{-1}, \;\; i = 0(1)N/2. \tag{4.2.24}$$

In the outer layer region $[\delta,1]$, assuming as in [54] that
$|u'(t)| \le C$ (or $\varepsilon^{-1}\exp(-\alpha t/\varepsilon) \le 1$), thus, application of Lemma 2.2.1 for $k=1$, leads to

$$|R_i^{(1)}| \le Ch, \quad i = N/2+1(1)N. \tag{4.2.25}$$

Following the same lines of discussion as above, we have

$$|R_i^{(1)}| \le CN^{-1}, \quad i = N/2+1(1)N, \tag{4.2.26}$$

$$|R_i^{(2)}| \leq 2CN^{-1}, \quad i = N/2 + 1(1)N, \tag{4.2.27}$$

and

$$|R_i^{(3)}| \leq 2CN^{-1}, \quad i = N/2 + 1(1)N. \tag{4.2.28}$$

From (4.2.26)-(4.2.28), we obtain for the outer region

$$|R_i| \leq CN^{-1}, \quad i = N/2 + 1(1)N. \tag{4.2.29}$$

Inequalities (4.2.24) and (4.2.29) immediately lead to the estimate (4.2.11). □

Lemma 4.2.4. *Suppose that τ_i is the solution of Problem (4.2.3)-(4.2.4). Then, we have*

$$||\tau_i||_{\infty,\psi_N} \leq C||R_i||_{\infty,\psi_N}. \tag{4.2.30}$$

Proof. The proof follows directly from (4.2.8) by taking $f \equiv R$ and $B \equiv 0$. □

We are now ready to present the main result of this chapter. The following theorem indicates that, in practice, the scheme (4.1.10)-(4.1.11) is first order convergent independently of the perturbation parameter on the piecewise-uniform Shishkin mesh.

Theorem 4.2.1. *Assume that the conditions of Lemma 2.2.1 are satisfied up to $k = 1$. Then the solution of the problems (4.1.10)-(4.1.11) converges to the solution of (1.3.1)-(1.3.2) and satisfies*

$$||u - y||_{\infty,\psi_N} \leq CN^{-1}. \tag{4.2.31}$$

Proof. The proof follows directly by combining the two previous lemmas. □

Remark 4.2.1. *Note that the above ε-uniform result does not contain the so called "locking factor" which usually surfaces when discretisations are made on Shishkin meshes. In fact, estimates of the type $||y - u||_{\infty,\psi_N} \leq CN^{-1} \ln N$ are encountered when the choice of the transition point is dependent on some factor of $\ln N$. Our choice of the transition point was inspired by [54], which uses a factor of $|\ln \varepsilon|$ (See (4.1.1)).*

4.3 Numerical verification

In this section we perform numerical experiments on two test singularly perturbed Volterra integro-differential equations.

Example 4.3.1. [63] *Consider the problem (1.3.1)-(1.3.2), where*

$$a(t) = t + 1,\ K(t,s) = t + s,$$
$$f(t) = \varepsilon \cos t + t \sin t + 2 \sin t + (t - 2t\varepsilon + \varepsilon^2) \exp\left(\frac{-t}{\varepsilon}\right) + t - 2t \cos t + \varepsilon t - \varepsilon^2,$$
$$u(0) = 1.$$

The exact solution to this problem is given by

$$u(t) = \sin t + \exp\left(\frac{-t}{\varepsilon}\right)$$

Example 4.3.2. [4] *Consider the problem (1.3.1)-(1.3.2) where*

$$a(t) = 1,\ K(t,s) = s,$$
$$f(t) = (2 + 9\varepsilon + \varepsilon t + 11t + t^2) \exp(-t) - 10(\varepsilon t + \varepsilon^2) \exp\left(\frac{-t}{\varepsilon}\right) + 5t^2 + 10\varepsilon^2 - 2,$$
$$u(0) = 10.$$

The exact solution to this problem is given by

$$u(t) = 10 - (10 + t) \exp(-t) + 10 \exp\left(\frac{-t}{\varepsilon}\right).$$

We calculated maximum point-wise errors for various values of ε and N. We have also calculated the computational rates of convergence. The maximum error $e_{\varepsilon,N}$ of the solution and the rates of convergence are evaluated using fomulae (2.5.1)-(2.5.4). Tables 4.1 and 4.2 display maximum point-wise errors along with the rate of convergence $r_{\varepsilon,k}$ for the two test examples. Clearly, it can be observed from these tables that the errors are of first order convergent as the theory indicates.

4.4 Conclusion

In this chapter we developed a descretization based on a piecewise-uniform mesh to solve (1.3.1)-(1.3.2) . We used the standard backward difference operator on a piecewise-uniform mesh of Shishkin type along with right and composite left side rectangle rules with weights and remainder terms in the integral form. It is shown that the method is robust with respect to the perturbation parameter. Two Examples were solved to show the applicability, efficiency and accuracy of the method.

Table 4.1: Results for Example 4.3.1: Maximum error and maximum rates of convergence obtained via FMFDM (4.1.10)-(4.1.11)

ε	$N = 40$	$N = 80$	$N = 160$	$N = 320$	$N = 640$	$N = 1280$	$N = 2560$
10^{-2}	6.23E-02	3.14E-02	1.57E-02	4.30E-02	6.82E-02	6.32E-02	3.69E-02
	0.96	0.14	-1.00	0.98	0.13	0.76	
10^{-4}	6.11E-02	3.08E-02	1.55E-02	7.74E-03	5.25E-03	1.46E-02	2.94E-02
	0.99	0.99	0.56	-1.47	1.01	0.72	
10^{-6}	5.95E-02	3.00E-02	1.51E-02	7.55E-03	3.78E-03	1.89E-03	9.46E-04
	0.99	0.99	0.99	0.99	0.12	-1.39	
10^{-8}	5.87E-02	2.96E-02	1.49E-02	7.45E-03	3.73E-03	1.87E-03	9.33E-04
	0.99	0.99	0.99	0.99	0.99	0.99	
10^{-10}	5.82E-02	2.94E-02	1.47E-02	7.39E-03	3.70E-03	1.85E-03	9.26E-04
	0.99	0.99	0.99	0.99	0.99	0.99	
10^{-12}	5.79E-02	2.92E-02	1.47E-02	7.36E-03	3.69E-03	1.84E-03	9.22E-04
	0.99	0.99	0.99	0.99	0.99	0.99	

Table 4.2: Results for Example 4.3.2: Maximum errors and maximum rates of convergence obtained via FMFDM (4.1.10)-(4.1.11)

ε	$N = 40$	$N = 80$	$N = 160$	$N = 320$	$N = 640$	$N = 1280$	$N = 2560$
10^{-2}	3.77E-01	2.10E-01	1.12E-01	5.76E-02	2.92E-02	1.47E-02	7.40E-03
	0.28	0.77	0.84	0.91	0.95	0.97	
10^{-4}	4.34E-01	2.18E-01	1.10E-01	5.55E-02	5.55E-02	1.47E-01	2.95E-001
	0.97	0.99	0.00	-1.40	-1.00	0.72	
10^{-6}	4.40E-01	2.22E-01	1.12E-01	5.58E-02	2.80E-02	1.40E-02	7.02E-03
	0.99	1.00	0.99	0.99	0.99	0.99	
10^{-8}	4.40E-01	2.23E-01	1.12E-01	5.61E-02	2.81E-02	1.40E-02	7.02E-03
	0.99	0.99	0.99	0.99	0.99	0.99	
10^{-10}	4.40E-01	2.23E-001	1.12E-01	5.61E-02	2.81E-02	1.41E-02	7.03E-03
	0.99	0.99	0.99	0.99	0.99	0.99	
10^{-12}	4.40E-01	2.23E-01	1.12E-01	5.61E-02	2.81E-02	1.41E-02	7.03E-03
	0.99	0.99	0.99	0.99	0.99	0.99	

We have noted that the numerical results corroborate the conclusions of the convergence analysis. However, rather than being robust for a wide range of ε, robustness is observed for only $\varepsilon < 10^{-8}$. To mitigate this drawback, we will use the well known Simpson and trapezoidal quadrature rules in the next chapter.

Chapter 5

New Parameter-Uniform Discretizations of SPVIDEs on a Piecewise Uniform Mesh.

In this chapter, we extend the method proposed in chapter 4. The new methods consist of backward finite difference scheme on a piecewise-uniform mesh of Shishkin type for the differential part. The first scheme is developed by blending the right side rectangle rule and the repeated Simpson quadrature rule and the second is obtained by combining the same right side rectangle rule and the repeated trapezoidal rule with weights and remainder terms in the integral form. We show that the two methods are first order convergent with a good improvement of the accuracy. The chapter is organised as follows. In Section 5.1 we describe the first scheme. Section 5.1.1 is devoted to the analysis of the scheme. The second scheme is given in Section 5.2. It's analysis is availabe in next section. In Section 5.3, we present numerical results. The chapter ends with concluding remarks.

5.1 Method I

To construct the fitted mesh scheme for solving the singularly perturbed problem (1.3.1)-(1.3.2), we again integrate (1.3.1) over the open interval (t_{i-1}, t_i):

$$\varepsilon h_i^{-1} \int_{t_{i-1}}^{t_i} u'(t)dt + h_i^{-1} \int_{t_{i-1}}^{t_i} a(t)u(t)dt + h_i^{-1} \int_{t_{i-1}}^{t_i} \left\{ \int_0^t K(t,s)u(s)ds \right\} dt = h_i^{-1} \int_{t_{i-1}}^{t_i} f(t)dt.$$

Using the right side rectangle rule, we have

$$\varepsilon u_{\widetilde{t},i} + a_i u_i + h_i^{-1}(t_i - t_{i-1}) \int_0^{t_i} K(t_i, s)u(s)dt + R_i^{(1)} + R_i^{(2)} = f_i, \tag{5.1.1}$$

where $R_i^{(1)}$and $R_i^{(2)}$ are respectively given by (4.1.4) and (4.1.6). Moreover applying the composite Simpson rule to the integral term in (5.1.1), we obtain

$$\begin{aligned}\int_0^{t_i} K(t_i, s)u(s)ds &= \frac{h_i}{3}K(t_i, t_i)u_i + \frac{h_i}{3}K(t_i, t_{i-1})u_{i-1} + \sum_{j=1}^{\lfloor (i/2 \rfloor} \frac{4}{3}h_{2j-1}K(t_i, t_{2j-1})u_{2j-1} \\ &+ \sum_{j=1}^{\lfloor (i-1)/2 \rfloor} \frac{2}{3}h_{2j}K(t_i, t_{2j})u_{2j} + R_i^{(3)}, \end{aligned} \tag{5.1.2}$$

where we have used (2.3.9) to calculate the remainder term

$$\begin{aligned} R_i^{(3)} &= \sum_{j=1}^{\lfloor (i/2 \rfloor} \int_{t_{j-1}}^{t_{2j-1}} (t_{2j-1} - s)\frac{d}{ds}[K(t_i, s)u(s)]ds + \\ &\sum_{j=1}^{\lfloor (i-1)/2 \rfloor} \int_{t_j}^{t_{2j}} (t_{2j} - s)\frac{d}{ds}[K(t_i, s)u(s)]ds, \end{aligned} \tag{5.1.3}$$

and $\lfloor (i-1)/2 \rfloor$ denotes the floor function of $(i-1)/2$. From (5.1.1) and (5.1.2), we have

$$\begin{aligned} &\varepsilon u_{\widetilde{t},i} + a_i u_i + \frac{h_i}{3}[K(t_i, t_i)u_i + K(t_i, t_{i-1})u_{i-1}] + \widetilde{K}(t_0, ..., t_{i-1}; u_0, ..., u_{i-1}) = R_i + f_i, \\ &i = 1(1)N, \end{aligned} \tag{5.1.4}$$

where we have

$$\widetilde{K}(t_0, ..., t_{i-1}; u_0, ..., u_{i-1}) = \left\{ \begin{array}{ll} 0 & \text{for } i = 1, \\ (4h_{2j-1}/3)K(t_i, t_{2j-1})u_{2j-1} & \text{for } i = 2, \\ \sum_{j=1}^{i/2} \frac{4}{3}h_{2j-1}K(t_i, t_{2j-1})u_{2j-1} & \\ + \sum_{j=1}^{\lfloor (i-1)/2 \rfloor} \frac{2}{3}h_{2j}K(t_i, t_{2j})u_{2j}, & \text{for } i > 2, \end{array} \right\} \tag{5.1.5}$$

and the discretization error is given by

$$\begin{aligned} R_i &= h_i^{-1} \int_{t_{i-1}}^{t_i} (t - t_{i-1})\frac{d}{dt}\left[a(t)u(t) - f(t)\right]dt \\ &+ h_i^{-1} \int_{t_{i-1}}^{t_i} \left[(t - t_{i-1})\frac{d}{dt}\int_0^t K(t, s)u(s)ds\right]dt \\ &+ \sum_{j=1}^{i/2} \int_{t_{i-1}}^{t_{2j-1}} (t_{2j-1} - s)\frac{d}{ds}[K(t_i, s)u(s)]ds \\ &+ \sum_{j=1}^{\lfloor (i-1)/2 \rfloor} \int_{t_j}^{t_{2j}} (t_{2j} - s)\frac{d}{ds}[K(t_i, s)u(s)]ds. \end{aligned} \tag{5.1.6}$$

Neglecting R_i in (5.1.4), we propose the following difference scheme for solving the problem (1.3.1)-(1.3.2):

$$L^N y_i \equiv \varepsilon y_{\widetilde{t},i} + a_i y_i + \frac{h_i}{3}[K(t_i,t_i)y_i + K(t_i,t_{i-1})y_{i-1}] + \widetilde{K}(t_0,...,t_{i-1};y_0,...,y_{i-1}) = f_i,$$
$$i = 1(1)N, \tag{5.1.7}$$
$$y_0 = \beta, \tag{5.1.8}$$

where $\widetilde{K}(t_0,...,t_{i-1},u_0,...,u_{i-1})$ is given by (5.1.5) by replacing the $u's$ by the $y's$. In matrix notation, the scheme (5.1.7)-(5.1.8) is the lower triangular linear system $AX = F$ where the various entries of the matrix A and components of the column-vector F are given by

$$\begin{aligned}
&A_{ii} = r_i^c, \quad i = 1(1)N,\\
&A_{i,i-1} = r^-_{1_{i,i-1}} \quad i = 2(2)N,\\
&A_{i,i-1} = r^-_{2_{i,i-1}} \quad i = 3(2)N,\\
&A_{i,j} = r^-_{3_{i,i-1}} \quad i = 3(1)N; j = 1(2)i-2,\\
&A_{i,j} = r^-_{4_{i,i-1}} \quad i = 3(1)N; j = 2(2)i-2,\\
&F_1 = f_1 - (-\tfrac{\varepsilon}{h_1} + \tfrac{h_1}{3}K_{10})\beta \quad i = 1,\\
&F_i = f_i, \quad i = 2(1)N,
\end{aligned}$$

with

$$\begin{aligned}
&r_i^c = \tfrac{\varepsilon}{h_i} + a_i + \tfrac{h_i}{3}K_{ii},\\
&r^-_{1_{i,i-1}} = \tfrac{-\varepsilon}{h_i} + \tfrac{h_i}{3}K_{i,i-1} + \tfrac{4}{3}h_{i-1}K_{i,i-1},\\
&r^-_{2_{i,i-1}} = \tfrac{-\varepsilon}{h_i} + \tfrac{h_i}{3}K_{i,i-1} + \tfrac{2}{3}h_{i-1}K_{i,i-1},\\
&r^-_{3_{i,i-1}} = \tfrac{4}{3}h_jK_{i,j},\\
&r^-_{4_{i,i-1}} = \tfrac{2}{3}h_jK_{i,j}.
\end{aligned}$$

In the rest of this section, we present some results whithout proofs. These results are needed to ascertain existence and uniqueness of the solution as well as the stability of the scheme. For the proofs of these results we refer the reader to Section 2.3.2 of Chapter 2.

Lemma 5.1.1. *Consider the following difference operator*

$$l^N y_i \equiv M_i y_i - Q_i y_{i-1}, \quad 1 \le i \le N, \tag{5.1.9}$$

where $M_i > Q_i > 0$ are given. The difference operator (5.1.9) satisfies the discrete maximum principle: Assume that the mesh function ψ_i satisfies $\psi_0 \ge 0$. Then the operator $l^N\psi_i \ge 0$, for all $i \ge 1$, implies that $\psi_i \ge 0$ for all $i \ge 0$

With the help of this discrete maximum principle, the following lemma which provides the bounds of the solution is obtained.

Lemma 5.1.2. *Let $l^N y_i$ be given by (5.1.9) and ϕ_i a nondecreasing mesh function . If $M_i - Q_i \geq \alpha > 0$, then for the solution of the difference initial value problem*

$$\begin{aligned} l^N y_i &= \phi_i, \quad i \geq 1, \\ y_0 &= \beta, \end{aligned}$$

the following inequality holds

$$||y_i||_\infty \leq |\beta| + \alpha^{-1} \max_{0 \leq i \leq N} |\phi_i|. \tag{5.1.10}$$

Lemma 5.1.3. *Suppose that*

$$\alpha + \frac{h_i}{3} K(t_i, t_i) \geq \alpha_* > 0, \quad i = 1(1)N, \tag{5.1.11}$$

then for the difference operator

$$l^N y_i = \varepsilon y_{\tilde{t},i} + a_i y_i + \frac{h_i}{3} K(t_i, t_i) y_i \tag{5.1.12}$$

we have

$$||y||_\infty \leq |y_0| + \alpha_*^{-1} \max_{0 \leq i \leq N} |l^N y_i| \tag{5.1.13}$$

Lemma 5.1.4. *Let the difference operator $l^N y_i$ be given by (5.1.12). Then for the difference problem (5.1.7)-(5.1.8) we have*

$$|l^N y_i| \leq ||f||_\infty + C \sum_{j=1}^{i} h_j |y_{j-1}| \quad 1 \leq i \leq N. \tag{5.1.14}$$

For this particular lemma, we provide the main lines of the proof as this is different from proofs in Chapter 2.

Proof. From scheme (5.1.7) we have

$$|l^N y_i| \leq |f_i| + \left| \sum_{j=1}^{\frac{i}{2}} \frac{4}{3} h_{2j-1} K(t_i, t_{2j-1}) u_{2j-1} \right| + \left| \sum_{j-1}^{\lfloor (i-1)/2 \rfloor} \frac{2}{3} h_{2j} K(t_i, t_{2j}) u_{2j} \right|.$$

If one classifies the weights in the summation and considers i, j as total mesh points for the partitions of odd and even mesh points, then one has

$$l^N y_i \leq ||f|| + |\sum_{j=1}^{i} \widetilde{w_{ij}} h_j K(t_i, t_j) u_{j-1}| \tag{5.1.15}$$

where

$$\widetilde{w_{ij}} = \begin{cases} \frac{4}{3} & 1 \le j \le i/2 \quad i,j \quad \text{(odd)} \\ \frac{2}{3} & 1 \le j \le \lfloor (i-1)/2 \rfloor \quad i,j \quad \text{(even)}. \end{cases} \tag{5.1.16}$$

The proposition of the lemma follows directly by taking into account the boundedness of $K(t,s)$.

□

Lemma 5.1.5. *Let the condition (5.1.11) be satisfied. Then for the solution of the difference scheme (5.1.7)-(5.1.8), we have*

$$|y_i| \le (\alpha_*^{-1}||f||_\infty + |\beta|)\exp(\alpha_*^{-1}Ct_i), \quad 1 \le i \le N. \tag{5.1.17}$$

5.1.1 Convergence analysis of method I

To investigate the convergence of our method, note that the error function $\tau_i = u_i - y_i$, $i \in [0,N]$, satisfies the discrete problem

$$\begin{aligned} l^N\tau_i \equiv\ & \varepsilon\tau_i + [a_iu_i - a_iy_i] + \frac{h_i}{3}[K(t_i,t_i)u_i - K(t_i,t_i)y_i] + \\ & \frac{h_i}{3}[K(t_i,t_{i-1})u_{i-1} + K(t_i,t_{i-1})y_{i-1}] + \widetilde{K} = R_i, \quad i = 1(1)N, \end{aligned} \tag{5.1.18}$$

$$\tau_0 = 0, \tag{5.1.19}$$

where u_i and y_i are solutions of the problem (1.3.1)- (1.3.2) and (5.1.7)-(5.1.8) respectively. Here the remainder term R_i is given by (5.1.6) and

$$\widetilde{K} = \begin{cases} 0, & \text{for } i = 1, \\ (4h_{2j-1}/3)[K(t_i,t_{2j-1})u_{2j-1} - K(t_i,t_{2j-1})y_{2j-1}], & \text{for } i = 2, \\ \sum\limits_{j=1}^{i/2} \frac{4}{3}h_{2j-1}[K(t_i,t_{2j-1})u_{2j-1} - K(t_i,t_{2j-1})y_{2j-1}] & \\ + \sum\limits_{j=1}^{\lfloor (i-1)/2 \rfloor} \frac{2}{3}h_{2j}[K(t_i,t_{2j})u_{2j} - K(t_i,t_{2j})y_{2j}] & \text{for } i = 3(1)N. \end{cases}$$

Lemma 5.1.6. *Let the assumptions of Lemma 2.2.1 be guaranteed up to $k = 1$. Then for the truncation error R_i, the following estimates holds:*

$$||R||_{1,\psi_N} \le CN^{-1} \tag{5.1.20}$$

Proof. The remainder term of the scheme (5.1.7) can be rewritten as

$$R_i = R_i^{(1)} + R_i^{(2)} + R_i^{(3)}, \tag{5.1.21}$$

where $R_i^{(1)}$ and $R_i^{(2)}$ are respectively given by (4.1.4) and (4.1.6) and

$$\begin{aligned} R_i^{(3)} \quad \leq \quad & \sum_{j=1}^{\frac{i}{2}} \int_{t_{j-1}}^{t_{2j-1}} (t_{2j-1} - s) \frac{d}{ds} K(t_i, s) u(s) ds + \\ & \sum_{j=1}^{\lfloor (i-1)/2 \rfloor} \int_{t_j}^{t_{2j}} (t_{2j} - s) \frac{d}{ds} K(t_i, s) u(s) ds. \end{aligned} \tag{5.1.22}$$

Following the discussions from Chapter 4 Section 4.2, the inequalities $R_i^{(1)}$ and $R_i^{(2)}$ immediately lead to

$$|R_i^{(1)}| \leq C\Big\{ h_i + \frac{1}{\varepsilon} \int_{t_{i-1}}^{t_i} \exp(-\alpha t/\varepsilon) dt \Big\}, \quad i = 1(1)N. \tag{5.1.23}$$

and

$$|R_i^{(2)}| \leq C h_i \quad i = 1(1)N. \tag{5.1.24}$$

Furthermore, for $R_i^{(3)}$, we rewrite

$$\begin{aligned} |R_i^{(3)}| \quad \leq \quad & \sum_{j=1}^{\frac{i}{2}} \int_{t_{j-1}}^{t_{2j-1}} (t_{2j-1} - s) \left| \frac{d}{ds} K(t_i, s) u(s) \right| ds \\ & + \sum_{j=1}^{\lfloor (i-1)/2 \rfloor} \int_{t_j}^{t_{2j}} (t_{2j} - s) \left| \frac{d}{ds} K(t_i, s) u(s) \right| ds. \end{aligned} \tag{5.1.25}$$

Using (5.1.16), the above inequality becomes

$$|R_i^{(3)}| \quad \leq \quad \left| \sum_{j=1}^{i} \int_{t_{j-1}}^{t_j} (t_j - s) \widetilde{w_{ij}} \frac{d}{ds} K(t_i, s) u(s) \right| ds. \tag{5.1.26}$$

Thus, by similar procedure as the one employed in deriving in (4.2.15), we get for $R_i^{(3)}$

$$|R_i^{(3)}| \leq C h_i, \quad i = 1(1)N, \tag{5.1.27}$$

where h_i is given by (4.2.17). Now, by a similar process to the one adopted in chapter 4 for the error analysis, the truncation error of the scheme (5.1.7)-(5.1.8) is examined separetely in the subdomains $[0, \delta]$ and $[\delta, 1]$ for $\delta = \alpha^{-1} \varepsilon |\ln \varepsilon|$. Therefore in $[0, \delta]$, using (4.2.19) and (4.2.20), we deduce from (5.1.23) that

$$|R_i^{(1)}| \leq C N^{-1}, \quad i = 1(1)N/2, \tag{5.1.28}$$

so that by similar arguments (5.1.24) and (5.1.27) become,

$$|R_i^{(2)}| \leq CN^{-1}, \quad i = 1(1)N/2, \tag{5.1.29}$$

$$|R_i^{(3)}| \leq CN^{-1}, \quad i = 1(1)N/2. \tag{5.1.30}$$

Combining (5.1.28)-(5.1.30) we obtain the estimate

$$|R_i| \leq CN^{-1}, \quad i = 1(1)N/2. \tag{5.1.31}$$

Next, in $[\delta, 1]$, recalling that $|u'(t)| \leq C$, hereby we get

$$|R_i^{(1)}| \leq Ch, \quad i = N/2 + 1(1)N. \tag{5.1.32}$$

In a similar way as above, we obtain

$$|R_i^{(1)}| \leq CN^{-1}, \quad i = N/2 + 1(1)N. \tag{5.1.33}$$

$$|R_i^{(2)}| \leq CN^{-1}, \quad i = N/2 + 1(1)N, \tag{5.1.34}$$

$$|R_i^{(3)}| \leq CN^{-1}, \quad i = N/2 + 1(1)N. \tag{5.1.35}$$

From (5.1.33)-(5.1.35) for the subdomain $[\delta, 1]$ we obtain

$$|R_i| \leq CN^{-1}, \quad i = N/2 + 1(1)N. \tag{5.1.36}$$

And this completes the proof. □

Lemma 5.1.7. *Under the conditions (5.1.11) and Lemma 5.1.5, the solution τ_i of the problem (5.1.18) and (5.1.19) satisfies*

$$||\tau_i||_{\infty,\psi_N} \leq \max_{0 \leq i \leq N} |R_i| \tag{5.1.37}$$

The main result of this paper is contained in the following theorem which establishes a first order ε-uniform error estimate.

Theorem 5.1.1. *Let the hypothesis of Lemma 2.2.1 be guaranteed up to $k = 1$. Then the following first order ε-uniform convergent inequality*

$$||u - y||_{\infty,\psi_N} \leq CN^{-1}$$

holds.

5.2 Method II

As indicated in the introduction of this chapter, the scheme we suggest in this section consists of the right side rectangle along with the repeated trapezoidal quadrature rule. Thus, consistently with the fitted mesh method constructed in chapters 4 as well as the one in the previous section, we have the following expression for u_i

$$u_{\tilde{t},i} + a_i u_i + \frac{h_i}{4} K(t_i, t_i) u_i + \frac{h_i}{4} K(t_i, t_{i-1}) u_{i-1} + \widetilde{K}(t_0, ..., t_{i-1}; u_0, ..., u_{i-1}) +$$
$$R_i = f_i \quad i = 1(1)N, \tag{5.2.1}$$

where

$$\widetilde{K}(t_0, ..., t_{i-1}; u_0, ..., u_{i-1}) = \begin{cases} 0 & \text{for } i = 1, \\ \sum_{j=1}^{i-1} \frac{h_j}{2} [K(t_i, t_j) u_j + K(t_i, t_{j-1}) u_{j-1}] & \text{for } i > 1, \end{cases}$$

and the discretization error is given by

$$R_i = -h_i^{-1} \int_{t_{i-1}}^{t_i} (t - t_{i-1}) \frac{d}{dt} [a(t)u(t) - f(t)] \, dt - h_i^{-1} \int_{t_{i-1}}^{t_i} (t - t_{i-1}) \frac{d}{dt} \Big[\int_0^t K(t, s) u(s) ds \Big] dt$$
$$+ \sum_{j=1}^{i} \int_{t_{j-1}}^{t_j} (t_j - s) \frac{d}{dt} [K(t_i, s) u(s) ds] \, . \tag{5.2.2}$$

Neglecting the remainder term in (5.2.1), the following difference scheme may be used to approximate (1.3.1)-(1.3.2).

$$L^N y_i \equiv \varepsilon y_{\tilde{t},i} + a_i y_i + \frac{h_i}{4} K(t_i, t_i) y_i + \frac{h_i}{4} K(t_i, t_{i-1}) y_{i-1} + \widetilde{K}(t_0, ..., t_{i-1}; y_i, ..., y_{i-1}) = f_i,$$
$$i = 1(1)N, \tag{5.2.3}$$
$$y_0 = \gamma_0, \tag{5.2.4}$$

where

$$\widetilde{K}(t_0, ...t_{i-1}; y_0, ..., y_{i-1}) = \begin{cases} 0 & \text{for } i = 1, \\ \sum_{j=1}^{i-1} \frac{h_j}{2} [K(t_i, t_j) y_j + K(t_i, t_{j-1}) y_{j-1}], & \text{for } i > 1. \end{cases}$$

The lower triangular system of linear equations (5.2.3)-(5.2.4) takes the form

$$AU = F, \tag{5.2.5}$$

where the various entries of the matrix A and components of the column-vector F are given by

$$\begin{aligned}
&A_{ii} = r_i^c, \quad i = 1(1)N,\\
&A_{i,i-1} = r_{i,i-1}^- \quad i = 2(1)N,\\
&A_{i,j} = r_{i,i-1}^- \quad i = 3(1)N; j = 1(1)i-1,\\
&F_1 = f_1 - \left(-\frac{\varepsilon}{h_1} + \frac{h_1}{4}K_{10}\right) y_0 \quad i = 1,\\
&F_i = f_i - \left(\frac{h_1}{2}K_{i0}\right) y_0 \quad i = 2(1)N,
\end{aligned}$$

where

$$\begin{aligned}
r_i^c &= \left(\frac{\varepsilon}{h_i}\right) + a_i + \frac{h_i}{4}K_{ii},\\
r_{i,i-1}^- &= \left(\frac{-\varepsilon}{h_i}\right) + \frac{h_i}{4}K_{i,i-1} + \frac{1}{2}h_{i-1}K_{i,i-1},\\
r_{i,i-1}^- &= \left(\frac{h_j + h_{j-1}}{2}\right) K_{i,j}.
\end{aligned}$$

Here, we refer to this scheme as FMFDM. The discrete operator in the FMFDM satisfies the following lemmas

Lemma 5.2.1. *Consider the following difference operator*

$$l^N y_i \equiv V_i y_i - W_i y_{i-1}, \quad 1 \le i \le N, \tag{5.2.6}$$

where $V_i > 0$ and $W_i > 0$ are given. Then, for all mesh function ξ_i such that $\xi_0 \ge 0$, $l^N \xi_i \ge 0$, for all $i \ge 1$, we have $\xi_i \ge 0$ for all $0 \le i \le N$.

An immediate consequence of the lemma above is the following boundedness result.

Lemma 5.2.2. *Let $l^N y_i$ be defined as in (5.2.6). If $V_i - W_i \ge \alpha > 0$, then for the solution of the difference initial value problem*

$$l^N y_i = G_i, \quad i \ge 1, \tag{5.2.7}$$

$$y_0 = \nu, \tag{5.2.8}$$

the following inequality holds

$$||y||_\infty \le |\mu| + \alpha^{-1} \max_{0 \le i \le N} |G_i|. \tag{5.2.9}$$

The proofs for the two previous lemmas are obtained by similar arguments to those used in proving Lemma 2.3.1.

Lemma 5.2.3. *Assume that*

$$\alpha + \frac{h_i}{4} K_{ii} \geq \alpha_* > 0, \quad i = 1(1)N, \tag{5.2.10}$$

then for the difference operator

$$l^N v_i = \varepsilon v_{\widetilde{t},i} + a_i v_i + \frac{h_i}{4} K_{ii} v_i, \tag{5.2.11}$$

where $K_{ii} = K(t_i, t_i)$ *we have*

$$||v_i||_\infty \leq |v_0| + \alpha \max_{0 \leq i \leq N} |l^N v_i|. \tag{5.2.12}$$

The proof can be easly deduced from Lemma 2.3.2

Lemma 5.2.4. *(Stability result). Let the difference operator* $l^N y_i$ *be given by (5.2.11). Then for difference problem (5.2.3)-(5.2.4) we have the following estimate*

$$l^N y_i \leq C \sum_{j=1}^{i} h_j |y_{j-1}| + ||f||_\infty, \quad 1 \leq i \leq N. \tag{5.2.13}$$

Proof similar to the one of Lemma 2.3.2.

Lemma 5.2.5. *Let (5.2.10) be satisfied, then for the solution of the difference scheme (5.2.3)-(5.2.4) we have the following estimate*

$$|y_i| \leq (\alpha_*^{-1} ||f||_\infty + |A|) \exp(\alpha_*^{-1} C t_i), \quad 1 \leq i \leq N. \tag{5.2.14}$$

Proof. See the one of Lemma 2.3.4

5.2.1 Convergence analysis of method II

Let $\tau_i = y_i - u_i$, $0 \leq i \leq N$, where y_i is the solution of (5.2.3)-(5.2.4) and u_i the solution of (1.3.1)-(1.3.2) at the mesh point t_i. Then for the error function τ_i, we have

$$\begin{aligned} L^N \tau_i =& \varepsilon \tau_{\widetilde{t},i} + [a_i y_i - a_i u_i] + \frac{h_i}{2}[K(t_i, t_i) y_i - K(t_i, t_i) u_i] + \\ & \frac{h_i}{2}[K(t_i, t_{i-1}) y_{i-1} - K(t_i, t_{i-1}) u_{i-1}] + \widetilde{K} + R_i \quad i = 1(1)N, \end{aligned} \tag{5.2.15}$$

$$\tau_0 = 0, \tag{5.2.16}$$

where the remainder term R_i is given by (5.2.2) and

$$\widetilde{K} = \begin{cases} 0 & \text{for } i = 1, \\ \sum_{j=1}^{i} h_j \{[K(t_i, t_j) y_j - K(t_i, t_j) u_j] + [K(t_i, t_{j-1}) y_{j-1} - K(t_i, t_{j-1}) u_{j-1}]\} & \text{for } i > 1. \end{cases}$$

Lemma 5.2.6. *Under the requirements of Lemma 2.2.1, for the remainder term R_i of the scheme (5.2.3)-(5.2.4) the inequality*

$$||R||_{\infty,\psi_N} \leq CN^{-1} \tag{5.2.17}$$

holds.

Proof. The proof of this Lemma follows directly in view of the techniques and discussions used in proving Lemma 4.2.3 and 5.1.6 for the remainder terms.

Lemma 5.2.7. *Let (5.2.10) be satisfied. Then the solution τ_i of the problem (5.2.15)-(5.2.16) satisfies*

$$||\tau_i||_{\infty,\psi_N} \leq \max_{0\leq i\leq N}|R_i|. \tag{5.2.18}$$

Combining the results in the two previous lemmas, we have the convergence result

Theorem 5.2.1. *Let u be the solution of (1.3.1)-(1.3.2) and y the solution of (5.2.3)-(5.2.4). Under the conditions of Lemma 2.2.1 for $k = 1$, the inequality*

$$||y - u||_{\infty,\psi_N} \leq CN^{-1} \tag{5.2.19}$$

is true.

5.3 Numerical results

In this section, we test the two numerical methods described in this chapter. To this end, the two Volterra integro-differential equations solved in chapter two are again considered here. The maximum errors along with the rates of convergence are given in tabular form and evaluated using the fomulae (2.5.1)-(2.5.4).

Example 5.3.1. [63]

Consider problem (1.3.1)-(1.3.2) with

$$a(t) = t + 1,\ K(t,s) = t + s,$$

$$f(t) = \varepsilon\cos t + t\sin t + 2\sin t + (t - 2t\varepsilon + \varepsilon^2)\exp\left(\frac{-t}{\varepsilon}\right) + t - 2t\cos t + \varepsilon t - \varepsilon^2,$$

$$u(0) = 1.$$

The exact solution to this problem is given by

$$u(t) = \sin t + \exp\left(\frac{-t}{\varepsilon}\right).$$

Example 5.3.2. [4]

Consider problem(1.3.1)-(1.3.2) with

$$a(t) = 1,\ K(t,s) = s,$$
$$f(t) = (2 + 9\varepsilon + \varepsilon t + 11t + t^2)\exp(-t) - 10(\varepsilon t + \varepsilon^2)\exp\left(\frac{-t}{\varepsilon}\right) + 5t^2 + 10\varepsilon^2 - 2,$$
$$u(0) = 10.$$

The exact solution to this problem is given by

$$u(t) = 10 - (10 + t)\exp(-t) + 10\exp\left(\frac{-t}{\varepsilon}\right).$$

Our theoretical analysis shows that the two methods developed are of first order uniformly convergent independently of the perturbation parameter ε as mentioned in theorems 5.1.1 and 5.2.1 . This is confirmed by numerical results presented in tables 5.1-5.4 where we have computed the maximum errors $e_{\varepsilon,N}$ and the corresponding rates of convergence $r_{\varepsilon,k}$.

Table 5.1: Results for Example 5.3.1: Maximum errors and maximum rates of convergence obtained via FMFDM (5.1.7)-(5.1.8)

ε	$N = 40$	$N = 80$	$N = 160$	$N = 320$	$N = 640$	$N = 1280$	$N = 2560$
10^{-2}	5.60E-03	1.12E-02	2.22E-02	4.31E-02	8.11E-02	1.32E-02	1.00E-02
	0.14	-100	0.98	0.95	-0.95	0.61	
10^{-3}	6.21E-03	3.14E-03	1.58E-03	7.98E-04	4.93E-04	2.44E-04	1.58E-04
	0.99	0.93	0.99	0.99	0.98	0.98	
10^{-4}	6.21E-03	3.14E-03	1.58E-03	7.90E-04	3.97E-04	1.94E-04	1.48E-04
	0.99	0.99	0.99	1.00	0.99	0.98	
10^{-5}	6.21E-03	3.14E-03	1.58E-03	7.90E-04	3.95E-04	1.98E-04	9.90E-05
	0.99	0.99	0.99	0.99	0.99	0.98	
$\vdots$	$\vdots$	$\vdots$	$\vdots$	$\vdots$	$\vdots$	$\vdots$	$\vdots$
E_N	6.21E-03	3.14E-03	1.58E-03	7.90E-04	3.95E-04	1.98E-04	9.90E-05
r_N	0.98	0.99	0.99	0.99	0.99	0.99	

Table 5.2: Results for Example 5.3.2: Maximum errors and maximum rates of convergence obtained via FMFDM (5.1.7)-(5.1.8)

ε	$N = 40$	$N = 80$	$N = 160$	$N = 320$	$N = 640$	$N = 1280$	$N = 2560$
10^{-2}	6.02E-02	8.18E-02	6.98E-02	3.98E-02	2.29E-02	1.24E-02	6.44E-03
	-0.97	0.92	-0.62	0.00	0.64	0.81	
10^{-3}	2.26E-02	1.25E-02	5.71E-03	3.10E-03	1.45E-03	1.60E-02	7.79E-03
	0.98	0.95	0.98	0.97	0.95	0.77	
10^{-4}	2.16E-02	1.11E-02	5.61E-03	2.83E-03	1.42E-03	7.42E-03	3.64E-04
	0.98	0.99	0.99	0.99	0.99	0.99	
10^{-5}	2.16E-02	1.11E-02	5.61E-03	2.83E-03	1.42E-03	7.10E-04	3.55E-04
	0.98	0.99	0.99	0.99	0.99	0.98	
$\vdots$	$\vdots$	$\vdots$	$\vdots$	$\vdots$	$\vdots$	$\vdots$	$\vdots$
E_N	2.16E-02	1.11E-02	5.61E-03	2.83E-03	1.42E-03	7.10E-04	3.55E-04
r_N	0.98	0.99	0.99	0.99	0.99	0.99	

Table 5.3: Results for Example 5.3.1: Maximum errors and maximum rates of convergence obtained via FMFDM (5.2.3)-(5.2.4)

ε	$N = 40$	$N = 80$	$N = 160$	$N = 320$	$N = 640$	$N = 1280$	$N = 2560$
10^{-2}	2.93E-02	1.49E-02	4.30E-02	6.82E-02	6.32E-02	3.69E-02	1.01E-2
	1.00	1.00	1.00	1.00	1.00	1.00	
10^{-3}	2.91E-02	1.46E-02	7.28E-03	5.25E-03	1.46E-02	2.94E-02	6.64E-03
	1.00	1.00	1.00	1.00	1.00	1.00	
10^{-4}	2.89E-02	1.45E-02	7.23E-03	3.62E-03	1.81E-03	1.75E-03	5.85E-04
	1.00	1.00	1.00	1.00	1.00	1.00	
10^{-5}	2.87E-02	1.44E-02	7.20E-03	3.60E-03	1.80E-03	9.01E-04	4.50E-04
	1.00	1.00	1.00	1.00	1.00	1.00	
$\vdots$	$\vdots$	$\vdots$	$\vdots$	$\vdots$	$\vdots$	$\vdots$	$\vdots$
E_N	2.85E-02	1.43E-02	7.17E-03	3.58E-03	1.79E-03	8.95E-04	4.47E-04
r_N	1.00	1.00	1.00	1.00	1.00	1.00	

Table 5.4: Results for Example 5.3.2: Maximum errors and maximum rates of convergence via obtained FMFDM (5.2.3)-(5.2.4)

ε	$N = 40$	$N = 80$	$N = 160$	$N = 320$	$N = 640$	$N = 1280$	$N = 2560$
10^{-2}	2.30E-01	1.19E-01	6.02E-02	3.03E-02	1.52E-02	2.84E-02	5.65E-02
	0.98	0.98	0.99	-0.90	-0.99	-0.98	
10^{-3}	2.30E-01	1.17E-01	6.01E-02	3.06E-02	1.51E-02	7.53E-03	4.86E-03
	0.97	0.98	0.99	0.99	0.62	0.99	
10^{-4}	2.30E-01	1.18E-01	6.02E-02	3.01E-02	1.51E-02	7.64E-03	3.86E-03
	0.97	0.98	0.99	0.99	0.99	0.99	
10^{-5}	2.30E-01	1.18E-01	6.02E-02	3.01E-02	1.51E-02	7.64E-03	3.86E-03
	0.97	0.98	0.99	0.99	0.99	0.99	
$\vdots$	$\vdots$	$\vdots$	$\vdots$	$\vdots$	$\vdots$	$\vdots$	$\vdots$
E_N	2.30E-01	1.18E-01	6.02E-02	3.01E-02	1.51E-02	7.64E-03	3.86E-03
r_N	0.97	0.98	0.99	0.99	0.99	0.99	

5.4 Conclusion

In this chapter, we proposed two fitted finite difference schemes to solve (1.3.1)-(1.3.2). While the first one is developed using the right side rectangle rule along with the repeated Simpson's quadrature rule to discrete the integral part of the problem, the second consisted in a combination of the right side rectangle rule with the repeated trapezoidal integration. In both cases, the backward difference operator have been utilized to discretize the derivative part of the problem. In order for the two methods to be ε-uniform, a piecewise-uniform mesh of Shishkin type was considered.

We have shown that the proposed schemes are both uniformly convergent of order one with respect to the perturbation parameter and of the mesh parameter. However, as compared to the method of the previous chapter, we have noticed that the two methods are more accurate. Numerical computations have been performed on two Volterra equations to illustrate our theoretical results.

In the next chapter we suggest a new fitted operator finite difference method.

Chapter 6

A new Exponentially Fitted Operator Finite Difference Method for SPVIDEs

In this chapter, we introduce a new discretization of (1.3.1)-(1.3.2). The aim of the discretization is to improve results obtained via the method of chapter 2. The present method falls under the class of FOFDMs.

The method uses the right side rectangle rule together with the method of integral identities and the exponential basis function to derive the fitting factors which helps in discretizing the derivative part of the problem. Then the trapezoidal rule with the weights and remainder terms in the integral form is used to deal with the integral part. This is what demarcates this method from the one in chapter 2 and others found in the literature.

The overall method is analysed for convergence and stability and found to be of first order convergence. In comparison to the method of Chapter 2, the present method is more accurate in the sense that it produces small nodal maximum errors.

The rest of this chapter is organized as follows. The numerical method is derived in Section 6.1. In section 6.2 we presents some qualitative results regarding the scheme. Section 6.3 is devoted to the error analysis. Numerical results are presented in Section 6.4. A short conclusion and discussion are given in Section 6.5.

6.1 Derivation of the scheme

In this section the mesh is taken to be uniform. As before, let N be a positive integer. We consider the following uniform partition of the interval $[0,1]$ which we denote by $\bar{\psi}^N$: $t_0 = 0,\ \ t_i = t_0 + ih,\ \ i = 1(1)N,\ \ t_N = 1$ where $h = 1/N$, the step-size.

We first construct the numerical method.

To get started, we consider the identity (2.3.1) i.e.,

$$\chi_i^{-1}h^{-1}\int_{t_{i-1}}^{t_i} Lu\varphi_i(t)dt = \chi^{-1}h^{-1}\int_{t_{i-1}}^{t_i} f(t)\varphi_i(t)dt, \quad i = 1(1)N, \tag{6.1.1}$$

where the exponential function $\varphi_i(t)$ and χ_i are respectively variants of (2.3.2) and (2.3.3) given by

$$\varphi_i(t) = \exp\left(\frac{a_i}{\varepsilon}(t - t_i)\right), \tag{6.1.2}$$

$$\chi_i = h^{-1}\int_{t_{i-1}}^{t_i} \varphi_i(t)dt = \frac{1 - \exp(-\rho a_i)}{\rho a_i}, \tag{6.1.3}$$

$(\rho = h/\varepsilon)$.

We note that the exponential basis function $\varphi_i(t)$ satisfies (2.3.4) and (2.3.5). Thus, equation (6.1.1) is written in the form

$$\chi_i^{-1}h^{-1}\varepsilon\int_{t_{i-1}}^{t_i} u'(t)\varphi_i(t)dt + \chi_i^{-1}h^{-1}a_i\int_{t_{i-1}}^{t_i} u(t)\varphi_i(t)dt + \chi_i^{-1}h^{-1}\int_{t_{i-1}}^{t_i}\varphi_i(t)\left(\int_0^t K(t,s)u(s)ds\right)dt = f_i - R_i^{(1)}, \tag{6.1.4}$$

where

$$R_i^{(1)} = \chi_i^{-1}h^{-1}\int_{t_{i-1}}^{t_1}[a(t) - a(t_i)]u(t)\varphi_i(t)dt + \chi_i^{-1}h^{-1}\int_{ti-1}^{t_i}[f(t_i) - f(t)]\varphi_i(t)dt.$$

Using quadrature rules (2.3.7) for $\sigma = 1$ and (2.3.8) on the interval $[t_i - t_{i-1}]$ and taking into considerartion equation (2.3.4), (6.1.4) is reduced to

$$\begin{aligned}
&\varepsilon u_{\tilde{t},i}\left[\chi_i^{-1}h^{-1}\int_{t_{i-1}}^{t_i}\varphi_i(t)dt + \chi_i^{-1}h^{-1}a_i\int_{t_{i-1}}^{ti}(t - t_i)\varphi_i(t)dt\right]\\
&+ a_i\chi_i^{-1}h^{-1}\int_{t_{i-1}}^{t_i}\varphi_i(t)dtu_i + \chi_i^{-1}h^{-1}\int_{t_{i-1}}^{t_i}\varphi_i(t)dt\int_0^{t_i}K(t_i,s)u(s)ds +\\
&+ \chi_i^{-1}h^{-1}\int_{t_{i-1}}^{t_i}\varphi_i(t)dt\times\int_{t_{i-1}}^{t_i}\frac{d}{d\eta}\left[\int_0^{\eta}K(\eta,s)u(s)ds\right][H(T-\eta)-1]d\eta\\
=&\varepsilon\Delta_i u_{\tilde{t},i} + a_i u_i + \int_0^{t_i}K(t_i,s)u(s)ds + \chi_i^{-1}h^{-1}\int_{t_{i-1}}^{t_i}\varphi_i(t)dt\times\\
&\int_{t_{i-1}}^{t_i}\frac{d}{d\eta}\left[\int_0^{\eta}K(\eta,s)u(s)ds\right][H(T-\eta)-1]d\eta,
\end{aligned}$$

where we have used (2.3.5),

$$\Delta_i = 1 + \chi_i^{-1} h^{-1} a_i \int_{t_{i-1}}^{ti} (t - t_i)\varphi_i(t)dt, \tag{6.1.5}$$

and $H(T-\eta)$ is a Heaviside function. Moreover, applying the repeated trapezoidal integration to the integral in the last expression we obtain

$$\int_0^{t_i} K(t_i, s)u(s)ds = \frac{h}{4}K(t_i, t_i)u_i + \frac{h}{4}K(t_i, t_{i-1})u_{i-1} + \frac{h}{2}\widetilde{K}(t_0, ...t_{i-1}; u_0, ..., u_{i-1}) + R_i^{(3)}$$

which together with (6.1.4) lead to the following expression for $u(t_i)$:

$$\begin{aligned} &\varepsilon\Delta_i u_{\widetilde{t},i} + a_i u_i + \frac{h}{4}K(t_i, t_i)u_i + \frac{h}{4}K(t_i, t_{i-1})u_{i-1} + \\ &\frac{h}{2}\widetilde{K}(t_0, ...t_{i-1}; u_0, ..., u_{i-1}) + R_i = f_i, \quad i = 1(1)N, \end{aligned} \tag{6.1.6}$$

where

$$\begin{aligned} R_i &= -\chi_i^{-1}h^{-1}\int_{t_{i-1}}^{t_1}[a(t) - a(t_i)]u(t)\varphi_i(t)dt + \chi_i^{-1}h^{-1}\int_{ti-1}^{t_i}[f(t_i) - f(t)]\varphi_i(t)dt + \\ &\chi_i^{-1}h^{-1}\int_{t_{i-1}}^{t_i}\varphi_i(t)dt \times \int_{t_{i-1}}^{t_i}\frac{d}{d\eta}\left[\int_0^{\eta}K(\eta, s)u(s)ds\right][H(T-\eta) - 1]d\eta + \\ &\sum_{j=1}^{i}\int_{t_{j-1}}^{t_j}(t_j - \eta)\frac{d}{ds}[K(t_i, \eta)u(\eta)]d\eta. \end{aligned} \tag{6.1.7}$$

and

$$\widetilde{K}(t_0, ..., t_{i-1}; u_0, ..., u_{i-1}) = \begin{cases} 0 & \text{for } i = 1, \\ \sum_{j=1}^{i-1}[K(t_i, t_j)u_j + K(t_i, t_{j-1})u_{j-1}] & \text{for } i > 1. \end{cases}$$

Simplifying (6.1.5), we get

$$\Delta_i = \frac{\rho a_i \exp(\rho a_i)}{(1 - \exp(-\rho a_i))}.$$

Neglecting R_i in (6.1.6) we obtain the following exponential finite difference scheme to approximate (1.3.1)-(1.3.2):

$$\begin{aligned} L^h y_i &\equiv \varepsilon\Delta_i y_{\widetilde{t},i} + a_i y_i + \frac{h}{4}K(t_i, t_i)y_i + \frac{h}{4}K(t_i, t_{i-1})y_{i-1} + \\ &\quad \frac{h}{2}\widetilde{K}(t_0, ...t_{i-1}; y_0, ..., y_{i-1}) = f_i, \quad i = 1(1)N, \end{aligned} \tag{6.1.8}$$

$$y_0 = \gamma_0, \tag{6.1.9}$$

where

$$\widetilde{K}(t_0, ...t_{i-1}; y_0, ..., y_{i-1}) = \begin{cases} 0 & \text{for } i = 1, \\ \sum_{j=1}^{i-1}[K(t_i, t_j)y_j + K(t_i, t_{j-1})y_{j-1}] & \text{for } i > 1. \end{cases}$$

The lower triangular system of linear equation (6.1.8)-(6.1.9) takes the form

$$AU = F,$$

where the entries of the matrix A and column vector F are given by:

$$\begin{aligned}
&A_{ii} = r_i^c, \quad i = 1(1)N,\\
&Ai, i-1 = r_{i,i-1}^- \quad i = 2(1)N,\\
&Ai, j = r_{i,i-1}^- \quad i = 3(1)N; j = 1(1)i-1,\\
&F = f_1 - \left(-\frac{\varepsilon\Delta_1}{h} + \frac{h}{4}KK_1\right) y_0 \quad i = 1,\\
&F_i = f_i - \left(\frac{h}{2}KK_i\right) y_0 \quad i = 2(1)N,
\end{aligned}$$

with

$$\begin{aligned}
r_i^c &= \frac{\varepsilon\Delta_i}{h} + a_i + \frac{h}{4}K_{ii},\\
r_{i,i-1}^- &= \frac{-\varepsilon\Delta_i}{h} + \frac{h}{4}K_{i,i-1} + \frac{1}{2}hK_{i,i-1},\\
r_{i,i-1}^- &= \frac{h}{2}K(t_i, t_j).
\end{aligned}$$

In the next section, we present some useful facts of the scheme above.

6.2 Some qualitative results regarding the scheme

The results which we present (in form of lemmas) are similar to those encountered in chapter 2. For this reason, as they are similar, proofs are not provided. However, where necessary, we provide an indication of the mains ideas of the proof.

Lemma 6.2.1. *Let the difference operator*

$$l^h y_i = E_i y_i - H_i y_{i-1}, \quad 1 \le i \le N, \tag{6.2.1}$$

be given, where $E_i > H_i > 0$. Then the difference operator (6.2.1) satisfies the following discrete maximum principal: if $ly_i \ge 0$, $\forall\ i \ge 0$ and $y_0 \ge 0$, then $y_i \ge 0$, $\forall\ i \ge 0$.

Lemma 6.2.2. *Let $l^h y_i$ be defined as in (6.2.1). If $E_i - H_i \ge \alpha > 0$, then for the solution of the difference initial value problem*

$$\begin{aligned}
l^h y_i &= F_i, \quad i \ge 1,\\
y_0 &= \mu
\end{aligned}$$

the following inequality holds

$$||y_i||_\infty \leq |\mu| + \alpha^{-1} \max_{0\leq i\leq N} |F_i|. \tag{6.2.2}$$

Proof. Following the technique of proof given in Lemma 2.3.1, we can prove the present lemma.

Lemma 6.2.3. *Let the condition*

$$\alpha + \frac{h}{4} K_{ii} \geq \alpha_* > 0, \quad i = 1(1)N \tag{6.2.3}$$

be guaranteed. Then for the difference operator

$$l^h v_i = \varepsilon \theta_i v_{\tilde{t},i} + a_i v_i + \frac{h}{4} K_{ii} v_i \tag{6.2.4}$$

we have

$$||v_i||_\infty \leq |v_0| + \alpha \max_{0\leq i\leq N} |l^h v_i| \tag{6.2.5}$$

where $K_{ii} = K(t_i, t_i)$.

Proof. The proof can be easly established by following similar arguments as the ones in (2.3.2).

Lemma 6.2.4. *(Stability result) Let the difference operator $l^h y_i$ be defined by (6.2.4). Then for difference problem (6.1.8)-(6.1.9) we have*

$$l^h y_i \leq Ch \sum_{j=1}^{i} |y_{j-1}| + ||f||_\infty, \quad 1 \leq i \leq N \tag{6.2.6}$$

Lemma 6.2.5. *Let (6.2.3) be satisfied, then for the solution of the difference scheme (6.1.8)-(6.1.9) we have the following estimate*

$$|y_i| \leq (\alpha_*^{-1} ||f||_\infty + |A|) \exp(\alpha_*^{-1} C t_i), \quad 1 \leq i \leq N. \tag{6.2.7}$$

6.3 Error analysis of the scheme

The main lines for the analysis of the uniform convergence given in this section are similar to the ones from Chapter 2 Section (2.4). Let $z_i = y_i - u_i$, where y_i and u_i are solution of problems

(6.1.8)-(6.1.9) and (1.3.1)-(1.3.2) respectively at the mesh point t_i. Then for the error function z_i, we have

$$L^h z_i = R_i, \quad i = 1(1)N, \tag{6.3.1}$$

$$z_0 = 0, \tag{6.3.2}$$

where R_i is defined by (6.1.7).

Lemma 6.3.1. *Under the requirements that $a, f \in C^1$, and $K \in C_0^1$ the remainder term (6.1.7) of the scheme (6.1.8)-(6.1.9) satisfies*

$$||R||_{\infty,\psi_h} \leq Ch \tag{6.3.3}$$

Proof. The local truncation error R_i has the form $R_i = R_i^{(1)} + R_i^{(2)} + R_i^{(3)}$ where

$$R_i^{(1)} = -\chi_i^{-1}h^{-1}\int_{t_{i-1}}^{t_1}[a(t)-a(t_i)]u(t)\varphi_i(t)dt + \chi_i^{-1}h^{-1}\int_{ti-1}^{t_i}[f(t_i)-f(t)]\varphi_i(t)dt \tag{6.3.4}$$

$$R_i^{(2)} = \chi_i^{-1}h^{-1}\int_{t_{i-1}}^{t_i}\varphi_i(t)dt \times \int_{t_{i-1}}^{t_i}\frac{d}{d\eta}\left[\int_0^{\eta}K(\eta,s)u(s)ds\right][H(T-\eta)-1]d\eta \tag{6.3.5}$$

$$R_i^{(3)} = \sum_{j=1}^{i}\int_{t_{j-1}}^{t_j}(t_j-\eta)\frac{d}{ds}[K(t_i,\eta)u(\eta)]d\eta. \tag{6.3.6}$$

Using the mean value theorem, (see discussions in Lemma 2.4.4), we have for $R_i^{(1)}$:

$$\begin{aligned} |a(t)-a(t_i)| &= |a'(\vartheta_i)||t-t_i| \leq C_1 h, \quad \vartheta_i \in (t_i,t), \\ |f(t_i)-f(t)| &= |f'(\upsilon_i)||t_i-t| \leq C_2 h, \quad \upsilon_i \in (t,t_i). \end{aligned}$$

And so, it is easy to see that

$$R_i^{(1)} \leq Ch. \tag{6.3.7}$$

Likewise, by arguments analogous to those in the proof of (2.2.2) and (2.4.9), we have

$$\begin{aligned} R_i^{(2)} =& \int_{t_{i-1}}^{t_i}\left\{K(\eta,\eta)u\eta + \int_0^{\eta}\frac{\partial}{\partial_\eta}\Big[K(\eta,s)u(s)\Big]ds\right\}[H(t-\eta)-1]d\eta \\ \leq& C\left\{\int_{t_{i-1}}^{t_i}|u(\eta)|d\eta + \int_{t_{i-1}}^{t_i}\left|\int_0^{\eta}u(s)ds\right|d\eta\right\} \\ \leq& Ch. \end{aligned} \tag{6.3.8}$$

and

$$|R_i^{(3)}| \leq \Big|\sum_{j=1}^{i}\int_{t_{j-1}}^{t_j}(t_j-s)\frac{\partial}{\partial t}K(t_i,s)u(s)ds\Big| + \Big|\sum_{j=1}^{i}\int_{t_{j-1}}^{t_j}(t_j-s)K(t_i,s)u(s)ds\Big|,$$
$$\leq Ch_i\Big[\int_0^{t_i}|u(s)|ds + \int_0^{t_i}|u'(s)|ds\Big]$$
$$\leq Ch_i \quad i = 1(1)N. \tag{6.3.9}$$

Therefore, from (6.3.7)-(6.3.9), the proof is completed □

Lemma 6.3.2. *Let inequality (6.2.3) be satisfied. Then the solution z_i of the problem (6.3.1)-(6.3.2) satisfies*

$$||z_i||_{\infty,\psi_h} \leq \max_{0\leq i\leq N}|R_i|. \tag{6.3.10}$$

Combining the lemmas 6.3.1 and 6.3.2, we obtain the following main result.

Theorem 6.3.1. *Assume that u is the exact solution of problem (1.3.1)-(1.3.2) and y its numerical solution obtained via (6.1.8)-(6.1.9). Then, under assumptions that $a, f \in C^1(I)$ and $K \in C_0^1$, we have*

$$||y-u||_{\infty,\psi_h} \leq Ch \tag{6.3.11}$$

6.4 Numerical results

In this section, we test the two numerical methods described in this chapter. To this end, two Volterra integro-differential equations are presented and the maximum errors along with the rates of convergence are given in tabular form. The maximum errors at all the mesh points are evaluated using the formula

$$e_{\varepsilon,N} := \max_{[0\leq j\leq 1]}|u(x_j)-y(x_j)| \tag{6.4.1}$$

for the different values of N. The numerical rates of convergence are calculated using the formula

$$r_{\varepsilon,k} := \log_2\left(\frac{e_{N_{k,\varepsilon}}}{e_{2N_{k,\varepsilon}}}\right), k = 1,2,3,... \tag{6.4.2}$$

The test examples are considered over the interval $I = [0,1]$.

Example 6.4.1. [63] *Consider problem (1.3.1)-(1.3.2) where the coefficient functions are given by*

$$a(t) = t + 1,\ K(t,s) = t + s,$$
$$f(t) = \varepsilon \cos t + t \sin t + 2 \sin t + (t - 2t\varepsilon + \varepsilon^2) \exp\left(\frac{-t}{\varepsilon}\right) + t - 2t \cos t + \varepsilon t - \varepsilon^2,$$
$$u(0) = 1.$$

The exact solution to this problem is given by

$$u(t) = \sin t + \exp\left(\frac{-t}{\varepsilon}\right).$$

Table 6.1: Results for Example 6.4.1: Maximum errors and maximum rates of convergence obtained via EFOFDM (6.1.8)-(6.1.9)

ε	$N = 40$	$N = 80$	$N = 160$	$N = 320$	$N = 640$	$N = 1280$	$N = 2560$	
10^{-1}	4.61E-02	2.10E-01	4.58.E-01	6.77.01	8.23E-01	8.23E-01	9.07E-01	
	1.00	1.00	1.02	1.00	1.01	1.01	1.02	
10^{-2}	8.13E-03	4.07E-03	2.03E-03	1.02E-03	5.08E-04	2.24E-04	1.26E-04	
	1.00	1.00	1.00	1.00	1.00	1.01	1.00	
10^{-3}	8.13E-03	4.07E-03	2.04E-03	1.02E-03	5.09E-04	2.24E-04	1.27E-04	
	1.00	1.00	1.00	1.00	1.00	1.01	1.00	
10^{-4}	8.13E-03	4.07E-03	2.04E-03	1.02E-03	5.09E-04	2.24E-04	1.27E-04	
	1.00	1.00	1.00	1.00	1.00	1.01	1.00	
10^{-5}	8.13E-03	4.07E-03	2.04E-03	1.02E-03	5.09E-04	2.24E-04	1.27E-04	
	1.00	1.00	1.00	1.00	1.00	1.01	1.00	
$\vdots$	$\vdots$	$\vdots$	$\vdots$	$\vdots$	$\vdots$	$\vdots$	$\vdots$	
E_N	8.13E-03	4.07E-03	2.04E-03	1.02E-03	5.09E-04	2.24E-04	1.27E-04	
r_N	1.00	1.00	1.00	1.00	1.00	1.01	1.00	

The analysis summarised in Theorem 6.3.1 shows that the proposed numerical method is first order uniformly convergent independently of the perturbation parameter. These theoretical results are confirmed numerically in Table 6.1 where we computed the maximum errors $e_{\varepsilon,N}$ and the corresponding rates of convergence $r_{\varepsilon,k}$.

6.5 Conclusion

We designed and implemented a fitted operator finite difference method for solving singularly perturbed Volterra integro-differential equations. The method was developed utilizing the method of integral identity with the use of exponential basis function and interpolating quadrature rules with weight and remainder term in the integral form. We showed through an error analyis that the proposed method is ε-convergent. For illustration purposes, an example was solved via the proposed method and results corroborate the theoretical findings.

Chapter 7

Concluding Remarks and Directions for Future Research

This chapter focuses on a brief review of the work done in the previous chapters and highlights the main observations in this work. This dissertation mainly contributed to the investigation, design and analysis of robust numerical methods for solving singularly perturbed Volterra integro-differential equations.

Since the problem under study is composed of a differential operator and an integral operator, to construct the discrete problems, we used the fitted finite difference methods for the differential part and various suitably chosen interpolating quadrature rules to deal with the integral operator.

The general observation that we made throughout this thesis is that the blend of the midpoint difference operator with trapezoidal integration on piecewise uniform Shishkin meshes led to an almost second order convergence scheme. However, using the method of integral identities with weight and remainder terms in integral form, notwithstanding the fast convergence quadrature rules used, we obtained first-order accurate convergence schemes. This unexpected behaviour was observed when combining right side rectangle rule with trapezoidal and Simpson's rule, respectively. Numerical results were presented in each chapter to attest our theoretical findings.

Now we summarise the work by chapter. An exponentially fitted finite difference method was considered in Chapter 2. We first presented qualitative results which play a primordial role throughout the work in the analysis of the numerical methods. Next we provide a numerical method which was analyzed for convergence and stability. The analysis carried out shows that the method is first order convergent in the maximum norm.

Chapter 3 dealt with a robust computational method on a piecewise uniform mesh. The scheme was developed on the basis of a method consisting of a midpoint difference operator along with trapezoidal integration. The proposed numerical method presents uniform convergence of almost second order. This theoretical result is confirmed numerically through some test examples.

In chapter 4, on a piecewise uniform partition, we proposed a computational numerical method which is based on the right and repeated left side rectangle rules with weights and remainder terms in the integral form. It is proved that the proposed scheme converges ε-uniformly with first-order accuracy. We however observe that the method is ε-uniform convergent for $\varepsilon << 1$. To avoid this drawback, we proposed two numerical methods in Chapter 5. Both methods involve right side rectangle rule with Simpson and trapezoidal schemes respectively. In order for these two methods to be ε-convergent, we used piecewise uniform meshes of Shishkin type. As expected, we noted that the two methods are significantly more accurate than the method of Chapter 4.

We constructed a new exponential fitted operator finite difference method (EFOFDM) in Chapter 6. First, we computed a fitting factor using the exponential basis function which plays an important role in discretizing the differential part of the problem. Then, we used the trapezoidal rule to discretize the rest of the problem. The numerical computations show that the method is stable and robust,i.e.; converges for all the values of ε and have a first-order convergent.

Much work is still to be done. One can use the techniques developed here for nonlinear singularly perturbed Volterra integro-differential equations. An attempt in this regard have been made by Şevgin [54]. We would like to deepen these approaches by extending them to various classes of singularly perturbed Volterra equations. Currently we are working in this direction.

Bibliography

[1] D.N. de G. Allen and R.V. Southwell, Relaxation methods applied to determine the motion, in two dimensions, of viscours fluid past a fixed cylinder, *The Quarterly Journal of Mechanics & Applied Mathematics*, **8** (1955) 129-145.

[2] G.M. G.M. Amiraliyev and B.Yilmaz, Fitted difference method for a singularly perturbed Initial value problem, *International Journal of Mathematics and Computation*, **22** (2014) 1-10.

[3] G.M. Amiraliyev and H. Duru, A uniformly convergent difference method for the periodical boundary value problem, *Computers & Mathematics with Applications*, **46(5)** (2003) 695-703.

[4] G.M. Amiraliyev and S. Şevgin, Uniform difference method for singularly perturbed Volterra integro-differential equations, *Applied Mathematics and Computation*, **179(2)** (2006) 731-741.

[5] G.M. Amiraliyev, On difference schemes for problems of the theory of dispersive waves *Soviet Mathematics Doklady*, **42** (1991) 235-238.

[6] G.M. Amiraliyev and Y.D. Mamedov, Difference schemes on the uniform mesh for singular perturbed pseudo-parabolic equations, *Turkish Journal of Mathematics*, **19** (1995) 207-222.

[7] M. Aigo, On the numerical approximation of Volterra integral equations of the second kind using quadrature rules, *International Journal of Advanced Scientific and Technological Research*, **1** (2013) 558-564.

[8] J.S. Angell and W.E. Olmstead, Singular perturbation analysis of an integrodifferential equation modelling filament stretching, *Zeitschrift für angewandte Mathematik und Physik ZAMP*, **36(3)** (1985) 487-490.

[9] J.S. Angell and W.E. Olmstead, Singularly perturbed Volterra integral equations II, *SIAM Journal on Applied Mathematics*, **47(6)** (1987) 1150-1162.

[10] E.B.M. Bashier and K.C. Patidar, A novel fitted operator finite difference method for singularly perturbed delay parabolic partial differential equation, *Applied Mathematics and Computation* **217** (2011) 4728-4739.

[11] N.S. Bakhvalov, Towards optimization of methods for solving boundary value problems in the presence of boundary layers, *Zh. Vychisl. Mat. i Mat. Fiz.*, **9**(1969) 841-859.

[12] C.T. Baker, A perspective on the numerical treatment of Volterra equations *Journal of Computational and Applied Mathematics*, **125(1)** (2000) 217-249.

[13] A. Bellour and M. Bousselsal, Numerical solution of delay integro-differential equations by using Taylor collocation method, *Mathematical Methods in the Applied Sciences*, **37(10)** (2014) 1491-1506.

[14] S. Bhalekar and J.Patade, A Novel Third Order Numerical Method for Solving Volterra Integro-Differential Equations, *ArXiv Preprint ArXiv:* (2016) 1604.08863.

[15] A.M. Bijura, Initial-layer theory and model equations of Volterra type, *IMA Journal of Applied Mathematics*, **71(3)** (2006) 315-331.

[16] C. Clavero and J.L. Gracia, On the uniform convergence of a finite difference scheme for time dependent singularly perturbed reaction-diffusion problem, *Applied Mathematics and Computation*, **216(5)** (2010) 1478-1488.

[17] B. De Good approximation by splines with variable knots, *Spline Functions and Approximation Theory*, **21** (1973) 57-72.

[18] P. Das, Robust numerical schemes for singularly perturbed boundary-value problems on adaptive meshes, Ph.D. thesis, Indian Insitute of Technology Guwahati, 2013.

[19] W.H. Enright and W.B. Hayes, Robust and reliable defect control for Runge-Kutta methods, *ACM Transactions on Mathematical Software (TOMS)*, **33(1)** (2007) 1-19.

[20] P.A. Farrell, J.J.H Miller, E. O'Riordan *Robsut Computationl Techniquesfor Boundary Layers.* Chapman & Hall/CRC Press, Boca Raton (2000).

[21] E.C. Gartland, Graded-mesh difference schemes for singularly perturbed two-point boundary value problems, *Mathematics of Computation*, **51** (1988) 631-657.

[22] J. Grasman Small random perturbatios of dynamical systems with applications in population genetics, *Asymptotics Analysis*, Lecture notes in Math., **711** (1979) 158-175.

[23] D. He and L. Xu, Integrodifferential inequality for stability of singularly perturbed impulsive delay integrodifferential equations, *Journal of Inequalities and Applications*, **2009(1)** (2009) 369-185.

[24] P.W. Hemker, G.I. Shishkin and L.P. Shishkina, The use of defect correction for the solution of parabolic singular perturbation problems, *ZAMM-Journal of Applied Mathematics and Mechanics/Zeitschrift für Angewandte Mathematik und Mechanik*, **77(1)** (1997) 59-74.

[25] V. Horvat, Tension spline collocation methods for singularly perturbed Volterra integrodifferential and Volterra integral equations, *Journal of Computational and Applied Mathematics*, **140(1)** (2002) 381-402.

[26] G.S. Jordan A nonlinear, singularly perturbed Volterra integrodifferential equation of nonconvolution type, *Proceedings of the Royal Society of Edinburgh: Section A Mathematics*, **80(3-4)** (1987) 235-247.

[27] G.S. Jordan, Some nonlinear singularly perturbed Volterra integrodifferential equations, *Volterra Equations* (1979) 107-119.

[28] G.S. Jordan, Some nonlinear singularly perturbed volterra integrodifferential equations, *Volterra Equations*, (1979) 107-119.

[29] M. Kadalbajoo and K.C. Patidar, A survey of numerical techniques for solving singularly perturbed ordinary differential equations, *Applied Mathematics and Computation*, **130(2)** (2002) 457-510.

[30] M. Kadalbajoo and K.C. Patidar, K.K. Sharma, ε-Uniformly convergent fitted methods for the numerical solution of the problems arising from singularly perturbed general DDEs, *Applied mathematics and computation*, **182** (2006) 119-139.

[31] , M. Kadalbajoo and V. Gupta, Numerical solution of singularly perturbed convection-diffusion problem using parameter uniform B-spline collocation method, *Journal of Mathematical Analysis and Applications*, **355(1)** (2009) 439-452.

[32] M. Kadalbajoo and D. Kumar A Computational method for singularly perturbed nonlinear differential-difference equation with small shirft *Applied Mathematical Modlling* **34** (2010) 2584-2596.

[33] J.P. Kauthen, Implicit Runge-Kutta methods for some integrodifferential-algebraic equations, *Applied Numerical Mathematics*, **13(1-3)** (1993) 125-134.

[34] J.P. Kauthen, Implicit Runge-Kutta methods for singularly perturbed integro-differential systems, *Applied Numerical Mathematics*, **18(1)** (1995) 201-210.

[35] J.P. Kauthen, A survey of singularly perturbed Volterra equations, *Applied Numerical Mathematics*, **24(2)** (1997) 95-114.

[36] R.B. Kellogg and A. Tsan, Analysis of some difference approximations for a singular perturbation problem without turning points, *Kellogg, R Bruce and Tsan, Alice*, **32 (144)** (1978) 1025-1039.

[37] T. Koto, Stability of Runge-Kutta methods for delay integro-differential equations, *Journal of Computational and Applied Mathematics*, **145(2)** (2002) 483-492.

[38] M. Kudu, I. Amirali and G.M. Amiraliyev, A finite-difference method for a singularly perturbed delay integro-differential equation, *Journal of Computational and Applied Mathematics*, **308** (2016) 379-390.

[39] V. Kumar, Fitted Mesh Methods for the Numerical Solutions of Singularly Perturbed Problems, Ph.D. Thapar University Ptiala, 2013.

[40] M. Kumari and G. Nath, Unsteady MHD mixed convection flow over an impulsively stretched permeable vertical surface in a quiescent fluid, *International Journal of Nonlinear Mechanics*, **45 (3)** (2010) 310-319.

[41] T.Linß An upwind difference scheme on a novel Shishkin-type mesh for a linear convection-diffusion problem, *Journal of Computational and Applied Mathematics*, **110(1)** (1999) 93-104.

[42] A.S. Lodge, J.B. McLeod and J.A. Nohel, A nonlinear singularly perturbed Volterra integrodifferential equation occurring in polymer rheology, *Proceedings of the Royal Society of Edinburgh: Section A Mathematics*, **80(1-2)** (1978) 99-137.

[43] R.E. Mickens, *Nonstandard Finite Difference Models of Differential Equations*, World Scientific, Singapore, 1994.

[44] J.J.H. Miller, E. O'Riordan and G. I. Shishkin, *Fitted numerical methods for singular perturbation problems: error estimates in the maximum norm for linear problems in one and two dimensions*, World Scientific, Singapore, 2012.

[45] R.E. Moore, *Methods and Applications of interval analysis*, SIAM, Philadelphia, 1979.

[46] J.B. Munyakazi and K.C. Patidar Limitations of Richardsons extrapolation for a high order fitted mesh method for self-adjoint singularly perturbed problems, *Journal of Applied Mathematics and Computing*, **32(1)** (2010) 219-236.

[47] K.C. Patidar, High order fitted operator numerical method for self-adjoint singular perturbation problems, *Applied Mathematics and Computation*, **171(1)** (2005) 547-566.

[48] K.C. Patidar and K.K. Sharma, Uniformly convergent non-standard finite difference methods for singularly perturbed differential-difference equations with delay and advance*International Journal for Numerical Methods in Engineering*, **66(2)** (2006) 272-296.

[49] L. Prandtl. Uber flussigkeits-bewegung bei kleiner reibung, *In Verhandlungen, III Inter. Math. Kongresses, Tuebner, Leipzig*, (1905) 484-491.

[50] Y. Raffoul and H. Rai, Uniform Stability In Nonlinear Infinite Delay Volterra Integrodifferential Equations Using Lyapunov Functionals, *Nonautonomous Dynamical Systems*, **3(1)** (2016) 14-23.

[51] H.G. Roos, M. Stynes and L. Tobiska, *Robust numerical methods for singularly perturbed differential equations: convection-diffusion-reaction and flow problems*, Springer Science & Business Media, **24** 2008.

[52] R. Saadati, B. Raftari, H. Abibi, S.M. Vaezpour and S. Shakeri, A comparison between the variational iteration method and trapezoidal rule for solving linear integro-differential equations, *World Applied Sciences Journal*, **4(3)** (2008) 321-325.

[53] A.A. Salama and D.J. Evans, Fourth order scheme of exponential type for singularly perturbed Volterra integro-differential equations *International Journal of Computer Mathematics*, **77(1)** (2010) 153-164.

[54] S. Şevgin, Numerical solution of a singularly perturbed Volterra integro-differential equation, *Advances in Difference Equations*, **2014(1)** (2014) 1-15.

[55] M. Shakourifar and W.H. Enright, Reliable approximate solution of systems of Volterra integro-differential equations with time-dependent delays, *SIAM Journal on Scientific Computing*, **33(3)** (2011) 1134-1158.

[56] M. Shakourifar and W.H. Enright, Superconvergent interpolants for collocation methods applied to Volterra integro-differential equations with delay, *BIT Numerical Mathematics*, **52(3)** (2012) 725-740.

[57] M. Stynes and H.G. Roos, The midpoint upwind scheme, *Applied Numerical Mathematics*, **23(3)** (1997) 361-374.

[58] N. Sultana, *Volterra difference equations*, Missouri University of Science and Technology, 2015.

[59] G.I. Shishkin A difference scheme for a singularly perturbed parabolic equation with a discontinuous boundary condition, *Zh. Vychisl. Mat. Mat. Fiz.*, **28** (1988) 1679-1692.

[60] K. Surla, Exponential function as boundary layer functions, *Novi Sad Journal of Mathematics*, **28(3)** (1998) 159-176.

[61] J. Zhao, Y. Fan and Y. Xu, Delay-dependent stability analysis of symmetric boundary value methods for linear delay integro-differential equations, *Numerical Algorithms*, **65(1)** (2014) 125-151.

[62] Y. Zhao and F. Zhao, The Analytical Solution of Parabolic Volterra Integro-Differential Equations in the Infinite Domain, *Entropy*, **18(10)** (2016) 344.

[63] C. Zhongdi and X. Lifeng, A parameter robust numerical method for a singularly perturbed Volterra equation in security technologies, *Matrix*, **1** (2006) 20-22.

[64] R. Vulanović Mesh construction for discretization of singularly perturbed boundary value problems, PhD thesis, University of Novi Sad, 1986.

[65] R. Vulanović Non-equidistant generalizations of the Gushchnin-Shchennikov Scheme, *Z. Angew. Math. Mesh.*, **67** (1987) 625-632.

[66] A.M. Wazwaz, *A first course in integral equations*, World Scientific, Singapore, 2015.

[67] S. Wu and S. Gan, Errors of linear multistep methods for singularly perturbed Volterra delay-integro-differential equations, *Mathematics and Computers in Simulation*, **79** (2009) 3148-3159.